Title
Characterization of a Novel Population of Olfactory Neurons

Author
Israel, Samuel Harris

Publication Date
2017

Peer reviewed|Thesis/dissertation

Characterization of a Novel Population of Olfactory Neurons

By

Samuel H Israel

A dissertation submitted in partial satisfaction of the

requirements for the degree of

Doctor of Philosophy

in

Neuroscience

in the

Graduate Division

of the

University of California, Berkeley

Committee in charge:

Professor John Ngai, Chair

Professor Kristin Scott

Professor Gian Garriga

Professor Richard Harland

Summer 2017

Abstract

Characterization of a Novel Population of Olfactory Neurons

Samuel H Israel

Doctor of Philosophy in Neuroscience

University of California, Berkeley

Professor John Ngai, Chair

Zebrafish have become a useful model for understanding olfactory circuitry and social behaviors. Combined with the benefits of optical transparency and fast developmental speed, the large clutch sizes of zebrafish larvae make this animal a desirable choice for large scale drug screens that may be affecting the olfactory system (McCarroll et al., 2016). Zebrafish olfactory anatomy consists of one olfactory epithelium (OE) that exposes at least five classes of olfactory sensory neurons (OSNs) to chemical ligands in the water (Ahuja et al., 2014; Wakisaka et al., 2017; Yoshihara, 2008). OSNs then project axons to the olfactory bulb, which then send projections to higher order brain regions (Yoshihara, 2014). In each step of the olfactory signaling process, ligand information is coded in the receptors, OSNs, and brain areas that each ligand, or suite of ligands, activates. However, to make comparisons with the mammalian olfactory systems, we need to understand how the circuitry of the zebrafish olfactory system differs from mammals. In mice, for instance, two different olfactory systems exist in the nose: the main olfactory epithelium (MOE) and the vomeronasal olfactory system (VNO). These two sensory systems contain OSNs that diverge in morphology and projection targets. Some are important in learned behaviors while others play a role in innate behaviors. In zebrafish, there is only one epithelium that contains a variety of cell types and projection targets. How does this system differentiate between learned and innate behaviors? Understanding why these differences have evolved this way might help us make better comparative studies between different animal groups. New behavioral assays and gene trap techniques have emerged as a powerful way to probe the structure and function of zebrafish olfactory behaviors (Koide et al., 2009; Yabuki et al., 2016). This dissertation examines the circuitry of the zebrafish olfactory system and innate behaviors using gene trapping, single cell RNA sequencing, immunohistochemistry, in situ hybridization, and novel behavioral assays. The following was determined: (1) A new class of unipolar olfactory sensory neuron (OSN) exists in zebrafish larvae that projects directly to the telencephalon and fish amygdala from the anterior olfactory epithelium (OE); (2) Two types of bipolar OSNs project to the mG2 and mG3 glomeruli of the olfactory bulb and express the ora4 and ora6 receptors respectively; (3) Larval zebrafish display thigmotaxis when exposed to fish skin extract; (4) This behavior is absent in fish with olfactory nerve lesions; and (5) Ablation of telencephalon projecting OSNs suggest that these neurons may play a role in thigmotaxis. These results provide a new look at how olfactory circuitry is organized in the larval zebrafish and how these circuits may play a role in innate fear behavior.

Table of Contents

Abstract

Chapter 1: The neural structure and function of vertebrate olfactory and fear behaviors

1.1 Olfactory Systems- Genetic and Anatomic Organization **1**
1.2 Zebrafish Olfactory Anatomy **3**
1.3 Zebrafish Behavioral Circuits **8**
1.4 Fear Circuitry in the Amygdala **13**
1.5 Zebrafish Amygdala Anatomy **15**
References **21**

Chapter 2: Identification of a new class of olfactory neurons

Background **38**
Methods **39**
Results **44**
Discussion **47**
References **62**

Chapter 3: A hardwired circuit for olfactory-guided fear in larval zebrafish

Background **67**
Methods **68**
Results **70**
Discussion **73**
References **82**

List of Figures and Tables

Figure 1.1 Olfactory sensory neurons of the zebrafish olfactory system.

Figure 1.2 Olfactory bulb organization in the larval zebrafish.

Figure 1.3 Olfactory bulb organization in the adult zebrafish.

Figure 1.4 Development of the telencephalon in tetrapod vs. actinopterygian lineage.

Figure 2.1 SAGFF91b gene trap zebrafish line with Gal4FF expression in OSNs and the forebrain.

Figure 2.2 Ablation of OSN terminals in the SAGFF91b line reveals organization of heterogeneous population of OSNs

Figure 2.3 Heatmap of ora receptor expression reveals elevated levels of ora6 and ora4 in GFP positive cells

Figure 2.4 ora6 RNA in-situ expression overlaps with OSNs projecting to the OB

Figure 2.5 ora6 and ora4 RNA in-situ expression overlaps with OSNs projecting to the mG3 and mG2 glomeruli within the OB

Figure 2.6 Expression of GFP and emx3 in the pallium of adult SAGFF91b fish

Figure 2.7 Anatomic map of OSNs within the SAGFF91b line

Figure 3.1 5 dpf larval zebrafish exhibit thigmotaxis when exposed to a skin extract containing an alarm pheromone.

Figure 3.2 Larval zebrafish thigmotaxis behaviors are not caused by putative adult zebrafish alarm pheromones.

Figure 3.3 Alarm pheromone behaviors are mediated by the olfactory system.

Figure 3.4 Larval zebrafish alarm pheromone response represents fear.

Figure 3.5 Alarm pheromone behaviors are partially mediated by the telencephlon projections.

Supplementary Figure 3.1 4 dpf larval zebrafish exhibit thigmotaxis when placed with many other fish larvae and exposed to skin extract.

Table 1 Cell counts and statistics for GFP positive OSNs in the SAGFF91b line

Table 2 Cell counts and statistics for ora6 GFP double labeled OSNs in the SAGFF91b line, with telencephalon or olfactory bulb ablations

Table 3 Cell counts and statistics for ora6 GFP double labeled OSNs in the SAGFF91b line, with mG2 or mG3 ablations

Table 4 Cell counts and statistics for ora4 GFP double labeled OSNs in the SAGFF91b line, with mG2 or mG3 ablations.

Acknowledgments

To my wife Dror, I could have never completed this project without your love and support. You helped me through all of the frustrating moments of my dissertation. Thank you for cheering me up every day. To my parents, thank you for always believing in me and being positive. Our family trips were a highlight of my grad school experience. To my brother, thank you for your endless political commentary and giving me a useful distraction from graduate school. To my friends, thank you for keeping me sane. To Michael Sanchez, Levi Gadye, and Diya Das, thanks for helping lighten the mood in and out of lab. To Scott Laughlin and Russell Fletcher, thank you for your mentorship and guidance as I worked my way through many dead ends. To Ariane Bauhdhuin, thank you so much for your magical lab help. Your skills with the cryostat are unmatched. To my advisor John Ngai, thank you for giving me the opportunity to grow in your lab. No matter where my life takes me, I will always remember to think like a scientist and question everything. To the Ngai lab, thank you for being my home for the past few years.

Chapter 1: The neural structure and function of vertebrate olfactory and fear behaviors

1.1 Olfactory Systems- Genetic and Anatomic Organization

Olfactory Signaling Pathways

Olfaction begins when odorant molecules bind to receptors on the ends of specialized sensory neurons. Almost all receptors within the vertebrate olfactory system are seven-pass transmembrane G-protein coupled receptors (GPCRs). After the ligand (odorant) binds to the extracellular binding domain of the GPCR, G-proteins signal through intracellular second messengers that eventually open ion channels and depolarize the cell. This causes action potentials to propagate down the axon to the olfactory bulb within the brain (Manzini and Korsching, 2011). While each GPCR might show a binding preference for odorants with a particular molecular feature, an individual receptor can be broadly tuned to many molecules with many molecular features. Additionally, one odorant molecule may bind to many receptors with varying strengths. Variations in the structural features of the ligand would elicit different responses in a different subset of receptors. The combinatorial code of receptor binding results in the perception of a unique smell (Repicky and Luetje, 2009; Saito et al., 2009). Of course, the "smell" one detects from most environments includes a complex mix of odorants, each activating a unique set of receptors. How an animal detects a smell is therefore dependent on the variety of cells and receptors present in the nose.

Receptor Family Organization

Most vertebrates express one olfactory GPCR in each olfactory neuron, and expression of all other receptors are shut down within that neuron. Olfactory receptors can be broadly grouped into 5 GPCR families: ORs, TAARs, V1Rs, V2Rs, and FPRs (Dalton and Lomvardas, 2015). One non-GPCR family is the MS4As. These 4-pass transmembrane spanning receptors are expressed in the necklace sensory neurons, and each neuron can express many MS4A receptors (Greer et al., 2016). Members of each receptor family bind with a range of odorants that share common characteristics. ORs bind a structurally diverse array of small organic molecules, TAARs bind odorants containing amine groups, while V2Rs bind larger peptide and protein molecules that function as pheromone and kairomone cues (Abe and Touhara, 2014; Liberles, 2015; Malnic et al., 2010; Papes et al., 2010). In the main olfactory epithelium (MOE) of mice, neurons expressing ORs and TAARs are spread through the main olfactory epithelium into spatially restricted zones. The majority of ciliated cells in the MOE express members of the canonical OR family, which are divided into two groups: ORI and ORII (Buck and Axel, 1991; Freitag et al., 1995; Ressler et al., 1993). A minority of these neurons express receptors in the trace amine associated receptor (TAAR) family (Johnson et al., 2012; Liberles and Buck, 2006). In mice, the TAAR receptor family is very small (only 14 functional receptors). Most tetrapods (mammals and amphibians) have an accessory olfactory system that begins with odorant detection in the vomeronasal organ (VNO), a sensory epithelium separate from the MOE that detects pheromones and large water-soluble chemicals. The mouse VNO is divided into two layers. Microvillous sensory neurons populate both of the layers. Microvillus cells in the apical layer express Vomeronasal type 1 Receptors (V1R), while microvillous cells in the basal layer express Vomeronasal type 2 receptors (V2R). Neurons that express V2Rs do not adhere strictly to the one-neuron one receptor rule since these neurons express a chaperone V2R that is required

for amino acid detection and intracellular trafficking of the non-chaperone receptor (DeMaria et al., 2013; Dulac and Axel, 1995; Herrada and Dulac, 1997; Ryba and Tirindelli, 1997; Silvotti et al., 2007). The last group of receptors is the small Formyl Peptide Receptor (FPR) family. Neurons expressing FPRs are sparsely distributed in both layers of the vomeronsal organ (Liberles et al., 2009; Rivière et al., 2009).

Higher Order Olfactory Anatomy

Beyond the MOE and VNO, neurons in the sensory epithelia send axons to the main olfactory bulb (MOB) and accessory olfactory bulb (AOB) respectively. Neurons that express identical receptors project onto glomeruli in the outer layer of the olfactory bulb. Each glomerulus represents the axon terminals of neurons expressing the same receptor, and the positions of each glomerulus are somewhat fixed between individuals (Mombaerts, 2004). Odorants that bind to a particular receptor will then activate a distinct subset of glomeruli that correspond to that receptor, and therefore will be represented by a unique spatiotemporal activity map within the OB (Lin et al., 2006). Neurons in the accessory olfactory system display a different projection pattern from the MOB. The AOB does contain glomeruli, however unlike the MOB, neurons expressing the same V1R or V2R converge onto large subsets of AOB glomeruli. VNO neurons that express the same receptor send axons to as many as 30 glomerular targets, which are only roughly the same between individuals (Wagner et al., 2006). The location in the glomerular layer of the AOB is indicative of the identity of a group of cues, not one particular receptor cue like the MOE-MOB system. The main olfactory system has the ability to detect a wide range of cues and a large range of concentrations with low selectivity, while the accessory olfactory system detects a narrow range of cues with high selectivity. This high selectivity can sometimes be tuned to single molecules that determine the survival of a species (large molecules in predator urine). Both systems are tuned for detecting different types of cues (Dulac and Wagner, 2006).

Activity in the main and accessory olfactory bulb drive both learned and innate behaviors via connections to more central brain regions. The largest projection area from the MOB is the piriform cortex, a three layered cortical structure in the temporal lobe, where mitral and tufted cells from the MOB spread out in unique patterns that encode odor identity. The diffuse projection patterns differ between individuals. Neurons in the piriform cortex that respond to a given odorant, are not only distributed in a random fashion, their receptive fields are non-contiguous and non-overlapping. One odorant may activate different groups of piriform neurons depending on the identity of other odorants in the odor mix (Choi et al., 2011; Sosulski et al., 2011; Stettler and Axel, 2009). This organizational principle differs from the spatially segregated patterns of the MOB. It also differs from the organization of other neocortical sensory areas where cells with similar or overlapping receptive fields are located in close proximity to one another and tuning varies smoothly across the cortices.

Odor representations also send projections into other targets of the olfactory bulb such as the cortical amygdala, lateral entorhinal cortex, and olfactory tubercule, a subdivision of the ventral striatum. While connections to these areas are less well understood, a rough projection map has been observed. Single dendrites from mitral and tufted cells extend into glomeruli of the MOB and parallel axon branches extend into MOB targets in characteristic patterns. The patterns may give rise to the distinct roles each area has in olfactory processing. Unlike the piriform cortex, the cortical amygdala receives inputs from individual MOB glomeruli in spatially restrictive patterns that are roughly common between individuals. These inputs result in behaviors that are

spatially biased to innately relevant odors, such as the mouse avoidance behaviors to TMT, a chemical component in fox urine. This hardwiring seems to mediate instinctive responses to predator odors (Root et al., 2014; Sosulski et al., 2011).

In contrast to the main olfactory sensory system, the accessory olfactory system projects neurons in a more conserved and stereotypical fashion between individuals. Neurons expressing V1Rs project their axons to the anterior AOB (aAOB) while V2Rs project to the posterior AOB (pAOB). In the AOB, dendrites from single mitral cells are activated by many glomeruli often responding to the same vomeronasal receptor. Mitral cells then send axons into the medial amygdala (MeA) primarily, and also the bed nucleus of the stria terminalis (BST). Neurons in the MeA respond to higher level categorical information and sharpened receptive field compared to the AOB. MeA cells can distinguish female, predator cues, and opposite sex stimuli for conspecific urine, which the AOB cannot (Bergan et al., 2014). From the MeA, neurons send projections to hypothalamic nuclei involved in reproductive and stress response (Mohedano-Moriano et al., 2007). The main and accessory olfactory systems remain distinct in both their function, genetics, and anatomy, thus allowing higher order brain areas to trigger distinct behaviors based on the activation of different olfactory receptors.

1.2 Zebrafish Olfactory Anatomy

The mammalian olfactory system provides a solid basis for understanding both learned and innate olfactory circuitry in other organisms. The zebrafish olfactory system shares many of the same features as other mammals, such as the presence of an olfactory epithelium containing sensory cells that express OR and TAAR receptors, an olfactory bulb, where OE neurons send projection axons, and olfactory driven innate behaviors. Unlike the mammalian system, the zebrafish only has one olfactory epithelium and even though four of the five receptor families exist in the zebrafish genome, each family has evolved and expanded in very different ways. Sensory neurons in the zebrafish OE also show a variety of cellular morphologies, some of which are not present in the mammalian OE.

Cellular Organization and Receptor Expression in the Zebrafish OE

In the zebrafish there is only one olfactory organ (the olfactory rosette or olfactory epithelium), which contains olfactory sensory neurons (OSNs) of at least five different morphological types: ciliated, microvillous, crypt, kappe, and pear cells, all of which send axons to the olfactory bulb via the tightly bundled olfactory nerve. The two predominant OSNs are the ciliated and microvillous cells. Ciliated OSNs are long bipolar cells that project a single ciliated dendritic knob into the nasal cavity and an unbranched axon into the olfactory bulb. Within the OE, ciliated neurons are located deep in the basal layer. The microvillous cells are more rounded bipolar cells that send tens of short microvilli into the nasal cavity and are located in the more superficial layer of the olfactory epithelium (Ahuja et al., 2014; Hansen and Zeiske, 1993, 1998). Uniquely in fish there at least three other OSN types that are not present in mammals, and are summarized in figure 1.1. Crypt cells account for only a small population in the OE and are located in the most apical OE layer. Their signature characteristic is an extremely rounded almost spherical shape. They project both microvilli and short cilia into the nasal cavity. They show expression of the S100 calcium-binding protein and tropomypsin receptor kinase A (TrkA), which is the receptor for nerve growth factor (Catania et al., 2003; Germanà et al., 2004,

2007). Kappe cells resemble crypt cells in their round morphology and location in the apical most layer of the OE. Their distinguishing feature is a raised tip with microvilli (resembling a cap) and expression of the G-protein G-alpha o, which has been only observed previously in microvillous cells (Ahuja et al., 2014; Oka and Korsching, 2011). Pear cells are the most recently discovered OSN type. These cells bind to adenosine via the A2c receptor in a highly specific manner. Curiously, they express OMP and Gaolf, just like ciliated cells, even though their morphology is small & round, they are located near the apical end of the olfactory epithelium, and they project microvilli, not cilia, into the lumen (Wakisaka et al., 2017). Scattered throughout the OE are ciliated non-sensory cells, which help move mucus along the surface of the epithelium (Zeiske et al., 1992). Fig 1.1 displays a summary chart comparing the morphology and characteristics of all known fish OSNs.

As in mammals, the detection of odorants occurs through different families of GPCRs. Zebrafish contain ~140 OR genes, ~50 vomeronasal type 2 (V2R-like) genes, ~100 TAARs, and 6 ora receptor genes (V1R-like) (Alioto and Ngai, 2005, 2006, Hashiguchi and Nishida, 2006, 2007; Saraiva and Korsching, 2007). Ciliated cells express ORs while microvillous cells express primarily V2R receptors (DeMaria et al., 2013; Yoshihara, 2008). Crypt cells have displayed expression of one of the ora family receptors, ora4 (Oka et al., 2012). The TAAR receptor family is also expressed in a much larger subset of OSNs when compared to other organisms (~100 fish TAARs compared to 6 human, 16 mouse, and 17 rat TAARs). The large diversity of TAARs in zebrafish suggests an evolutionary importance of amine detection and perhaps pheromone and kairomone detection as well. Similar behaviors have been observed in the (Dewan et al., 2013; Ferrero et al., 2011; Gloriam et al., 2005; Hussain et al., 2009; Shi and Zhang, 2009).

A major question in the zebrafish olfactory system is whether or not olfactory neurons follow the one-receptor one-neuron rule. This rule allows tuning of OSNs to a particular molecular receptive range. Double-fluorescence in situ hybridization experiments revealed that many combinations of 2 ORs do not overlap their expression (Sato et al., 2007). Furthermore, individual OR receptor expression ranges from 0.5% to 2% of overall receptor expression (Barth et al., 1996, 1997). These data support the one-receptor one-neuron rule, however experiments have been performed that show examples of one-neuron multiple-receptor expression. Within ciliated OSNs, a subpopulation expressing receptors in the OR103 family may express up to three receptors in the same cell (OR 103-1, 103-2, & 103-5) (Sato et al., 2007). Similar expression patterns have been observed in several populations of OSNs in *C. elegans* and *Drosophila*. A single AWC neuron in *C.elegans* expresses many receptors and displays appetitive behavioral responses to each odorant that activates the cell (Bargmann et al., 1993; Goldman et al., 2005; Troemel et al., 1995). This may imply that odorant detection of OR 103 receptors are redundant and discrimination between individual members is not evolutionarily important. Another example of one-neuron multiple-receptor expression is in microvillous cells, where almost all microvillous OSNs express the V2R-like receptor, V2rI1 (olfCc1, VR5.3) as a co-receptor (DeMaria et al., 2013). V2rI1 expression in microvillous cells resembles other co-expression systems in other animals such as the *Drosophila* Orco (Or83b) and mouse V2R2 olfactory receptors (DeMaria et al., 2013; Larsson et al., 2004; Martini et al., 2001). In zebrafish, OSNs have been shown to express either one receptor exclusively or many receptors, depending on the case. The functional relevance of these two systems has yet to be determined.

The repertoire of ligands that bind to each receptor class has been somewhat elucidated through electrophysiology experiments in other species of fish. Voltage clamp and patch clamp recordings have shown that in the rainbow trout and Cabinza grunt, ciliated and microvillous cells respond to amino acids, but through different signaling pathways (Sato and Suzuki, 2001; Schmachtenberg and Bacigalupo, 2004). Ciliated cells also respond to bile salts, and microvillous cells respond to nucleic acids (Hansen et al., 2003). Ligands for crypt cells have been harder to determine. They have been hypothesized to detect reproductive pheromones, since their density and depth in the OE varies depending on the season in carp (Hamdani et al., 2008). Also, in certain species of fish, crypt cell density is sex dependent (Bettini et al., 2012). In mature trout, depending on the sexual maturity and gender of the fish, crypt cells respond to reproductive pheromones of the opposite sex (Bazáes and Schmachtenberg, 2012). Crypt cells might respond differently to unique ligands as the fish matures through life.

Signal transduction pathways in ciliated and microvillous cells share many similarities with the mammalian system. Ciliated cells in both mammals and zebrafish express the olfactory-specific GTP-binding protein subunit (G_{olf}) and cyclic nucleotide-gated cation channel A2 subunit (CNGA2) (Brunet et al., 1996; Hansen et al., 2003; Sato et al., 2005). Microvillous cells in the zebrafish express the transient receptor potential channel C2 (TrpC2), which mimics the vomeronasal sensory neurons in mice. The TrpC2 mouse ortholog plays a critical role in the signal transduction of social and sexual behaviors (Kimchi et al., 2007; Leypold et al., 2002; Sato et al., 2005; Stowers et al., 2002). Unlike the mammalian system, zebrafish express the olfactory marker protein (OMP) only in ciliated cells. In the mouse, all OSNs in the MOE and VNO express OMP (Graziadei et al., 1980; Sato et al., 2005).

The three cellular types all send projections from the OE to the OB in a coarse spatial map and are shown in figure 1.2. Studies using double transgenic fluorescent labeling of ciliated and microvillous OSNs have shown that ciliated cells project to the dorsal and medial olfactory bulb, and microvillous cells project to the lateral olfactory bulb (Sato et al., 2005, 2007). Retrograde labeling of lipophilic tracer dye in the OB, and TrkA immunolabeling, have revealed that crypt cells project to the ventral olfactory bulb in carp and to a single olfactory bulb glomerulus (mdG2) in zebrafish (Ahuja et al., 2013; Gayoso et al., 2012; Hamdani and Døving, 2006).

Extrabulbar Projections

In many adult fish, including zebrafish, and amphibians, OSNs that bypass the OB have been discovered. The extrabulbar projecting OSNs originate in the OE and send axons to brain areas beyond the olfactory bulb (Gayoso et al., 2011; Honkanen and Ekström, 1990; Pinelli et al., 2004; Riddle and Oakley, 1992). In white sturgeon, OSNs send extrabulbar projections to the posterior tubercle in the diencephalon. In trout, extrabulbar fibers innervate the ventral nucleus of the ventral telencephalon (vV), dorsal telencephalon, and hypothalamus (Anadón et al., 1995; Becerra et al., 1994; Northcutt, 2011). Lipophilic tracer dye experiments have shown extrabulbar projections in adult zebrafish. OSNs with these projections terminate in the vV (Gayoso et al., 2011). The first description of extrabulbar projections in zebrafish larvae is revealed in this dissertation. These new OSNs project directly from the OE to the ventral telencephalon.

Olfactory Bulb Organization in Zebrafish

The zebrafish OB is subdivided into distinct bundles called glomeruli, much like the mammalian and insect systems, where information is transmitted from OSNs to second order mitral and tufted cells. The developing larval zebrafish has a small number of glomerular clusters called protoglomeruli (Dynes and Ngai, 1998). In the 5 day post fertilization (5dpf) aged fish, there are 5 protoglomeruli: posterior (pG), lateral (lG), dorsal (dG), antero-ventral (avG), and medial (mG), which are further subdivided into 6 more distinct clusters (mG1-6) (Fig 1.2) (Braubach et al., 2012; Koide et al., 2011). The adult zebrafish OB contains ~140 glomeruli, many of which are indistinguishable, tiny, or fused together (Baier and Korsching, 1994; Braubach et al., 2012). However, a unique feature of the zebrafish OB is how glomeruli are grouped into clusters, which are displayed in figure 1.3. The adult has ~9 clusters grouped by region: dorsal (dG), dorso-lateral (dlG), lateral (lG), medio-anterior (maG), medio-posterior (mpG), medio-dorsal (mdG), ventro-anterior (vaG), ventro-medial (vmG) and ventro-posterior (vpG) (Fig 1.3). While it is unclear whether all OSNs of the same receptor type project to stereotyped glomerular clusters, like the mammalian system, it has been shown that single OSNs project onto glomerular targets in a predetermined and reproducible way (Lakhina et al., 2012). This suggests that receptor expression drives the axon growth to its glomerular target in the OB.

Glomerular clusters play an important role as functional units of olfactory coding in both the mouse and fish. Different structural and functional odor categories activate glomerular clusters in odor maps. Studies using voltage-sensitive dyes, calcium indicators, and immunohistochemical analysis have uncovered the activation pattern of glomeruli in response to a variety of odors. Amino Acids, which activate microvillous cells, also activate multiple glomeruli in the lG cluster. Subdividing the amino acid odorants by structural characteristics such as side chain length, hydrophobicity, and pH has revealed a combinatorial code within spatially defined glomeruli within the lateral cluster (Friedrich and Korsching, 1997, 1998; Fuss and Korsching, 2001; Hansen et al., 2003; Speca et al., 1999). These functional data have been further supported by behavioral data showing the dependence of lateral glomeruli for amino acid detection (Koide et al., 2009). Bile acids, which activate ciliated cells, show strong responses in the dG and vmG clusters. Nucleotides, which activate a subset of ciliated cells, show activity in lG2 (Friedrich and Korsching, 1998; Yoshihara, 2014). Amines are hypothesized to play an important role the fish olfactory system due to the large abundance of TAAR receptors in the zebrafish genome. Amines and nucleotides have been shown to activate the dlG glomerular cluster, which is almost solely devoted to amine detection. Distinct glomeruli with in the dlG are activated by structurally distinct catagories of amines, much like the way lG is subdivided for amino acid characteristics (Yoshihara, 2014).

Higher Order Olfactory Centers in the Fish Brain

Second order projections from the OB are propagated through mitral cells to a variety of distinct areas throughout the zebrafish telencephalon and diencephalon. There are four main projection areas: dorsal telencephalon, ventral telencephalon (vV), the posterior tuberculum (PT), and the right habenula (rHb). Approximately one third of all neurons projecting out of the OB send axons back into the OB ipsilaterally, contralaterally or both. While the functional mechanisms of higher order areas have yet to be elucidated, many experiments have uncovered the complete axon projection map out of the zebrafish OB with single cell neuron labeling techniques (Miyasaka et al., 2009, 2014; Nikonov et al., 2005).

The Telencephalon

The telencephalon contains two OB projection areas, the dorsal and ventral telencephalon. More specifically, the posterior zone within the dorsal telencephalon (Dp) receives the largest number of OB projections. Neurons from every OB glomerular cluster project axons to the Dp with extensive overlap. These anatomical connections form broad and sparse representations of OB topographical information (Miyasaka et al., 2014). Additional imaging studies have shown that neurons within the Dp respond to distinct groups of odors and odor molecular features from many different OB glomeruli (Yaksi et al., 2009). The broad, sparse, higher order projections of the Dp resemble the associative learning olfactory cortices in other animals such as the piriform cortex in mammals and mushroom body in *Drosophila* (Caron et al., 2013; Ghosh et al., 2011; Igarashi et al., 2012; Jefferis et al., 2007; Lin et al., 2007; Miyamichi et al., 2011; Sosulski et al., 2011).

The Vv has historically been linked to the mammalian septal area due to the expression of molecular markers used to delineate brain areas in mammals. The Vv receives massive inputs from a select group of glomerular clusters: maG, vaG, vmG, and dG. In the OB, these clusters are innervated by ciliated OSNs that express ORs and respond to bile acids and prostaglandins (Ganz et al., 2012; Miyasaka et al., 2014; Wullimann and Mueller, 2004). Based on the output projections of the vV to the preoptic and hypothalamic areas, it is thought that the role of the vV and its projection inputs may be to decode odor and pheromone signals into social and endocrine based responses (Rink and Wullimann, 2004).

Both the Dp and vV receive extensive neuromodulatory inputs from the locus coeruleus, raphe nuclei, and posterior tubercle, which contain noradrenergic, serotonergic, and dopaminergic neurons respectively. Interestingly, dopaminergic inputs to the Dp selectively decrease inhibitory but not excitatory odor responses, which was supported further by calcium imaging experiments showing that the magnitude of odor responses increased with increased dopamine levels (Rink and Wullimann, 2004; Schärer et al., 2012). These experiments suggest that dopamine mediates odor response gain during learning.

The Diencephalon

While not as extensive as the telencephalon, direct projections from the OB reach as far as the posterior tuberculum (PT) and right habenula (rHb) in the diencephalon. The PT is associated with the hypothalamus and contains groups of dopaminergic neurons. Although sparse, neurons from all OB glomerular clusters emerge through the posterior telencephlon and innervate the PT (Miyasaka et al., 2014; Schweitzer et al., 2012). This pattern of innervation suggests that the PT responds to a wide range of odor inputs. Experiments in sea lamprey have shown that neurons in the OB-PT pathway play a role in olfactory driven locomotor activity. Stimulation of the medial OB generated responses in reticulospinal cells in the ventral root of the spinal cord, resembling fictive motion. Dopaminergic neurons in the PT relayed information from the OB to the spinal cord, displaying the first functional connection between the olfactory system and spinal motor networks in vertebrates (Derjean et al., 2010; Ren et al., 2009).

The habenula (Hb) is a highly conserved structure among vertebrates and shows heterogeneity in both structure and function between left and right sides within a single animal. The medial and

lateral habenulae in mammals correspond to the dorsal and ventral habenulae in fish (Amo et al., 2010). Asymmetric projections from two glomerular OB clusters (mdG and vmG) innervate the medial compartment of the right habenula (Miyasaka et al., 2009, 2014). The strongly biased connections from these two glomerular clusters imply a hardwired circuit that may be part of innate olfactory behaviors. Outputs from the Hb project to many areas in the brainstem including the interpeduncular nucleus, the raphe nuclei, the substantia nigra, and the ventral tegmental area (Hikosaka, 2010; Tomizawa et al., 2001). Specifically, the right habenula (rHb), which receives all inputs form the OB, projects to the ventral part of the interpenduncular nucleus. Interestingly, the habenula and interpeduncular nucleus have both shown involvement with the motor behavior in dopaminergic circuits in mammals (Hikosaka, 2010). Furthermore, experiments in zebrafish have shown that genetically inactivating rHb neurons alters responses to conditioned fear stimuli (Agetsuma et al., 2010; Lee et al., 2010). These experiments imply a role for the habenula in learned fear behaviors driven by olfaction.

1.3 Zebrafish Behavioral Circuits

Zebrafish have become a widely used model organism for many areas of neuroscience and development studies. Since the 1930s, zebrafish have been the focus of laboratory research because of their adaptability to a variety of water conditions, and ease of raising and breeding in captivity, not to mention their fast developmental speed and transparency through larval stages (Engeszer et al., 2007; Roosen-Runge, 1938). Zebrafish are naturally found in Southeast Asia, and live in shallow, slow moving water (shallow streams and rice paddies). Thanks to the implementation of genetic approaches to study neural circuit development in Zebrafish, and recent large scale genetic screens, Zebrafish have become a widely used model system in neuroscience (Grunwald and Eisen, 2002; Scott et al., 2007; Streisinger et al., 1981).

More recently, zebrafish have become a popular system to study behavior. Even at 3 days old zebrafish larvae display a broad array of behaviors while only containing ~100,000 neurons (0.000001x the number of human neurons). More remarkably, larval zebrafish contain the same overall vertebrate body structure. Vertebrate anatomical features as well as specific circuits and cell classes are conserved in zebrafish (Hashimoto and Hibi, 2012; Hoon et al., 2014). Genetic expression systems such as Gal4-UAS have been used to create numerous driver and reporter transgenic lines of zebrafish to study learned and innate behavioral circuits.

In the 3-6 day old fish, most behaviors are innate, almost reflexive responses that are stereotyped across individuals. Visual behaviors such as prey capture, navigation and predator avoidance develop almost as soon as retinal ganglion cells reach their central targets (~3dpf). Auditory and touch related behaviors such as the startle response, vestibular-ocular reflex, and rheotaxsis (reflex to move in the opposite direct of flowing water) have been used to study hair cells function in vertebrates (Bhandiwad et al., 2013; Bianco et al., 2012; Oteiza et al., 2017; Yang et al., 2017). The olfactory system in zebrafish mediates a wide variety of behaviors such as foraging for food, olfactory imprinting, reproduction/mating, and a wide variety of different fear and anxiety behaviors, all of which begin at the larval stage of zebrafish development (Orger, 2016; Yang et al., 2017; Yoshihara, 2014).

Visual Behavior in the Larval Zebrafish

Avoiding capture from a predator and hunting prey are two important visually guided behaviors that are hardwired in the larval circuitry. Both behaviors rely on the optic tectum (OTc, the homologue of the mammalian superior colliculus) for visual detection. By immobilizing larval zebrafish heads in agarose, and mimicking the approach of a predator, via video, fish were observed to vigorously flip their tails (looming escape response). Activation of retinal gangion cells in the OTc was observed during the looming escape response, and laser ablation of these cells abolished the response altogether (Temizer et al., 2015).

In a similar experimental setup, larval zebrafish heads were immobilized and a video that evoked the prey capture response was used to dissect the underlying neural circuitry for that behavior. Larval zebrafish naturally tracked large, dark, and fast moving spots on a video screen with their eyes. The movement mimics the natural motion of a paramecium that larvae eat as prey. Cells in the OTc were also activated during tracking behavior (observed by calcium imaging) and were shown to be vital components of a larger model for prey recognition and hunting behavior. Cells in the OTc trigger reticulospinal neurons which in turn, recruit spinal circuits to induce turning toward a visual target (Bianco and Engert, 2015).

The circuit level experiments have been accompanied by comprehensive population level experiments, which observe activation of almost every neuron in the fish brain during the onset of a visual stimulus in real time. Using light sheet microscopy, population level neuronal activity is measured during bouts of fictive motion, where fish larvae are immobilized and the surrounding environment moves in response to fish motor circuit activation (Ahrens et al., 2012, 2013; Portugues et al., 2014). Visual reflexes like the optokinetic response (rotational motion reflex), have activated sparse and widely distributed groups of neurons in the ventral cerebellum, pre-tectum, and rostral medulla, all areas that integrate visual and motor behaviors (Portugues et al., 2014). Importantly, the patterns of activity were consistent across different fish, implying a level of stereotypy that will aid in uncovering complete innate behavior circuitry across vertebrates.

Vestibular/Auditory Behavior in Larval Zebrafish

Zebrafish sense auditory and physical (vestibular) information through the use of hair cells, which, like mammals, detect physical vibrations. Zebrafish have two hair cell systems: the inner ear, which mimics the inner ear of mammals by detecting rotational and bi directional motion; and the lateral line, which not only detect sound but also the direction and speed of water motion around the body of the fish. The lateral line consists of small bundles of hair cells that wrap around the sides of the fish's midsection.

The startle response is a reflex that has been observed in many species of fish. By simply tapping on a dish or creating a loud and sudden tone, fish react by bending into a "C" shape away from the stimulus, and then straighten out and swim rapidly away (Eaton et al., 1977; Kimmel et al., 1974). Startle behavior relies on the Mauthner cell circuit. Hair cells in the fish inner ear respond to high frequency sound waves (>100Hz) and through auditory afferent neurons send excitatory signals to the large Mauthner cells in the hindbrain. Mauthner cells are very large and have two long dendrites that use both electrical and chemical synapses to propagate information to the trunk muscles in the zebrafish spine (Medan and Preuss, 2014; Nicolson et al., 1998). One action potential from either Mauthner cell is sufficient to activate spinal neurons that synapse directly

onto trunk muscles on the contralateral side and inhibit the ipsilateral side (Fetcho and Faber, 1988; Nissanov et al., 1990). Ablation of the Mauthner cells eliminates the startle response (Issa et al., 2011; Zottoli et al., 1999).

The vestibular-ocular reflex (VOR) is a reflex that fish use to maintain gaze of the eyes while the body is moved rotationally. Body motion is detected by lateral line hair cells. In experiments where larval zebrafish were immobilized in agarose and rotated around a fixed axis, both eyes rotate counter to the axis of motion to maintain gaze. Zebrafish with genetically mutated tip links in their hair cells lost their VOR (Mo et al., 2010). Laser ablation studies in second order neurons of the tangential nucleus show that these neurons also play a role in VOR circuitry (Bianco et al., 2012).

Rheotaxis (alignment in a stream) is also mediated in part by the lateral line hair cells. Perturbation of a healthy lateral line system disables the ability of larval zebrafish to align properly in a moving stream and display rheotaxis (Suli et al., 2012). Specifically, it is the lack of the posterior lateral line system that induces a significant decrease in a fish's orienting behavior (Oteiza et al., 2017). Easy access to the lateral line and inner ear hair cells make auditory/ vestibular behaviors nice targets for circuit level neuroscience research.

Olfactory Behaviors in Zebrafish

In most animal species, searching for food, mating, and avoiding danger are some of the most important tenants of survival. Olfactory signals elicit these behaviors in many mammals through odorants in the air and pheromones by tactile touch. Odorants and pheromones in aquatic environments activate olfactory neural circuits mediating many innate and conditioned behaviors in zebrafish.

Attraction toward a food source (not to be confused with prey capture) is fundamental for survival. Amino acids, while an important foods source themselves, can also signal feeding cues by acting as odorants on the zebrafish olfactory system. Adult fish have exhibited increased turning and attractive behaviors towards amino acids (Braubach et al., 2009; Steele et al., 1990, 1991). Using genetic, anatomic and behavioral approaches, zebrafish that normally showed attraction toward amino acids lost that attraction when synaptic transmission was blocked to the lateral glomeruli (lG) in the OB (Koide et al., 2009). The lG is innervated primarily by microvillous cells, which express V2Rs. Projections from the lG target the Dp, vV in the telencephalon and sparse projections to the rHb (Miyasaka et al., 2014). Clearly, microvillous cells leading to the lG play a significant role in amino acid appetitive behavior. Innate avoidance behaviors can also be observed when fish are exposed to the death associated diamine compound cadaverine. Decaying fish release cadaverine, which is then detected by surrounding fish via the receptor TAAR13c (Hussain et al., 2013). Adult fish show a strong avoidance behavior to cadaverine. How amino acid and diamine information is read by higher order neurons in the telencephalon remains a mystery.

Reproductive behaviors in fish have also been linked to olfactory and pheromone detection. In goldfish, two reproductive steroids are secreted from female goldfish during their preovulatory cycle that affect male behavior: 17α, 20β-dihydroxy-4-pregnen-3-one (17,20P) and its sulfated form (17,20P-S). Males detect these as pheromones, which then change their endocrine gonad

responses (Sorensen et al., 1998; Stacey et al., 1989). In zebrafish, 17,20P-S appears as an active pheromone by activating a subset of ciliated OSNs and a few glomeruli in the maG glomerular cluster (Friedrich and Korsching, 1998). During zebrafish and goldfish ovulation, prostaglandin F2α (PGF2α) and its metabolite 15-keto-PGF2α are secreted in female urine. Male fish display a variety of behaviors when exposed to these pheromones including increased swimming activity, attraction to females, nudging, and quivering. Using voltage sensitive dyes, PGF2α and 15-keto-PGF2α activate two glomeruli in the vmG OB cluster in zebrafish (Friedrich and Korsching, 1998; Sorensen et al., 1988; Yabuki et al., 2016). Receptors and higher order neural circuits for reproductive behaviors are yet to be discovered. More recently, ora1 of the V1R-like family of receptors, was shown to be activated by 4-hydroxyphenylacetic acid (pHPAA), a putative pheromone that causes an increase in ovipositioning frequency in mating pairs (Behrens et al., 2014). Cells expressing ora1 and neural circuits responding to pHPAA are still unknown.

Olfactory imprinting behaviors have been widely studied in Salmon. As juveniles, salmon imprint the odors they are exposed to in their native streams. After migrating to sea to become adults, they return to the streams of their birth for the reproduction of their own offspring. They navigate to their natal streams by using the olfactory cues of their environment (Dittman and Quinn, 1996; Scholz et al., 1976; Yamamoto et al., 2010). While zebrafish don't display this behavior in the wild, experiments have shown that adult zebrafish can remember artificial odorants exposed to them as juveniles using a Y-maze preference test (Harden et al., 2006).

Anxiety Behavior in Zebrafish

Zebrafish adults and larvae display numerous anxiety behaviors from all of their sensory systems. Investigators have likewise developed key assays to observe these behaviors. Two of the most common assays, the novel tank test and the light-dark preference test have been used to investigate responses to potentially threatening stimuli and innate preferences for dark vs. bright areas (scototaxsis). Another useful new tool is the open field test, which assays the animal's innate fear of open spaces and tendency to seek comfort along the edges of an enclosure (thigmotaxsis). All of these assays can lead to a better understanding of fear and anxiety in the brain.

The Alarm Response

The first known observation of anxiety behaviors in fish came from the famed ethologist, Karl von Frisch, who, years before his Nobel Prize winning discoveries in honey bee sensory perception, noticed that minnows swimming in the ponds near his home would display "frightened" reactions to an accidentally injured fish. How, he wondered, did the surrounding fish notice this injury? Using tank experiments where an injured fish was placed inside a tank of healthy swimming fish, he hypothesized that injury to the skin caused an unknown alarm substance, or Schreckstoff (scary stuff), to be released and exposed to the surrounding fish causing a behavioral change (von Frisch, 1938). Over 40 years later, investigators determined that there are in fact specific cells in fish skin, club cells, which release an alarm substance only when the skin is damaged. The substance is then detected by the olfactory system of the surrounding fish to signal danger (Kasumyan and Lebedeva, 1975; Lebedeva et al., 1975; Pfeiffer, 1977; Waldman, 1982). A more recent adaption of this behavior makes use of conspecific skin extracts to induce a tank diving behavior when fish are placed into a novel tank (NTT, Novel Tank Test). When exposed to a skin extract fish display a quick burst of swimming

followed by freezing at the bottom of the tank. Approximately two thirds of all freshwater fish species (members of the superorder Ostariophysi) display tank diving behavior (Speedie and Gerlai, 2008; Yoshihara, 2014). Much work has been done to identify the active components of the alarm substance, but there has been little conclusive evidence identifying the native alarm chemical. One molecule, hypoxanthine-3*N*-oxide, was shown to cause tank diving behavior in adults only (Pfeiffer et al., 1985). Chondroitin sulfate is another molecule that was seen to cause some behavioral changes in adult fish (Mathuru et al., 2012). Replicating these results has been difficult, and conclusive evidence proving that these compounds are part or all of the native alarm substance is weak. Hypoxanthine-3*N*-oxide has not even been identified as a native component of the skin. Neither chemical shows fear behaviors in larval fish (Yoshihara, 2014; unpublished observations). The true nature of the alarm substance may be a complex mixture of chemicals, and the subsequent alarm behavior may be detected by higher order integration of many activated OB glomeruli. Identification of the alarm substance is ongoing.

Thigmotaxis and the Open Field Test

Thigmotaxis is a term used to describe the movement of an organism either away from an object that provides a mechanical stimulus, and in many animals is used to describe the "wall-hugging" behavior that is observed when an animal is experiencing stress and anxiety. The tendency for animals to avoid open spaces when anxious has been observed in almost every animal, but its use as a test for psychopharmalogical studies began in mice in the 1930s (Candland and Nagy, 1969; Choleris et al., 2001; Hall and S., 1934). The Open Field Test (OFT) was designed as a way to measure thigmotaxsis, and is broadly defined as "an enclosed open area where an animal is placed and some form of behavior, usually activity, is measured" (Choleris et al., 2001). Along with the elevated plus maze (another measure of anxiety behavior in rodents) the open field assay was used as a way to study and develop anxiolytic drugs like diazepam (Choleris et al., 2001; Menard and Treit, 1999; Schmitt and Hiemke, 1998; Tye et al., 2011). OFT has become one of the most widely used tests in preclinical studies using rodent models (Schnörr et al., 2012).

OFT has more recently been used to measure fear behavior in zebrafish. First used as a method to observe anxiety in adult fish caused by placement in a new environment (Stewart et al., 2010, 2012), the assay was quickly adapted to observe anxiety in fish larvae. The use of anxiolytic (anxiety reducing) and anxiogenic (anxiety increasing) drugs has become a powerful tool in behavioral anxiety research. Using larval zebrafish's innate avoidance of dark spaces, OFT was used to test the effects of anxiolytic drugs (diazepam) and anxiogenic drugs (caffeine) on larval anxiety behavior. By measuring the average distance larvae travel on the edges of the wells of 24-well plates, investigators were able to observe that anxiolytics significantly attenuate thigmotaxsis while anxiogenics enhance it (Schnörr et al., 2012).

Recently, experimenters have used the OFT in zebrafish larvae as a way to probe for new drugs that target altered signaling pathways associated with anxiety disorders. Signaling molecules, such as the second messenger cyclic AMP (cAMP), are important for the control of learning, memory, and mood (Maurice et al., 2014). Intracellular levels of cAMP are controlled by phosphodiesterases (PDEs). In particular, *PDE4* genes play a significant role in controlling cAMP levels in the CNS, and polymorphisms in human *PDE4B* are associated with schizophrenia and psychosis (Maurice et al., 2014; Millar et al., 2005, 2007; Xu et al., 2011).

Using OFT in zebrafish larvae, Lundegaard et al. were able to show that blocking PDE function with PDE inhibitors causes an increase in thigmotaxsis in large groups of fish larvae. They then used this model to successfully screen for new suppressors of zebrafish anxiety behaviors (Lundegaard et al., 2015). These experiments not only show the ease of using the OFT with fish larvae, they highlight how well zebrafish larvae can be used as a model for drug discovery in humans.

1.4 Fear Circuitry in the Amygdala

One of the most highly conserved areas of the brain across species, and one that is heavily responsible for fear and anxiety processing, is the amygdala. A complete understanding of the alarm behavior and innate circuitry in fish would be incomplete without an in-depth look at amygdalar structures in fish and what the corresponding anatomy reveals in other animals, including humans, rodents, and reptiles. For decades, the amygdala has been studied in rodents, but research into the amygdala has uncovered a remarkable conservation across species with zebrafish being a recent addition (Janak and Tye, 2015; Perathoner et al., 2016). This conservation between species gives an added importance to amygdala and fear/anxiety research in zebrafish.

The amygdala was first described in the early 19th century as, “an almond-shaped mass of gray matter in the anterior portion of the human temporal lobe” (Burdach, 1819; Perathoner et al., 2016). Since its first anatomical discovery, the amygdala has been implicated in a variety of emotional states in primates and rodents. Lesion studies in non-human primates showed that bilateral ablation of the temporal lobe impaired the animal’s ability to understand the meaning of the sounds, sights, and “other impressions” that may reach him, but did not lower the ability of the animal to hear, see, and sense the world generally (Brown and Schafer, 1888). Other lesioning studies showed a decrease in aggression, fear, and defensive behaviors as well as “an impairment in acquiring behavioral responses to shock-predictive cues” after bilateral amygdalar ablation in Rhesus monkeys (Klüver and Bucy, 1937; Weiskrantz and Lawrence, 1956). Further lesioning experiments in rodents and humans have revealed a strong conservation between amygdalar structure and function across species, especially when it comes to the impairment and recognition of fear conditioning (Adolphs et al., 1994; Anderson and Phelps, 2001; Blanchard and Blanchard, 1972; LeDoux et al., 1990). These studies allowed investigators a way to observe the neural circuitry of innate and conditioned fear circuits.

The amygdala, or amygdaloid complex, is considered one of the most heterogeneous structures in the brain. It is made up of numerous nuclei that originate from differentiated parts of the cortex, claustrum, and striatum. They include 1) the basolateral complex (BLA), which is subdivided into the lateral (LA), basal (BA), and basomedial (BM) nuclei; 2) the extended amygdala, which includes the central (CeA), medial (MeA) and cortical (CoA) nuclei as well as the bed nucleus of the stria terminalis (BNST); and 3) the intercalated cell masses (Duvarci and Pare, 2014; Janak and Tye, 2015; Sah et al., 2003). Each of these areas represents unique cell types and functionality.

Basolateral (Pallial) Amygdala

The BLA was the original complex discovered in the amygdala. It represents the interface between sensory input and emotional memory/output for many sensory systems (Fernando et al., 2013; Hermans et al., 2014). Information from the various sensory cortices and sensory thalamus send strong connections to the LA, which then projects strongly to the BA, BM, and CeA. The BLA also makes strong connections to several cortices, especially the midline and orbital prefrontal cortices (PFC), hippocampus (HPC), and sensory association areas (Freese and Amaral, 2005; McDonald, 1998). The strong reciprocal connections between the BLA and sensory cortices, especially the excitatory projections, may explain the relative enlargement of the BLA compared to the CeA between rodents and higher organisms such as the cat and primates (Chareyron et al., 2011).

After extensive intra-amygdala processing, the translation of BLA signals to behavioral output is primarily done through the striatum, BNST, hypothalamus, and CeA (Buffalari and See, 2010; Duvarci and Pare, 2014; Janak and Tye, 2015). As a whole, The BLA is comprised of ~80% glutamatergic neurons (~20% GABAergic neurons). Most neurons in the other subdivisions (central, medial nuclei, and the intercalated cell masses) are GABAergic (Duvarci and Pare, 2014).

Medial and Cortical (Extended) Amygdala

Sensory signals from the vomeronasal and main olfactory systems project to the MeA and CoA respectively. The MeA receives inputs almost exclusively from the AOB (Swanson and Petrovich, 1998). Output neurons from the MeA project to hypothalimc nuclei involved in a variety of social, defensive, and innate fear responses, and when these projections are disrupted severe deficits in social and predator recognition are observed (Choi et al., 2005; Ferguson et al., 2001; Li et al., 2004; Lin et al., 2011; Petrovich et al., 2001). One common characteristic of higher processing centers in the brain is the presence of sparse coding, which is a reflection of increasingly complex sensory representations (Olshausen and Field, 1996; Poo and Isaacson, 2011). The MeA is no exception. Activity in the MeA is about threefold less than the AOB to any given olfactory stimulus. MeA neurons respond to vomeronasal stimuli with significantly more specificity for behaviorally distinct classes of stimuli than AOB neurons. Stimuli include conspecific male and female urine and predator urine (Bergan et al., 2014). Additionally, selectivity in MeA neurons toward sexual dimorphic stimuli only occurs in adult animals. This suggests that innate sexually dimorphic circuits toward sex cues within the MeA do not develop until adulthood (Bergan et al., 2014).

The majority of neurons from the MOB project primarily to the piriform cortex (PCx), but a significant number of projections target the posterolateral cortical amygdala (plCoA). Unlike the PCx, the plCoA plays a critical role in the generation of innate odor-driven behaviors, receiving hardwired inputs from the olfactory bulb (Root et al., 2014; Sosulski et al., 2011). Similar to the PCx however, is how the plCoA organizes sensory information for aversive and appetitive odor driven behaviors. Recent experiments have shown that neurons in the plCoA and PCx display similar odor tuning properties, information about odor identity, chemical class and odor valence. Neural ensembles within these two areas show a similar capacity to encode odor identity information and concentration. Most surprisingly, there is no apparent spatial order to the tuning properties within the PCx or the plCoA (Iurilli and Datta, 2017). Some novel mechanisms may

explain how innate behaviors are encoded in the plCoA. Either 1) there is a hardwired decoder that is specified during development, 2) there are rare labeled lines that are broadly dispersed to identify odor identity, or 3) there are input neurons from the PCx that add additional information after learning has occurred to encode the valence of a particular odor (Iurilli and Datta, 2017). In any of these cases, it is clear that odor-driven innate behaviors can be supported by a highly distributed neural code.

1.5 Zebrafish Amygdala Anatomy

Numerous studies have shown that the functional and circuit level components of the amygdala are conserved across species (Folgueira et al., 2012; Maximino et al., 2013; O'Connell and Hofmann, 2011; von Trotha et al., 2014). However, even though teleost fish have become a popular model for neurobiology, neuropharmacology, and behavioral research, anatomical differences between the telencephalon of teleost fish and terrestrial vertebrates have created challenges when pursuing translational studies. Many lines of evidence lead to an amygdala like area in the medial zone of teleost fish, but because of the many nuclei and developmental tissues that make up the amygdala (in all animals) it is challenging to make concrete connections between homologous amygdalar structures. For instance, one common method of identifying the medial amygdala in birds is to identify afferent projections from the VNO (O'Connell and Hofmann, 2011). Because fish do not have a VNO, and because of the divergent way the teleost brain develops (Døving and Trotier, 1998; Nieuwenhuys, 2009, 2011), identifying amygdala homologues has been accomplished through a comprehensive comparative analysis of the topology, molecular marker, and even behavioral analysis between the teleost and mammalian brain.

Zebrafish Forebrain Development

In all vertebrates, the early developing brain can be subdivided into three portions: Rhombencephalon (hindbrain), Mesencephalon (midbrain), and Prosencephalon (forebrain). As the animal develops, the proencephalon divides into the telencephalon and diencephalon. In mammals these forebrain structures further develop into the cerebral cortex, white matter, and basal ganglia (telencephalon) and the thalamus, hypothalamus, subthalamus, epithalamus, and pretectum (diencephalon) (Kandel et al., 2014). A closer inspection at the telencephalon reveals a further subdivision into dorsal and ventral sections, often referred to as the pallium and subpallium respectively (Wullimann and Mueller, 2004). The mammalian amygdala is located along the junction of this division. The basolateral nuclei reside in the pallium (pallial amygdala), while the CeA, MeA, and CoA are located in the subpallium (extended amygdala) (LeDoux, 2007).

Zebrafish Amygdala Subdivisions

Interestingly, the telencephalon of ray-finned fishes (actinopterygian lineage) does not develop in the same way as mammals (summarized in figure 1.4). The ventral telencephalon (subpallium) closely resembles the mammalian subpallium, where the septal nuclei and the striatum have been homologized to the ventral telencephalon structures in fish (Braford, 2009). The dorsal telencephalon (pallium) diverges significantly from mammalian anatomy however. In tetrapods,

the pallium forms through an evagination of the neural tube (inward folding movement), but in the actinopterygian lineage of fish, the dorsal telencephalon forms through an eversion of the neural tube (outward folding movement) (Nieuwenhuys, 2009). To make things more complicated, this eversion is incomplete because there is a radial migration event of cell masses across the pallium (Fig 1.4A) (Mueller et al., 2011).

A more complete understanding of the location of homologous structures is provided by comparative gene expression during telencephalon development. Subpallial markers for the developing medial amygdala in tetrapods include *Dlx2, Nkx2.1, Dlx1, GAD67, Lhx6,* and *Lhx7* (Moreno et al., 2009; Puelles et al., 2000). Teleost fish express *dlx2b* and *nk2.1b* in the dorsal section of the ventral telencephalon (Vd), with *dlx2b* expression extending to the dorsal subpallum, immediately adjacent to Vd (Ganz et al., 2012; Mueller et al., 2008; Rohr et al., 2001). *dlx2b* is therefore a favorable marker for the medial amygdala in teleosts. More recently, the transcription factor Orthopedia (Otp) has been suggested as a medial amygdala marker in zebrafish and goldfish due to direct projections from medial OB OSNs to Otp expressing cells in the intermediate nucleus of the ventral telencephalon (Biechl et al., 2017; Levine and Dethier, 1985). *lhx7* expression in Vd of medaka fish and *lhx6* and *lhx7* RNA transcripts in the ventral section of the ventral telencephalon (Vv) of zebrafish make these good markers of the CeA and BNST.

Markers for the pallial amygdala in tetrapods include *tbr1*, *lhx9*, and *emx1* (Puelles et al., 2000; Rétaux et al., 1999). Here, expression in teleost fish is mixed. *lhx9* is expressed in the dorsal telencephalon of medaka and Mexican tetra, *Astyanax mexicanus* (Alunni et al., 2004; Menuet et al., 2007). *emx1,2,& 3* and *tbr1* are all expressed in the medial section of the dorsal telencephalon (Dm) of cyprinid fish, which includes zebrafish (Ganz et al., 2014; Mione et al., 2001; Morita et al., 1995). Additionally, markers of the basolateral amygdala in rat – the cannabinoid receptor gene (cb1) – is expressed within the dorsal telencephalon (Dm) of teleost fish (Harvey-Girard et al., 2013; Lam et al., 2006; Mailleux and Vanderhaeghen, 1992).

The ultimate test of amygdala identity is pairing structure with function. Conditioning studies have revealed that lesions in the Dm lead to a reduction of conditioned avoidance and conditioned taste aversion in goldfish (Martín et al., 2011; Portavella et al., 2004). Both are charactersitics of BLA lesions in rats (Pape and Pare, 2010; Yamamoto et al., 1995). Further evidence to support the Dm and Vv as locations for the zebrafish pallial and extended amygdala, come from activation studies in zebrafish. During light avoidance, an innate behavior in larval zebrafish, neurons in the Dm are activated and identified by c-fos early neuron marker expression (Lau et al., 2011). Calcium imaging studies have shown activity within the Dm during aversive reinforcement learning in zebrafish (Aoki et al., 2013). Taken together, these experiments support the idea that the Dm in fish corresponds to the basolateral complex (pallial amygdala) and the Vd and Vv correspond to the extended amygdala (Fig 1.4B).

Despite the abundance of molecular support, there is still little concrete evidence that the pallial or extended amygdala in zebrafish play a role in fear behavior. Since there is no VNO in zebrafish it is difficult to confirm the identity of OSNs that signal innate behaviors in zebrafish. In this dissertation, I will present evidence of a newly discovered groups of OSNs in the OE that project directly to the zebrafish amygdala. I will also attempt to characterize the role these OSNs

play in larval fear behavior using a novel open field test. Furthermore, I will uncover new expression data for the ora6 receptor, a V1r-like receptor that may also function as pheromone receptor in zebrafish.

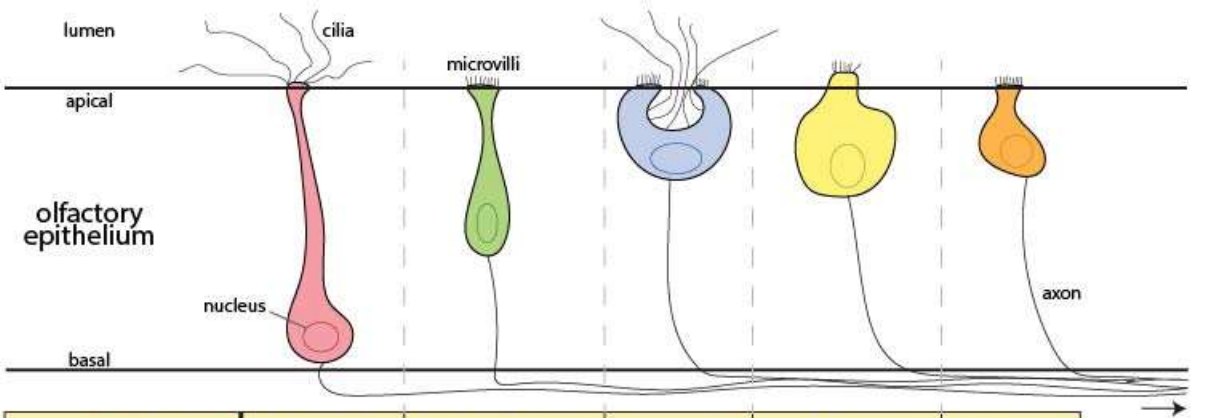

OSN type	ciliated	microvillous	crypt	kappe	pear
receptors	OR & TAAR	V2R	V1R (ora4)	?	A2c
G-protein	$G\alpha_{olf}$	?	$G\alpha_{i}$	$G\alpha_{o}$	$G\alpha_{olf}$
channel	CNGA2	TrpC2	?	?	?
other genes	OMP	-	S100, TrkA	-	OMP, ACIII
known ligands	amines, bile acids, $PGF_{2\alpha}$	amino acids	?	?	adenosine
major OB targets:					
larvae	dG, avG	IG	mG	?	?
adult	maG, vaG vmG, dG dlG, mpG	IG	mdG2	mdG5	IG2

Figure 1.1 Olfactory sensory neurons of the zebrafish olfactory system.
Comparison of morphology, receptors, ligands and other characteristics of all known olfactory sensory neurons in the zebrafish. (**Top**) illustration of cell shape, placement in the OE, and the presence of cilia or microvilli in fish OSNs. (**Bottom**) table comparing known genes, ligands, and projection targets between different OSN types.

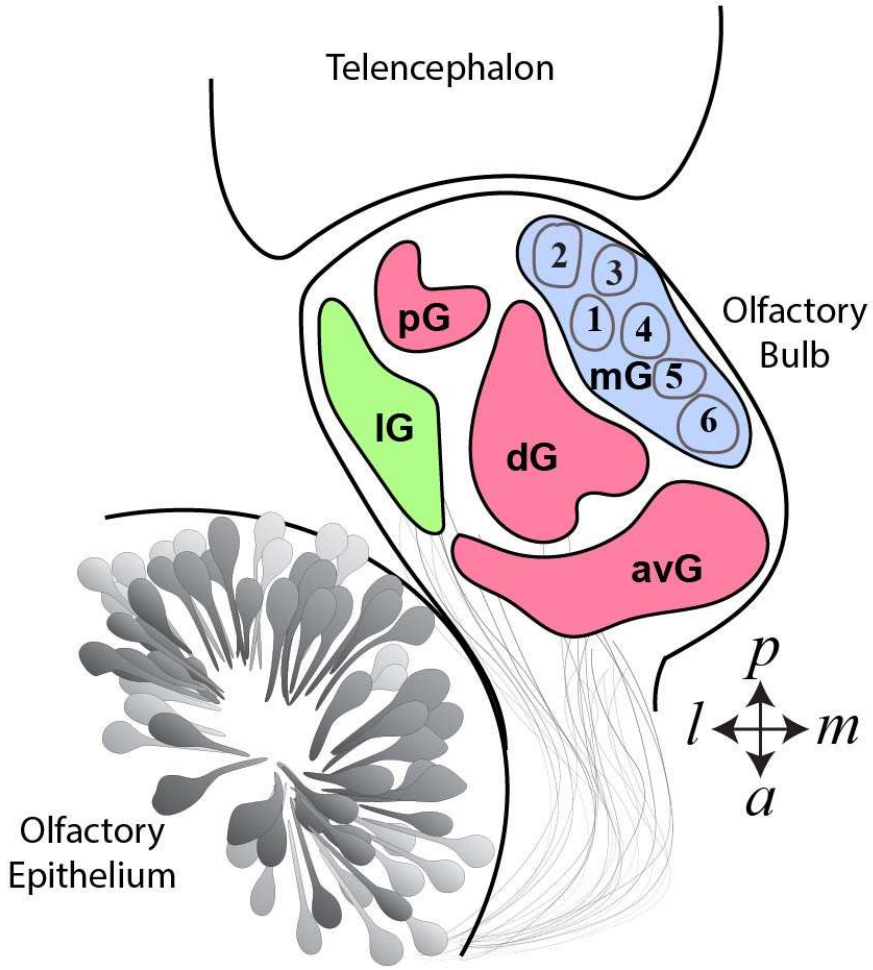

Figure 1.2 Olfactory bulb organization in the larval zebrafish.
Location and morphology of the 5 protoglomerular clusters in the larval zebrafish olfactory bulb. Cilliated cells project to pG, dG, and avG (red areas). Microvillous cells project to lG (green area). Crypt cells project to mG (blue area). lG, lateral; pG, posterior; dG, dorsal; avG, anteroventral; mG, medial glomeruli; *l*, lateral; *m*, medial; *a*, anterior; *p*, posterior.

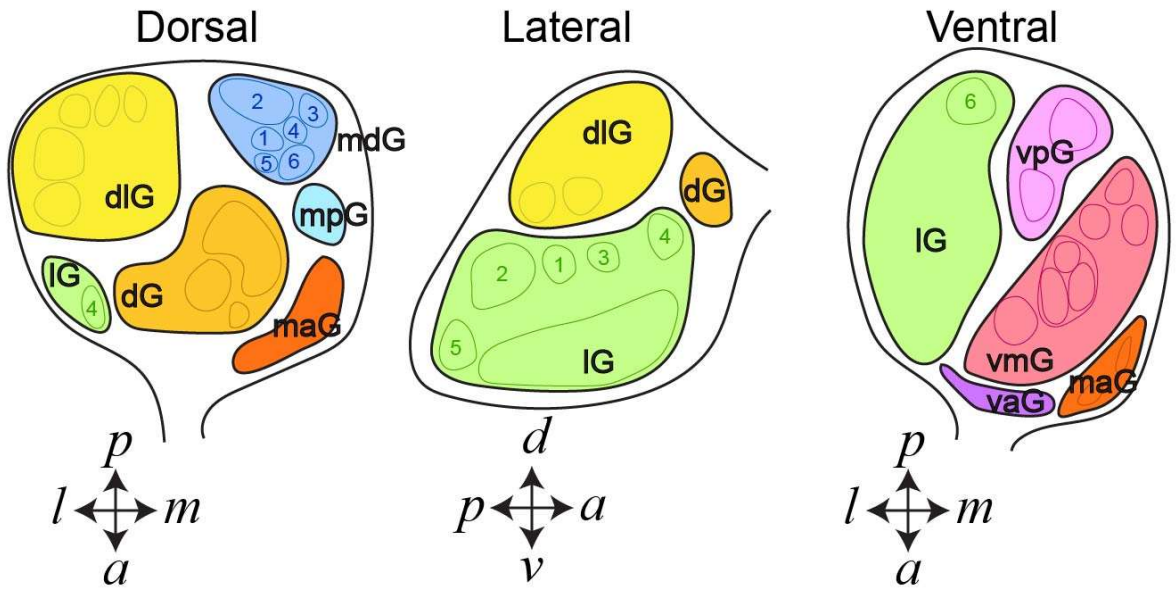

Figure 1.3 Olfactory bulb organization in the adult zebrafish.
Location and morphology of 9 glomerular clusters in the adult zebrafish olfactory bulb, viewed from three different vantage points; dorsal, lateral and ventral. dG, dorsal; dlG, dorso-lateral; lG, lateral; maG, medio-anterior; mpG, medio-posterior; mdG, medio-dorsal; vaG, ventro-anterior; vmG, ventro-medial; vpG, ventro-posterior glomeruli; *l*, lateral; *m*, medial; *a*, anterior; *p*, posterior; *d*, dorsal; *v*, ventral. Adapted from Yoshihara, 2014.

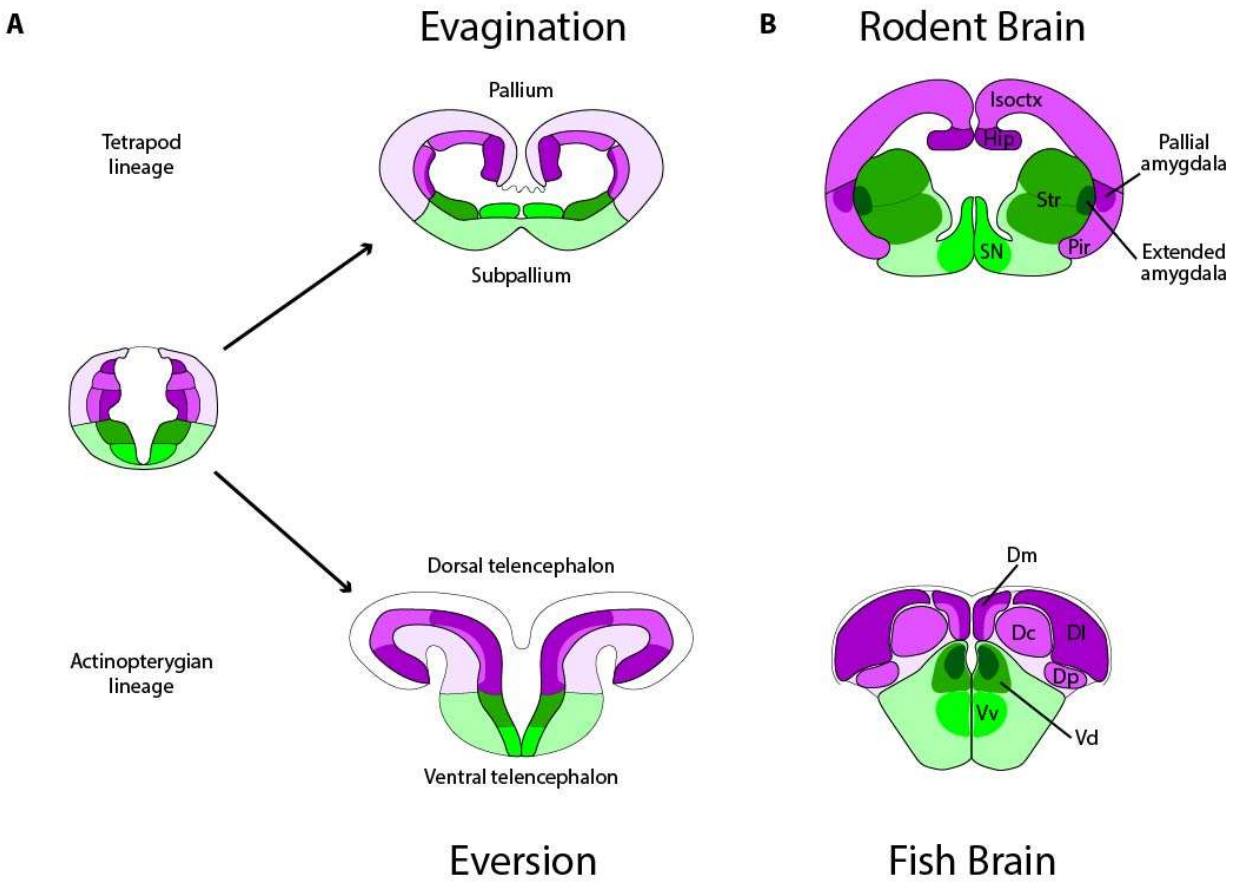

Figure 1.4 Development of the telencephalon in tetrapod vs. actinopterygian lineage. Comparison of tetrapod and actinopterygian telencephalon anatomy during development (**A**) and adult (**B**). Coronal sections. (**A**) During development, the neural tube in the tetrapod lineage (**top**) undergoes an evagination event while the neural tube in the actinopterygian lineage (**bottom**) undergoes an eversion (outward folding) event. (**B**) In the rodent brain, the pallial amygdala develops from the ventral pallium (dark purple), and the extended amygdala develops from the striatal subpallium (dark green). The corresponding area for the pallial amygdala in the fish brain develops into the medial and lateral zones of the dorsal telencephalon (Dm, Dl). The extended amygdala develops into the dorsal zone of the ventral telencephalon (Vd). Purple, dorsal (pallial) telencephalon; Green, ventral (subpallial) telencephalon; Isoctx, isocortex; Hip, hippocampus; Str, striatum; SN, septal nuclei; Pir, piriform cortex; Dm, medial; Dc, central; Dl, lateral; Dp, posterior zones of the dorsal telencephalon; Vd, dorsal; Vv, ventral zones of the ventral telencephalon. Adapted from Perathoner et al., 2016.

References:

Abe, T., and Touhara, K. (2014). Structure and function of a peptide pheromone family that stimulate the vomeronasal sensory system in mice. Biochem. Soc. Trans. *42*.

Adolphs, R., Tranel, D., Damasio, H., and Damasio, A. (1994). Impaired recognition of emotion in facial expressions following bilateral damage to the human amygdala. Nature *372*, 669–672.

Agetsuma, M., Aizawa, H., Aoki, T., Nakayama, R., Takahoko, M., Goto, M., Sassa, T., Amo, R., Shiraki, T., Kawakami, K., et al. (2010). The habenula is crucial for experience-dependent modification of fear responses in zebrafish. Nat. Neurosci. *13*, 1354–1356.

Ahrens, M., Li, J., Orger, M., Robson, D., Schier, A.F., Engert, F., and Portugues, R. (2012). Brain-wide neuronal dynamics during motor adaptation in zebrafish. Nature.

Ahrens, M., Orger, M., Robson, D., Li, J., and Keller, P. (2013). Whole-brain functional imaging at cellular resolution using light-sheet microscopy. Nat. Methods.

Ahuja, G., Ivandic, I., Saltürk, M., Oka, Y., Nadler, W., and Korsching, S.I. (2013). Zebrafish crypt neurons project to a single, identified mediodorsal glomerulus. Sci. Rep. *3*, 2063.

Ahuja, G., Nia, S.B., Zapilko, V., Shiriagin, V., Kowatschew, D., Oka, Y., and Korsching, S.I. (2014). Kappe neurons, a novel population of olfactory sensory neurons. Sci. Rep. *4*, 4037.

Alioto, T., and Ngai, J. (2005). The odorant receptor repertoire of teleost fish. BMC Genomics *6*, 173.

Alioto, T., and Ngai, J. (2006). The repertoire of olfactory C family G protein-coupled receptors in zebrafish: candidate chemosensory receptors for amino acids. BMC Genomics *7*, 309.

Alunni, A., Blin, M., Deschet, K., Bourrat, F., Vernier, P., and Rétaux, S. (2004). Cloning and developmental expression patterns of Dlx2, Lhx7 and Lhx9 in the medaka fish (Oryzias latipes). Mech. Dev. *121*, 977–983.

Amo, R., Aizawa, H., Takahoko, M., Kobayashi, M., Takahashi, R., Aoki, T., and Okamoto, H. (2010). Identification of the zebrafish ventral habenula as a homolog of the mammalian lateral habenula. J. Neurosci. *30*, 1566–1574.

Anadón, R., Manso, M.J., Rodríguez-Moldes, I., and Becerra, M. (1995). Neurons of the olfactory organ projecting to the caudal telencephalon and hypothalamus: a carbocyanine-dye labelling study in the brown trout (Teleostei). Neurosci. Lett. *191*, 157–160.

Anderson, A.K., and Phelps, E.A. (2001). Lesions of the human amygdala impair enhanced perception of emotionally salient events. Nature *411*, 305–309.

Aoki, T., Kinoshita, M., Aoki, R., Agetsuma, M., Aizawa, H., Yamazaki, M., Takahoko, M., Amo, R., Arata, A., Higashijima, S.-I., et al. (2013). Imaging of Neural Ensemble for the Retrieval of a Learned Behavioral Program. Neuron 1–14.

Baier, H., and Korsching, S. (1994). Olfactory glomeruli in the zebrafish form an invariant pattern and are identifiable across animals. J. Neurosci. *14*, 219–230.

Bargmann, C.I., Hartwieg, E., and Horvitz, H.R. (1993). Odorant-selective genes and neurons mediate olfaction in C. elegans. Cell *74*, 515–527.

Barth, A.L., Justice, N.J., and Ngai, J. (1996). Asynchronous Onset of Odorant Receptor Expression in the Developing Zebrafish Olfactory System. Neuron *16*, 23–34.

Barth, A.L., Dugas, J.C., and Ngai, J. (1997). Noncoordinate Expression of Odorant Receptor Genes Tightly Linked in the Zebrafish Genome. Neuron *19*, 359–369.

Bazáes, A., and Schmachtenberg, O. (2012). Odorant tuning of olfactory crypt cells from juvenile and adult rainbow trout. J. Exp. Biol. *215*, 1740–1748.

Becerra, M., Manso, M.J., Rodriguez-Moldes, I., and Anadón, R. (1994). Primary olfactory fibres project to the ventral telencephalon and preoptic region in trout (Salmo trutta): a developmental immunocytochemical study. J. Comp. Neurol. *342*, 131–143.

Behrens, M., Frank, O., Rawel, H., Ahuja, G., Potting, C., Hofmann, T., Meyerhof, W., and Korsching, S. (2014). ORA1, a zebrafish olfactory receptor ancestral to all mammalian V1R genes, recognizes 4-hydroxyphenylacetic acid, a putative reproductive pheromone. J. Biol. Chem. *289*, 19778–19788.

Bergan, J.F., Ben-Shaul, Y., and Dulac, C. (2014). Sex-specific processing of social cues in the medial amygdala. Elife *3*, e02743.

Bettini, S., Lazzari, M., and Franceschini, V. (2012). Quantitative analysis of crypt cell population during postnatal development of the olfactory organ of the guppy, Poecilia reticulata (Teleostei, Poecilidae), from birth to sexual maturity. J. Exp. Biol. *215*, 2711–2715.

Bhandiwad, A.A., Zeddies, D.G., Raible, D.W., Rubel, E.W., and Sisneros, J.A. (2013). Auditory sensitivity of larval zebrafish (Danio rerio) measured using a behavioral prepulse inhibition assay. J. Exp. Biol. *216*, 3504–3513.

Bianco, I.H., and Engert, F. (2015). Visuomotor Transformations Underlying Hunting Behavior in Zebrafish. Curr. Biol. *25*, 831–846.

Bianco, I.H., Ma, L.-H., Schoppik, D., Robson, D.N., Orger, M.B., Beck, J.C., Li, J.M., Schier, A.F., Engert, F., and Baker, R. (2012). The Tangential Nucleus Controls a Gravito-inertial Vestibulo-ocular Reflex. Curr. Biol. *22*, 1285–1295.

Biechl, D., Tietje, K., Ryu, S., Grothe, B., Gerlach, G., and Wullimann, M.F. (2017). Identification of accessory olfactory system and medial amygdala in the zebrafish. Sci. Rep. *7*, 44295.

Blanchard, D.C., and Blanchard, R.J. (1972). Innate and conditioned reactions to threat in rats with amygdaloid lesions. J. Comp. Physiol. Psychol. *81*, 281–290.

Braford, M.R. (2009). Stalking the everted telencephalon: comparisons of forebrain organization in basal ray-finned fishes and teleosts. Brain. Behav. Evol. *74*, 56–76.

Braubach, O., Fine, A., and Croll, R. (2012). Distribution and functional organization of glomeruli in the olfactory bulbs of zebrafish (Danio rerio). J. Comp. Neurol. *520*, 2317–39, Spc1.

Braubach, O.R., Wood, H.-D., Gadbois, S., Fine, A., and Croll, R.P. (2009). Olfactory conditioning in the zebrafish (Danio rerio). Behav. Brain Res. *198*, 190–198.

Brown, S., and Schafer, E.A. (1888). An Investigation into the Functions of the Occipital and Temporal Lobes of the Monkey's Brain on JSTOR. Philos. Trans. R. Soc. London. B *179*, 303–327.

Brunet, L., Gold, G., and Ngai, J. (1996). General anosmia caused by a targeted disruption of the mouse olfactory cyclic nucleotide-gated cation channel. Neuron *17*, 681–693.

Buck, L., and Axel, R. (1991). A novel multigene family may encode odorant receptors: a molecular basis for odor recognition. Cell *65*, 175–187.

Buffalari, D.M., and See, R.E. (2010). Amygdala Mechanisms of Pavlovian Psychostimulant Conditioning and Relapse. (Springer Berlin Heidelberg), pp. 73–99.

Burdach, K. (1819). Vom Baue und Leben des Gehirns. Leipzig. Dyk.

Candland, D.K., and Nagy, Z.M. (1969). THE OPEN FIELD: SOME COMPARATIVE DATA. Ann. N. Y. Acad. Sci. *159*, 831–851.

Caron, S.J.C., Ruta, V., Abbott, L.F., and Axel, R. (2013). Random convergence of olfactory inputs in the Drosophila mushroom body. Nature *497*, 113–117.

Catania, S., Germanà, A., Laurà, R., Gonzalez-Martinez, T., Ciriaco, E., and Vega, J.A. (2003). The crypt neurons in the olfactory epithelium of the adult zebrafish express TrkA-like immunoreactivity.

Chareyron, L.J., Banta Lavenex, P., Amaral, D.G., and Lavenex, P. (2011). Stereological analysis of the rat and monkey amygdala. J. Comp. Neurol. *519*, 3218–3239.

Choi, G., Stettler, D., Kallman, B., Bhaskar, S., Fleischmann, A., and Axel, R. (2011). Driving Opposing Behaviors with Ensembles of Piriform Neurons. Cell *146*, 1004–1015.

Choi, G.B., Dong, H.-W., Murphy, A.J., Valenzuela, D.M., Yancopoulos, G.D., Swanson, L.W., and Anderson, D.J. (2005). Lhx6 delineates a pathway mediating innate reproductive behaviors from the amygdala to the hypothalamus. Neuron *46*, 647–660.

Choleris, E., Thomas, A.., Kavaliers, M., and Prato, F.. (2001). A detailed ethological analysis of the mouse open field test: effects of diazepam, chlordiazepoxide and an extremely low frequency pulsed magnetic field. Neurosci. Biobehav. Rev. *25*, 235–260.

Dalton, R.P., and Lomvardas, S. (2015). Chemosensory Receptor Specificity and Regulation. Annu. Rev. Neurosci. *38*, 331–349.

DeMaria, S., Berke, A., Name, E., Heravian, A., Ferreira, T., Ngai, J., California, B., DeMaria, S., Berke, A., Name, E., et al. (2013). Role of a Ubiquitously Expressed Receptor in the Vertebrate Olfactory System. J. Neurosci. *33*, 15235–15247.

Derjean, D., Moussaddy, A., Atallah, E., St-Pierre, M., Auclair, F., Chang, S., Ren, X., Zielinski, B., and Dubuc, R. (2010). A novel neural substrate for the transformation of olfactory inputs into motor output. PLoS Biol. *8*, e1000567.

Dewan, A., Pacifico, R., Zhan, R., Rinberg, D., and Bozza, T. (2013). Non-redundant coding of aversive odours in the main olfactory pathway. Nature 1–5.

Dittman, and Quinn (1996). Homing in Pacific salmon: mechanisms and ecological basis. J. Exp. Biol. *199*, 83–91.

Døving, K.B., and Trotier, D. (1998). Structure and function of the vomeronasal organ. J. Exp. Biol. *201*, 2913–2925.

Dulac, C., and Axel, R. (1995). A novel family of genes encoding putative pheromone receptors in mammals. Cell *83*, 195–206.

Dulac, C., and Wagner, S. (2006). Genetic Analysis of Brain Circuits Underlying Pheromone Signaling. Annu. Rev. Genet. *40*, 449–467.

Duvarci, S., and Pare, D. (2014). Amygdala Microcircuits Controlling Learned Fear. Neuron *82*, 966–980.

Dynes, J., and Ngai, J. (1998). Pathfinding of olfactory neuron axons to stereotyped glomerular targets revealed by dynamic imaging in living zebrafish embryos. Neuron *20*, 1081–1091.

Eaton, R.C., Bombardieri, R.A., and Meyer, D.L. (1977). The Mauthner-initiated startle response in teleost fish. J. Exp. Biol. *66*, 65–81.

Engeszer, R.E., Patterson, L.B., Rao, A.A., and Parichy, D.M. (2007). Zebrafish in The Wild: A Review of Natural History And New Notes from The Field. Zebrafish *4*, 21–40.

Ferguson, J.N., Aldag, J.M., Insel, T.R., and Young, L.J. (2001). Oxytocin in the medial amygdala is essential for social recognition in the mouse. J. Neurosci. *21*, 8278–8285.

Fernando, A.B.P., Murray, J.E., and Milton, A.L. (2013). The amygdala: securing pleasure and avoiding pain. Front. Behav. Neurosci. *7*, 190.

Ferrero, D.M., Lemon, J.K., Fluegge, D., Pashkovski, S.L., Korzan, W.J., Datta, S.R., Spehr, M., Fendt, M., and Liberles, S.D. (2011). Detection and avoidance of a carnivore odor by prey. Proc. Natl. Acad. Sci. U. S. A. *108*, 11235–11240.

Fetcho, J.R., and Faber, D.S. (1988). Identification of motoneurons and interneurons in the spinal network for escapes initiated by the mauthner cell in goldfish. J. Neurosci. *8*, 4192–4213.

Folgueira, M., Bayley, P., Navratilova, P., Becker, T., Wilson, S.W., and Clarke, J. (2012). Morphogenesis underlying the development of the everted teleost telencephalon. Neural Dev. *7*, 32.

Freese, J.L., and Amaral, D.G. (2005). The organization of projections from the amygdala to visual cortical areas TE and V1 in the macaque monkey. J. Comp. Neurol. *486*, 295–317.

Freitag, J., Krieger, J., Strotmann, J., and Breer, H. (1995). Two classes of olfactory receptors in xenopus laevis. Neuron *15*, 1383–1392.

Friedrich, R., and Korsching, S.I. (1997). Combinatorial and Chemotopic Odorant Coding in the Zebrafish Olfactory Bulb Visualized by Optical Imaging. Neuron *18*, 737–752.

Friedrich, R.W., and Korsching, S.I. (1998). Chemotopic, Combinatorial, and Noncombinatorial Odorant Representations in the Olfactory Bulb Revealed Using a Voltage-Sensitive Axon Tracer. *18*, 9977–9988.

von Frisch, K. (1938). Zur Psychologie des Fisch-Schwarmes. Naturwissenschaften *26*, 601–606.

Fuss, S.H., and Korsching, S.I. (2001). Odorant Feature Detection: Activity Mapping of Structure Response Relationships in the Zebrafish Olfactory Bulb. J. Neurosci. *21*.

Ganz, J., Kaslin, J., Freudenreich, D., Machate, A., Geffarth, M., and Brand, M. (2012). Subdivisions of the adult zebrafish subpallium by molecular marker analysis. J. Comp. Neurol. *520*, 633–655.

Ganz, J., Kroehne, V., Freudenreich, D., Machate, A., Geffarth, M., Braasch, I., Kaslin, J., and Brand, M. (2014). Subdivisions of the adult zebrafish pallium based on molecular marker analysis. F1000Research *3*, 308.

Gayoso, J., Castro, A., Anadón, R., and Manso, M.J. (2012). Crypt cells of the zebrafish Danio rerio mainly project to the dorsomedial glomerular field of the olfactory bulb. Chem. Senses *37*, 357–369.

Gayoso, J.Á., Castro, A., Anadón, R., and Manso, M.J. (2011). Differential bulbar and extrabulbar projections of diverse olfactory receptor neuron populations in the adult zebrafish (Danio rerio). J. Comp. Neurol. *519*, 247–276.

Germanà, A., Montalbano, G., Laurà, R., Ciriaco, E., Valle, M., and Vega, J. (2004). S100 protein-like immunoreactivity in the crypt olfactory neurons of the adult zebrafish. Neurosci. Lett. *371*, 196–198.

Germanà, A., Paruta, S., Germanà, G., Ochoa-Erena, F., Montalbano, G., Cobo, J., and Vega, J. (2007). Differential distribution of S100 protein and calretinin in mechanosensory and chemosensory cells of adult zebrafish (Danio rerio). Brain Res. *1162*, 48–55.

Ghosh, S., Larson, S.D., Hefzi, H., Marnoy, Z., Cutforth, T., Dokka, K., and Baldwin, K.K. (2011). Sensory maps in the olfactory cortex defined by long-range viral tracing of single neurons. Nature *472*, 217–220.

Gloriam, D.E.I., Bjarnadóttir, T.K., Yan, Y.-L., Postlethwait, J.H., Schiöth, H.B., and Fredriksson, R. (2005). The repertoire of trace amine G-protein-coupled receptors: large expansion in zebrafish. Mol. Phylogenet. Evol. *35*, 470–482.

Goldman, A.L., Van der Goes van Naters, W., Lessing, D., Warr, C.G., and Carlson, J.R. (2005). Coexpression of Two Functional Odor Receptors in One Neuron. Neuron *45*, 661–666.

Graziadei, G.A., Stanley, R.S., and Graziadei, P.P. (1980). The olfactory marker protein in the olfactory system of the mouse during development. Neuroscience *5*, 1239–1252.

Greer, P.L., Bear, D.M., Lassance, J.-M., Kirchner, R., Hoekstra, H.E., Datta Correspondence, S.R., Bloom, M.L., Tsukahara, T., Pashkovski, S.L., Masuda, F.K., et al. (2016). A Family of non-GPCR Chemosensors Defines an Alternative Logic for Mammalian Olfaction. Cell *165*, 1734–1748.

Grunwald, D.J., and Eisen, J.S. (2002). Headwaters of the zebrafish — emergence of a new model vertebrate. Nat. Rev. Genet. *3*, 717–724.

Hall, C.S., and S., C. (1934). Emotional behavior in the rat. I. Defecation and urination as measures of individual differences in emotionality. J. Comp. Psychol. *18*, 385–403.

Hamdani, E.H., and Døving, K.B. (2006). Specific projection of the sensory crypt cells in the olfactory system in crucian carp, Carassius carassius. Chem. Senses *31*, 63–67.

Hamdani, E.H., Lastein, S., Gregersen, F., and Døving, K.B. (2008). Seasonal variations in olfactory sensory neurons--fish sensitivity to sex pheromones explained? Chem. Senses *33*, 119–123.

Hansen, A., and Zeiske, E. (1993). Development of the olfactory organ in the zebrafish,Brachydanio rerio. J. Comp. Neurol. *333*, 289–300.

Hansen, A., and Zeiske, E. (1998). The peripheral olfactory organ of the zebrafish, Danio rerio: an ultrastructural study. Chem. Senses *23*, 39–48.

Hansen, A., Rolen, S.H., Anderson, K., Morita, Y., Caprio, J., and Finger, T.E. (2003). Correlation between olfactory receptor cell type and function in the channel catfish. J. Neurosci. *23*, 9328–9339.

Harden, M. V, Newton, L.A., Lloyd, R.C., and Whitlock, K.E. (2006). Olfactory imprinting is correlated with changes in gene expression in the olfactory epithelia of the zebrafish. J. Neurobiol. *66*, 1452–1466.

Harvey-Girard, E., Giassi, A.C.C., Ellis, W., and Maler, L. (2013). Expression of the cannabinoid CB1 receptor in the gymnotiform fish brain and its implications for the organization of the teleost pallium. J. Comp. Neurol. *521*, 949–975.

Hashiguchi, Y., and Nishida, M. (2006). Evolution and origin of vomeronasal-type odorant receptor gene repertoire in fishes. BMC Evol. Biol. *6*, 76.

Hashiguchi, Y., and Nishida, M. (2007). Evolution of trace amine associated receptor (TAAR) gene family in vertebrates: lineage-specific expansions and degradations of a second class of vertebrate chemosensory receptors expressed in the olfactory epithelium. Mol. Biol. Evol. *24*, 2099–2107.

Hashimoto, M., and Hibi, M. (2012). Development and evolution of cerebellar neural circuits. Dev. Growth Differ. *54*, 373–389.

Hermans, E.J., Battaglia, F.P., Atsak, P., de Voogd, L.D., Fernández, G., and Roozendaal, B. (2014). How the amygdala affects emotional memory by altering brain network properties. Neurobiol. Learn. Mem. *112*, 2–16.

Herrada, G., and Dulac, C. (1997). A novel family of putative pheromone receptors in mammals with a topographically organized and sexually dimorphic distribution. Cell *90*, 763–773.

Hikosaka, O. (2010). The habenula: from stress evasion to value-based decision-making. Nat. Rev. Neurosci. *11*, 503–513.

Honkanen, T., and Ekström, P. (1990). An immunocytochemical study of the olfactory projections in the three-spined stickleback, gasterosteus aculeatus, L. J. Comp. Neurol. *292*, 65–72.

Hoon, M., Okawa, H., Della Santina, L., and Wong, R.O.L. (2014). Functional architecture of the retina: Development and disease. Prog. Retin. Eye Res. *42*, 44–84.

Hussain, A., Saraiva, L., and Korsching, S.I. (2009). Positive Darwinian selection and the birth of an olfactory receptor clade in teleosts. Proc. Natl. Acad. Sci. *106*, 4313–4318.

Hussain, A., Saraiva, L., Ferrero, D., Ahuja, G., Krishna, V., Liberles, S., and Korsching, S. (2013). High-affinity olfactory receptor for the death-associated odor cadaverine. Proc. Natl. Acad. Sci. 1–10.

Igarashi, K., Ieki, N., An, M., Yamaguchi, Y., Nagayama, S., Kobayakawa, K., Kobayakawa, R., Tanifuji, M., Sakano, H., Chen, W.R., et al. (2012). Parallel Mitral and Tufted Cell Pathways Route Distinct Odor Information to Different Targets in the Olfactory Cortex. J. Neurosci. *32*, 7970–7985.

Issa, F.A., O'Brien, G., Kettunen, P., Sagasti, A., Glanzman, D.L., and Papazian, D.M. (2011). Neural circuit activity in freely behaving zebrafish (Danio rerio). J. Exp. Biol. *214*, 1028–1038.

Iurilli, G., and Datta, S.R. (2017). Population Coding in an Innately Relevant Olfactory Area. Neuron *93*, 1180–1197.e7.

Janak, P.H., and Tye, K.M. (2015). From circuits to behaviour in the amygdala. Nature *517*, 284–292.

Jefferis, G., Potter, C., Chan, A., Marin, E., Rohlfing, T., Maurer, C., and Luo, L. (2007). Comprehensive Maps of Drosophila Higher Olfactory Centers: Spatially Segregated Fruit and Pheromone Representation. Cell *128*, 1187–1203.

Johnson, M., Tsai, L., Roy, D., Valenzuela, D., Mosley, C., Magklara, A., Lomvardas, S., Liberles, S., and Barnea, G. (2012). Neurons expressing trace amine-associated receptors project to discrete glomeruli and constitute an olfactory subsystem. Proc. Natl. Acad. Sci.

Kandel, E.R., Schwartz, J.H., Jessell, T.M., Siegelbaum, S.A., and Hudspeth, A.J. (2014). Principles of Neural Science, Fifth Edition.

Kasumyan, A.O., and Lebedeva, N. (1975). New data on the nature of the alarm pheromone in cyprinids (Phoxinus phoxinus). J. Icthyology *19*, 109–114.

Kimchi, T., Xu, J., and Dulac, C. (2007). A functional circuit underlying male sexual behaviour in the female mouse brain. Nature *448*, 1009–1014.

Kimmel, C.B., Patterson, J., and Kimmel, R.O. (1974). The development and behavioral characteristics of the startle response in the zebra fish. Dev. Psychobiol. *7*, 47–60.

Klüver, H., and Bucy, P.C. (1937). "Psychic blindness" and other symptoms following bilateral temporal lobectomy in Rhesus monkeys. Am. J. Physiol.

Koide, T., Miyasaka, N., Morimoto, K., Asakawa, K., Urasaki, A., Kawakami, K., and Yoshihara, Y. (2009). Olfactory neural circuitry for attraction to amino acids revealed by transposon-mediated gene trap approach in zebrafish. Proc. Natl. Acad. Sci. *106*, 9884–9889.

Koide, T., Ohkura, M., Nakai, J., and Yoshihara, Y. (2011). In vivo imaging of neural activities along the olfactory circuitry in transgenic zebrafish. Neurosci. Res. *71*, e357.

Lakhina, V., Marcaccio, C., Shao, X., Lush, M., Jain, R., Fujimoto, E., Bonkowsky, J., Granato, M., and Raper, J. (2012). Netrin/DCC Signaling Guides Olfactory Sensory Axons to Their Correct Location in the Olfactory Bulb. J. Neurosci. *32*, 4440–4456.

Lam, C.S., Rastegar, S., and Strähle, U. (2006). Distribution of cannabinoid receptor 1 in the CNS of zebrafish. Neuroscience *138*, 83–95.

Larsson, M.C., Domingos, A.I., Jones, W.D., Chiappe, M.E., Amrein, H., and Vosshall, L.B. (2004). Or83b encodes a broadly expressed odorant receptor essential for Drosophila olfaction. Neuron *43*, 703–714.

Lau, B., Mathur, P., Gould, G., and Guo, S. (2011). Identification of a brain center whose activity discriminates a choice behavior in zebrafish. Proc. Natl. Acad. Sci. *108*, 2581–2586.

Lebedeva, N., Malyukina, G.A., and Kasumyan, A.O. (1975). The natural repellent in the skin of Cyprinids. J. Ichthyol. *15*, 472–480.

LeDoux, J. (2007). The amygdala. Curr. Biol. *17*, R868–R874.

LeDoux, J.E., Cicchetti, P., Xagoraris, A., and Romanski, L.M. (1990). The lateral amygdaloid nucleus: sensory interface of the amygdala in fear conditioning. J. Neurosci. *10*, 1062–1069.

Lee, A., Mathuru, A.S., Teh, C., Kibat, C., Korzh, V., Penney, T.B., and Jesuthasan, S. (2010). The habenula prevents helpless behavior in larval zebrafish. Curr. Biol. *20*, 2211–2216.

Levine, R.L., and Dethier, S. (1985). The connections between the olfactory bulb and the brain in the goldfish. J. Comp. Neurol. *237*, 427–444.

Leypold, B.G., Yu, C.R., Leinders-Zufall, T., Kim, M.M., Zufall, F., and Axel, R. (2002). Altered sexual and social behaviors in trp2 mutant mice. Proc. Natl. Acad. Sci. U. S. A. *99*, 6376–6381.

Li, C.-I., Maglinao, T.L., and Takahashi, L.K. (2004). Medial Amygdala Modulation of Predator Odor-Induced Unconditioned Fear in the Rat. Behav. Neurosci. *118*, 324–332.

Liberles, S.D. (2015). Trace amine-associated receptors: ligands, neural circuits, and behaviors. Curr. Opin. Neurobiol. *34*, 1–7.

Liberles, S.D., and Buck, L.B. (2006). A second class of chemosensory receptors in the olfactory epithelium. Nature *442*, 645–650.

Liberles, S.D., Horowitz, L.F., Kuang, D., Contos, J.J., Wilson, K.L., Siltberg-Liberles, J., Liberles, D.A., and Buck, L.B. (2009). Formyl peptide receptors are candidate chemosensory receptors in the vomeronasal organ. Proc. Natl. Acad. Sci. U. S. A. *106*, 9842–9847.

Lin, D., Boyle, M.P., Dollar, P., Lee, H., Lein, E.S., Perona, P., and Anderson, D.J. (2011). Functional identification of an aggression locus in the mouse hypothalamus. Nature *470*, 221–226.

Lin, D.Y., Shea, S.D., and Katz, L.C. (2006). Representation of Natural Stimuli in the Rodent Main Olfactory Bulb. Neuron *50*, 937–949.

Lin, H.-H., Lai, J.S.-Y., Chin, A.-L., Chen, Y.-C., and Chiang, A.-S. (2007). A Map of Olfactory Representation in the Drosophila Mushroom Body. Cell *128*, 1205–1217.

Lundegaard, P.R., Anastasaki, C., Grant, N.J., Sillito, R.R., Zich, J., Zeng, Z., Paranthaman, K., Larsen, A.P., Armstrong, J.D., Porteous, D.J., et al. (2015). MEK Inhibitors Reverse cAMP-Mediated Anxiety in Zebrafish. Chem. Biol. *22*, 1–12.

Mailleux, P., and Vanderhaeghen, J.J. (1992). Distribution of neuronal cannabinoid receptor in the adult rat brain: a comparative receptor binding radioautography and in situ hybridization histochemistry. Neuroscience *48*, 655–668.

Malnic, B., Gonzalez-Kristeller, D.C., and Gutiyama, L.M. (2010). Odorant Receptors. In The Neurobiology of Olfaction, (CRC Press/Taylor & Francis)

Manzini, I., and Korsching, S. (2011). The peripheral olfactory system of vertebrates: molecular, structural and functional basics of the sense of smell. E-Neuroforum *17*, 68.

Martín, I., Gómez, A., Salas, C., Puerto, A., and Rodríguez, F. (2011). Dorsomedial pallium lesions impair taste aversion learning in goldfish. Neurobiol. Learn. Mem. *96*, 297–305.

Martini, S., Silvotti, L., Shirazi, A., Ryba, N., and Tirindelli, R. (2001). Co-expression of putative pheromone receptors in the sensory neurons of the vomeronasal organ. J. Neurosci. *21*, 843–848.

Mathuru, A.S., Kibat, C., Cheong, W.F., Shui, G., Wenk, M.R., Friedrich, R.W., and Jesuthasan, S. (2012). Chondroitin Fragments Are Odorants that Trigger Fear Behavior in Fish. Curr. Biol. *22*, 538–544.

Maurice, D.H., Ke, H., Ahmad, F., Wang, Y., Chung, J., and Manganiello, V.C. (2014). Advances in targeting cyclic nucleotide phosphodiesterases. Nat. Rev. Drug Discov. *13*, 290–314.

Maximino, C., Lima, M.G., Oliveira, K.R.M., Batista, E. de J.O., and Herculano, A.M. (2013). "Limbic associative" and "autonomic" amygdala in teleosts: A review of the evidence. J. Chem. Neuroanat. *48*, 1–13.

McCarroll, M.N., Gendelev, L., Keiser, M.J., and Kokel, D. (2016). Leveraging Large-scale Behavioral Profiling in Zebrafish to Explore Neuroactive Polypharmacology. ACS Chem. Biol. *11*, 842–849.

McDonald, A.J. (1998). Cortical pathways to the mammalian amygdala. Prog. Neurobiol. *55*, 257–332.

Medan, V., and Preuss, T. (2014). The Mauthner-cell circuit of fish as a model system for startle plasticity. J. Physiol. Paris *108*, 129–140.

Menard, J., and Treit, D. (1999). Effects of centrally administered anxiolytic compounds in animal models of anxiety. Neurosci. Biobehav. Rev. *23*, 591–613.

Menuet, A., Alunni, A., Joly, J.-S., Jeffery, W.R., and Rétaux, S. (2007). Expanded expression of Sonic Hedgehog in Astyanax cavefish: multiple consequences on forebrain development and evolution. Development *134*, 845–855.

Millar, J.K., Pickard, B.S., Mackie, S., James, R., Christie, S., Buchanan, S.R., Malloy, M.P., Chubb, J.E., Huston, E., Baillie, G.S., et al. (2005). DISC1 and PDE4B Are Interacting Genetic Factors in Schizophrenia That Regulate cAMP Signaling. Science (80-.). *310*.

Millar, J.K., Mackie, S., Clapcote, S.J., Murdoch, H., Pickard, B.S., Christie, S., Muir, W.J., Blackwood, D.H., Roder, J.C., Houslay, M.D., et al. (2007). Disrupted in schizophrenia 1 and phosphodiesterase 4B: towards an understanding of psychiatric illness. J. Physiol. *584*, 401–405.

Mione, M., Shanmugalingam, S., Kimelman, D., and Griffin, K. (2001). Overlapping expression of zebrafish T-brain-1 and eomesodermin during forebrain development. Mech. Dev. *100*, 93–97.

Miyamichi, K., Amat, F., Moussavi, F., Wang, C., Wickersham, I., Wall, N., Taniguchi, H., Tasic, B., Huang, Z., He, Z., et al. (2011). Cortical representations of olfactory input by trans-synaptic tracing. Nature *472*, 191–196.

Miyasaka, N., Morimoto, K., Tsubokawa, T., Higashijima, S., Okamoto, H., and Yoshihara, Y. (2009). From the olfactory bulb to higher brain centers: genetic visualization of secondary olfactory pathways in zebrafish. J. Neurosci. *29*, 4756–4767.

Miyasaka, N., Arganda-Carreras, I., Wakisaka, N., Masuda, M., Sümbül, U., Seung, H.S., and Yoshihara, Y. (2014). Olfactory projectome in the zebrafish forebrain revealed by genetic single-neuron labelling. Nat. Commun. *5*, 3639.

Mo, W., Chen, F., Nechiporuk, A., and Nicolson, T. (2010). Quantification of vestibular-induced eye movements in zebrafish larvae. BMC Neurosci. *11*, 110.

Mohedano-Moriano, A., Pro-Sistiaga, P., Úbeda-Bañón, I., Crespo, C., Insausti, R., and Martinez-Marcos, A. (2007). Segregated pathways to the vomeronasal amygdala: differential projections from the anterior and posterior divisions of the accessory olfactory bulb. Eur. J. Neurosci. *25*, 2065–2080.

Mombaerts, P. (2004). Genes and ligands for odorant, vomeronasal and taste receptors. Nat. Rev. Neurosci. *5*, 263–278.

Moreno, N., González, A., and Rétaux, S. (2009). Development and evolution of the subpallium. Semin. Cell Dev. Biol. *20*, 735–743.

Morita, T., Nitta, H., Kiyama, Y., Mori, H., and Mishina, M. (1995). Differential expression of two zebrafish emx homeoprotein mRNAs in the developing brain. Neurosci. Lett. *198*, 131–134.

Mueller, T., Wullimann, M.F., and Guo, S. (2008). Early teleostean basal ganglia development visualized by Zebrafish Dlx2a, Lhx6, Lhx7, Tbr2 (eomesa), and GAD67 gene expression. J. Comp. Neurol. *507*, 1245–1257.

Mueller, T., Dong, Z., Berberoglu, M.A., and Guo, S. (2011). The dorsal pallium in zebrafish, Danio rerio (Cyprinidae, Teleostei). Brain Res. *1381*, 95–105.

Nicolson, T., Rüsch, A., Friedrich, R.W., Granato, M., Ruppersberg, J.P., and Nüsslein-Volhard, C. (1998). Genetic Analysis of Vertebrate Sensory Hair Cell Mechanosensation: the Zebrafish Circler Mutants. Neuron *20*, 271–283.

Nieuwenhuys, R. (2009). The forebrain of actinopterygians revisited. Brain. Behav. Evol. *73*, 229–252.

Nieuwenhuys, R. (2011). The development and general morphology of the telencephalon of actinopterygian fishes: synopsis, documentation and commentary. Brain Struct. Funct. *215*, 141–157.

Nikonov, A.A., Finger, T.E., and Caprio, J. (2005). Beyond the olfactory bulb: An odotopic map in the forebrain. Proc. Natl. Acad. Sci. U. S. A. *102*, 18688–18693.

Nissanov, J., Eaton, R.C., and DiDomenico, R. (1990). The motor output of the Mauthner cell, a reticulospinal command neuron. Brain Res. *517*, 88–98.

Northcutt, R.G. (2011). Olfactory projections in the white sturgeon, Acipenser transmontanus: an experimental study. J. Comp. Neurol. *519*, 1999–2022.

O'Connell, L.A., and Hofmann, H.A. (2011). The Vertebrate mesolimbic reward system and social behavior network: A comparative synthesis. J. Comp. Neurol. *519*, 3599–3639.

Oka, Y., and Korsching, S.I. (2011). Shared and unique G alpha proteins in the zebrafish versus mammalian senses of taste and smell. Chem. Senses *36*, 357–365.

Oka, Y., Saraiva, L., and Korsching, S.I. (2012). Crypt neurons express a single V1R-related ora gene. Chem. Senses *37*, 219–227.

Olshausen, B.A., and Field, D.J. (1996). Emergence of simple-cell receptive field properties by learning a sparse code for natural images. Nature *381*, 607–609.

Orger, M.B. (2016). The Cellular Organization of Zebrafish Visuomotor Circuits. Curr. Biol. *26*, R377–R385.

Oteiza, P., Odstrcil, I., Lauder, G., Portugues, R., and Engert, F. (2017). A novel mechanism for mechanosensory-based rheotaxis in larval zebrafish. Nature.

Pape, H.-C., and Pare, D. (2010). Plastic synaptic networks of the amygdala for the acquisition, expression, and extinction of conditioned fear. Physiol. Rev. *90*, 419–463.

Papes, F., Logan, D.W., and Stowers, L. (2010). The Vomeronasal Organ Mediates Interspecies Defensive Behaviors through Detection of Protein Pheromone Homologs. Cell *141*, 692–703.

Perathoner, S., Cordero-Maldonado, M.L., and Crawford, A.D. (2016). Potential of zebrafish as a model for exploring the role of the amygdala in emotional memory and motivational behavior. J. Neurosci. Res. *94*, 445–462.

Petrovich, G.D., Canteras, N.S., and Swanson, L.W. (2001). Combinatorial amygdalar inputs to hippocampal domains and hypothalamic behavior systems. Brain Res. Rev. *38*, 247–289.

Pfeiffer, W. (1977). The Distribution of Fright Reaction and Alarm Substance Cells in Fishes. Copeia *1977*, 653–665.

Pfeiffer, W., Riegelbauer, G., Meier, G., and Scheibler, B. (1985). Effect of hypoxanthine-3(N)-oxide and hypoxanthine-1(N)-oxide on central nervous excitation of the black tetra Gymnocorymbus ternetzi (Characidae, Ostariophysi, Pisces) indicated by dorsal light response. J. Chem. Ecol. *11*, 507–523.

Pinelli, C., D'Aniello, B., Polese, G., and Rastogi, R.K. (2004). Extrabulbar olfactory system and nervus terminalis FMRFamide immunoreactive components in Xenopus laevis ontogenesis. J. Chem. Neuroanat. *28*, 37–46.

Poo, C., and Isaacson, J.S. (2011). A major role for intracortical circuits in the strength and tuning of odor-evoked excitation in olfactory cortex. Neuron *72*, 41–48.

Portavella, M., Torres, B., and Salas, C. (2004). Avoidance response in goldfish: emotional and temporal involvement of medial and lateral telencephalic pallium. J. Neurosci. *24*, 2335–2342.

Portugues, R., Feierstein, C.E., Engert, F., and Orger, M.B. (2014). Whole-Brain Activity Maps Reveal Stereotyped, Distributed Networks for Visuomotor Behavior. Neuron *81*, 1328–1343.

Puelles, L., Kuwana, E., Puelles, E., Bulfone, A., Shimamura, K., Keleher, J., Smiga, S., and Rubenstein, J.L. (2000). Pallial and subpallial derivatives in the embryonic chick and mouse telencephalon, traced by the expression of the genes Dlx-2, Emx-1, Nkx-2.1, Pax-6, and Tbr-1. J. Comp. Neurol. *424*, 409–438.

Ren, X., Chang, S., Laframboise, A., Green, W., Dubuc, R., and Zielinski, B. (2009). Projections from the accessory olfactory organ into the medial region of the olfactory bulb in the sea lamprey (Petromyzon marinus): a novel vertebrate sensory structure? J. Comp. Neurol. *516*, 105–116.

Repicky, S.E., and Luetje, C.W. (2009). Molecular receptive range variation among mouse odorant receptors for aliphatic carboxylic acids. J. Neurochem. *109*, 193–202.

Ressler, K., Sullivan, S., and Buck, L. (1993). A zonal organization of odorant receptor gene expression in the olfactory epithelium. Cell *73*, 597–609.

Rétaux, S., Rogard, M., Bach, I., Failli, V., and Besson, M.J. (1999). Lhx9: a novel LIM-homeodomain gene expressed in the developing forebrain. J. Neurosci. *19*, 783–793.

Riddle, D.R., and Oakley, B. (1992). Immunocytochemical identification of primary olfactory afferents in rainbow trout. J. Comp. Neurol. *324*, 575–589.

Rink, E., and Wullimann, M.F. (2004). Connections of the ventral telencephalon (subpallium) in the zebrafish (Danio rerio). Brain Res. *1011*, 206–220.

Rivière, S., Challet, L., Fluegge, D., Spehr, M., and Rodriguez, I. (2009). Formyl peptide receptor-like proteins are a novel family of vomeronasal chemosensors. Nature *459*, 574–577.

Rohr, K.B., Barth, K.A., Varga, Z.M., and Wilson, S.W. (2001). The nodal pathway acts upstream of hedgehog signaling to specify ventral telencephalic identity. Neuron *29*, 341–351.

Roosen-Runge, E.C. (1938). ON THE EARLY DEVELOPMENT—BIPOLAR DIFFERENTIATION AND CLEAVAGE—OF THE ZEBRA FISH, BRACHYDANIO RERIO. Biol. Bull. *75*, 119–133.

Root, C.M., Denny, C.A., Hen, R., and Axel, R. (2014). The participation of cortical amygdala in innate, odour-driven behaviour. Nature *515*, 269–273.

Ryba, N.J., and Tirindelli, R. (1997). A New Multigene Family of Putative Pheromone Receptors. Neuron *19*, 371–379.

Sah, P., Faber, E.S.L., Lopez De Armentia, M., and Power, J. (2003). The amygdaloid complex: anatomy and physiology. Physiol. Rev. *83*, 803–834.

Saito, H., Chi, Q., Zhuang, H., Matsunami, H., and Mainland, J.D. (2009). Odor Coding by a Mammalian Receptor Repertoire. Sci. Signal. *2*.

Saraiva, L., and Korsching, S.I. (2007). A novel olfactory receptor gene family in teleost fish. Genome Res. *17*, 1448–1457.

Sato, K., and Suzuki, N. (2001). Whole-cell response characteristics of ciliated and microvillous olfactory receptor neurons to amino acids, pheromone candidates and urine in rainbow trout. Chem. Senses *26*, 1145–1156.

Sato, Y., Miyasaka, N., and Yoshihara, Y. (2005). Mutually Exclusive Glomerular Innervation by Two Distinct Types of Olfactory Sensory Neurons Revealed in Transgenic Zebrafish. J. Neurosci. *25*, 4889–4897.

Sato, Y., Miyasaka, N., and Yoshihara, Y. (2007). Hierarchical Regulation of Odorant Receptor Gene Choice and Subsequent Axonal Projection of Olfactory Sensory Neurons in Zebrafish. J. Neurosci. *27*, 1606–1615.

Schärer, Y.-P.Z., Shum, J., Moressis, A., and Friedrich, R.W. (2012). Dopaminergic modulation of synaptic transmission and neuronal activity patterns in the zebrafish homolog of olfactory cortex. Front. Neural Circuits *6*, 76.

Schmachtenberg, O., and Bacigalupo, J. (2004). Olfactory transduction in ciliated receptor neurons of the Cabinza grunt, Isacia conceptionis (Teleostei: Haemulidae). Eur. J. Neurosci. *20*, 3378–3386.

Schmitt, U., and Hiemke, C. (1998). Combination of open field and elevated plus-maze: A suitable test battery to assess strain as well as treatment differences in rat behavior. Prog. Neuro-Psychopharmacology Biol. Psychiatry *22*, 1197–1215.

Schnörr, S.J., Steenbergen, P.J., Richardson, M.K., and Champagne, D.L. (2012). Measuring thigmotaxis in larval zebrafish. Behav. Brain Res. *228*, 367–374.

Scholz, A.T., Horrall, R.M., Cooper, J.C., and Hasler, A.D. (1976). Imprinting to chemical cues: the basis for home stream selection in salmon. Science *192*, 1247–1249.

Schweitzer, J., Löhr, H., Filippi, A., and Driever, W. (2012). Dopaminergic and noradrenergic circuit development in zebrafish. Dev. Neurobiol. *72*, 256–268.

Scott, E.K., Mason, L., Arrenberg, A.B., Ziv, L., Gosse, N.J., Xiao, T., Chi, N.C., Asakawa, K., Kawakami, K., and Baier, H. (2007). Targeting neural circuitry in zebrafish using GAL4 enhancer trapping. Nat. Methods *4*, 323–326.

Shi, P., and Zhang, J. (2009). Extraordinary diversity of chemosensory receptor gene repertoires among vertebrates. Results Probl. Cell Differ. *47*, 1–23.

Silvotti, L., Moiani, A., Gatti, R., and Tirindelli, R. (2007). Combinatorial co-expression of pheromone receptors, V2Rs. J. Neurochem. *103*, 1753–1763.

Sorensen, P.W., Hara, T.J., Stacey, N.E., and Goetz, F.W. (1988). F prostaglandins function as potent olfactory stimulants that comprise the postovulatory female sex pheromone in goldfish. Biol. Reprod. *39*, 1039–1050.

Sorensen, P.W., Christensen, T.A., and Stacey, N.E. (1998). Discrimination of pheromonal cues in fish: emerging parallels with insects. Curr. Opin. Neurobiol. *8*, 458–467.

Sosulski, D., Bloom, M.L., Cutforth, T., Axel, R., and Datta, S. (2011). Distinct representations of olfactory information in different cortical centres. Nature *472*, 213–216.

Speca, D., Lin, D., Sorensen, P., Isacoff, E., Ngai, J., and Dittman, A. (1999). Functional identification of a goldfish odorant receptor. Neuron *23*, 487–498.

Speedie, N., and Gerlai, R. (2008). Alarm substance induced behavioral responses in zebrafish (Danio rerio). Behav. Brain Res. *188*, 168–177.

Stacey, N.E., Sorensen, P.W., Van Der Kraak, G.J., and Dulka, J.G. (1989). Direct evidence that 17α,20β-dihydroxy-4-pregnen-3-one functions as a goldfish primer pheromone: Preovulatory release is closely associated with male endocrine responses. Gen. Comp. Endocrinol. *75*, 62–70.

Steele, C.W., Owens, D.W., and Scarfe, A.D. (1990). Attraction of zebrafish, Brachydanio rerio, to alanine and its suppression by copper. J. Fish Biol. *36*, 341–352.

Steele, C.W., Scarfe, A.D., and Owens, D.W. (1991). Effects of group size on the responsiveness of zebrafish, Brachydanio rerio (Hamilton Buchanan), to alanine, a chemical attractant. J. Fish Biol. *38*, 553–564.

Stettler, D.D., and Axel, R. (2009). Representations of odor in the piriform cortex. Neuron *63*, 854–864.

Stewart, A., Cachat, J., Wong, K., Gaikwad, S., Gilder, T., DiLeo, J., Chang, K., Utterback, E., and Kalueff, A. V. (2010). Homebase behavior of zebrafish in novelty-based paradigms. Behav. Processes *85*, 198–203.

Stewart, A.M., Gaikwad, S., Kyzar, E., and Kalueff, A. V. (2012). Understanding spatio-temporal strategies of adult zebrafish exploration in the open field test. Brain Res. *1451*, 44–52.

Stowers, L., Holy, T.E., Meister, M., Dulac, C., and Koentges, G. (2002). Loss of Sex Discrimination and Male-Male Aggression in Mice Deficient for TRP2. Science (80-.). *295*.

Streisinger, G., Walker, C., Dower, N., Knauber, D., and Singer, F. (1981). Production of clones of homozygous diploid zebra fish (Brachydanio rerio). Nature *291*, 293–296.

Suli, A., Watson, G.M., Rubel, E.W., Raible, D.W., and Nicolson, T. (2012). Rheotaxis in Larval Zebrafish Is Mediated by Lateral Line Mechanosensory Hair Cells. PLoS One *7*, e29727.

Swanson, L.W., and Petrovich, G.D. (1998). What is the amygdala? Trends Neurosci. *21*, 323–331.

Temizer, I., Donovan, J.C., Baier, H., and Semmelhack, J.L. (2015). A Visual Pathway for Looming-Evoked Escape in Larval Zebrafish. Curr. Biol. *25*, 1823–1834.

Tomizawa, K., Katayama, H., and Nakayasu, H. (2001). A novel monoclonal antibody recognizes a previously unknown subdivision of the habenulo-interpeduncular system in zebrafish. Brain Res. *901*, 117–127.

Troemel, E.R., Chou, J.H., Dwyer, N.D., Colbert, H.A., and Bargmann, C.I. (1995). Divergent seven transmembrane receptors are candidate chemosensory receptors in C. elegans. Cell *83*, 207–218.

von Trotha, J.W., Vernier, P., and Bally-Cuif, L. (2014). Emotions and motivated behavior converge on an amygdala-like structure in the zebrafish. Eur. J. Neurosci.

Tye, K., Prakash, R., Kim, S.-Y., Fenno, L., Grosenick, L., Zarabi, H., Thompson, K., Gradinaru, V., Ramakrishnan, C., and Deisseroth, K. (2011). Amygdala circuitry mediating reversible and bidirectional control of anxiety. Nature *471*, 358–362.

Wagner, S., Gresser, A.L., Torello, A.T., and Dulac, C. (2006). A Multireceptor Genetic Approach Uncovers an Ordered Integration of VNO Sensory Inputs in the Accessory Olfactory Bulb. Neuron *50*, 697–709.

Wakisaka, N., Miyasaka, N., Koide, T., Masuda, M., Hiraki-Kajiyama, T., and Yoshihara, Y. (2017). An Adenosine Receptor for Olfaction in Fish. Curr. Biol. *27*, 1437–1447.e4.

Waldman, B. (1982). Quantitative and Developmental Analyses of the Alarm Reaction in the Zebra Danio, Brachydanio rerio. Copeia *1982*, 1–9.

Weiskrantz, L., and Lawrence (1956). Behavioral changes associated with ablation of the amygdaloid complex in monkeys. J. Comp. Physiol. Psychol. *49*, 381–391.

Wullimann, M.F., and Mueller, T. (2004). Teleostean and mammalian forebrains contrasted: Evidence from genes to behavior. J. Comp. Neurol. *475*, 143–162.

Xu, Y., Zhang, H.-T., and O'Donnell, J.M. (2011). Phosphodiesterases in the Central Nervous System: Implications in Mood and Cognitive Disorders. (Springer Berlin Heidelberg), pp. 447–485.

Yabuki, Y., Koide, T., Miyasaka, N., Wakisaka, N., Masuda, M., Ohkura, M., Nakai, J., Tsuge, K., Tsuchiya, S., Sugimoto, Y., et al. (2016). Olfactory receptor for prostaglandin F2α mediates male fish courtship behavior. Nat. Neurosci. *19*, 897–904.

Yaksi, E., von Saint Paul, F., Niessing, J., Bundschuh, S.T., and Friedrich, R.W. (2009). Transformation of odor representations in target areas of the olfactory bulb. Nat. Neurosci. *12*, 474–482.

Yamamoto, T., Fujimoto, Y., Shimura, T., and Sakai, N. (1995). Conditioned taste aversion in rats with excitotoxic brain lesions. Neurosci. Res. *22*, 31–49.

Yamamoto, Y., Hino, H., and Ueda, H. (2010). Olfactory Imprinting of Amino Acids in Lacustrine Sockeye Salmon. PLoS One *5*, e8633.

Yang, Q., Sun, P., Chen, S., Li, H., and Chen, F. (2017). Behavioral methods for the functional assessment of hair cells in zebrafish. Front. Med. 1–13.

Yoshihara, Y. (2008). Molecular Genetic Dissection of the Zebrafish Olfactory System.

Yoshihara, Y. (2014). Zebrafish Olfactory System. In The Olfactory System, (Tokyo: Springer Japan), pp. 71–96.

Zeiske, E., Theisen, B., and Breucker, H. (1992). Structure, development, and evolutionary aspects of the peripheral olfactory system. In Fish Chemoreception, (Dordrecht: Springer Netherlands), pp. 13–39.

Zottoli, S.J., Newman, B.C., Rieff, H.I., and Winters, D.C. (1999). Decrease in occurrence of fast startle responses after selective Mauthner cell ablation in goldfish (Carassius auratus). J. Comp. Physiol. A. *184*, 207–218.

Chapter 2: Identification of a new class of olfactory neurons

In this chapter, analysis of the single cell RNA sequencing data represents a collaboration with Russell Fletcher with input from Shinya Iguchi. R.F. created Figure 2.3 based on the data generated from my RNA sequencing experiments.

Background

Animals must make sense of the large amount of molecules they are exposed to in the environment, and through various chemosensory systems they detect these molecules and determine an appropriate behavioral response. Mammals use a set of highly organized olfactory systems to categorize and respond to chemical ligands. The two main subsystems, the main olfactory system and the vomeronasal system, both detect molecules through olfactory sensory neurons (OSNs) in the nose. In the main olfactory system, ciliated OSNs in the main olfactory epithelium (MOE) express odorant receptors (ORs) and trace amine-associated receptors (TAARs) that detect small and mostly volatile odorant molecules (Buck and Axel, 1991; Liberles and Buck, 2006; Mombaerts, 2004). OSNs then send axons into the olfactory bulb (OB) where mitral and tufted cells send further projections to the five areas of the olfactory cortex, which includes the piriform cortex, entorhinal cortex and amygdala (Ghosh et al., 2011; Haberly and Price, 1977; Miyamichi et al., 2011; Mori et al., 1983; Nagayama, 2010; Sosulski et al., 2011). This system plays a key role in learning and odor discrimination. In the vomeronasal system (VNO) microvillous cells in the vomeronasal epithelium (VOE) express type 1 and 2 vomeronasal receptors (V1r and V2r) that detect mostly large soluble molecules (Dulac and Axel, 1995; Herrada and Dulac, 1997; Matsunami and Buck, 1997; Ryba and Tirindelli, 1997). These OSNs make projections to the accessory olfactory bulb. From here, projections are sent mainly to the medial amygdala (Chamero et al., 2012). This system plays a key role in innate behavior detection. Large molecules from the urine of members of the opposite sex in the species are commonly detected through OSNs in the VNO (Flanagan et al., 2011).

While mammals share many highly organized olfactory systems, fish differ significantly. The zebrafish olfactory system consists of one epithelium that houses many OSN types including ciliated, microvillous, crypt, kappe, and pear cells, the later three of which are not present in tetrapods (Ahuja et al., 2014; Hamdani and Døving, 2007; Hansen and Finger, 2000; Hussain et al., 2009; Sato et al., 2005; Wakisaka et al., 2017). While ciliated and microvillous cells express ORs, Taars and V2r receptors, crypt cells seem to express only one V1r-like receptor, ora4, from the ora receptor family in fish (Oka et al., 2012; Saraiva and Korsching, 2007). Crypt cells have been shown to project to the medial olfactory bulb, and from there to higher processing centers in the brain such as the telencephalon and habenula (Biechl et al., 2017), areas that are important for fear processing (Agetsuma et al., 2010). The newly discovered pear cells detect adenosine and send projections to the lateral glomerulus, lG2 (Wakisaka et al., 2017).

The differences between mammals and fish show an interesting divergence in evolution. Mammals have two major olfactory systems each expressing one of two distinct OSN subtypes (ciliated and microvillous), while fish have one major olfactory system that expresses a variety of cell types. Understanding how these differences have evolved might help us make better comparative studies between different animal groups.

Zebrafish have become a useful model for understanding the complexities of olfactory signaling. In addition to the basic advantages such as optical transparency and fast developmental speed, zebrafish can be manipulated using forward genetic tools such as gene and enhancer trapping. Zebrafish also have the potential to be used in behavioral screens for drug tests (Oliveira, 2013).

Previously, gene trapping using the Tol2-mediated Gal4 method was used to observe a variety of olfactory epithelial cell subtypes (Asakawa et al., 2008a; Kawakami et al., 2004; Koide et al., 2009). One gene trap lines, SAGFF91b, display a number of OSNs that project to two medial glomeruli in the OB (mG2 and mG3). Here we examine the OSNs in the SAGFF91b line more closely and use single cell RNA-seq to show that OSNs projecting to mG2 and mG3 express the receptors ora4 and ora6 respectively. We also identify a novel OSN type that projects directly from the OE to the ventral telencephalon bypassing the OB. These OSNs show a unique unipolar morphology and are confined to the anterior-medial section of the OE, the first time a spatially segregated cell type has been observed in the larval zebrafish fish olfactory epithelium. We also show that these OSNs project to the fish pallial (medial) amygdala. Understanding new olfactory cell types within the zebrafish system will hopefully uncover a new mechanism for teleost olfactory detection.

Methods

Animals

Adult fish strains AB (wild type) and fish from the gene trap line SAGFF91b were kept at 28.5 °C on a 14-h light/10-h dark cycle. Embryos were obtained from natural spawnings and were maintained in embryo medium (150 mM NaCl, 0.5 mM KCl, 1.0 mM $CaCl_2$, 0.37 mM KH_2PO_4, 0.05 mM Na_2HPO_4, 2.0 mM $MgSO_4$, 0.71 mM $NaHCO_3$ in deionized (18.0 MΩ·cm) H_2O, pH 7.4) at 25 °C. In some cases, 131 M PTU was added 24 h after fertilization to prevent pigmentation. Embryos and larvae were developmentally staged according to Kimmel and coworkers (Kimmel et al., 1995).

The SAGFF91B transgenic fish was identified by a large scale genetic screen using a gene trap construct containing Gal4FF (Asakawa et al., 2008a; Kawakami et al., 2010), and in the case of SAGFF91B, the Gal4 expressing gene trap construct was integrated 7.8 kb upstream of the gene encoding retinal aldehyde reductase 12-like on chromosome 24.

Immunohistochemistry

Whole mount immunohistochemistry was performed as described previously (Miyasaka et al., 2005). Larvae (4-6 dpf) were fixed and permeabilized for double staining of GFP and SV2 as follows. Larvae were fixed in 10% formalin (3.7% formaldehyde, 0.8% MeOH) in phosphate-buffered saline (PBS) for 30 min at room temperature (RT) and then in 2% trichloroscetic acid (TCA) in PBS for 2.5h at RT. The fixed larvae were subsequently treated with collagenase (1mg/ml, Sigma) at 37°C for 20 min. PBS containing 0.1% Tween-20 was used as washing solution.

Antibodies used were as follows: chicken polyclonal anti-GFP antibody (1:200, Abcam); mouse monoclonal anti-SV2 antibody [1:50, supernatant, Developmental Studies Hybridoma Bank (DSHB) at University of Iowa]; Alexa488-conjugated goat anti-chicken IgG antibody (1:500, Invitrogen); Alexa568-conjugated goat anti-mouse antibody (1:1000, Invitrogen).

Olfactory Glomeruli Lesions

SAGFF(LF)91b fish were grown in the presence of 131 μM PTU from 1-3 dpf. At 4dpf, the fish were anesthetized with tricaine, and mounted in 1% ultralow melting point agarose with the dorsal surface of the olfactory system exposed. Olfactory bulb glomeruli, mG2 or mG3, or the axons of the telencephalon projection neurons were destroyed by creating regions of interest (ROI) around the glomeruli in question and irradiating at 810nm (75% power at 2 frames/sec, Zeiss LSM 780 NLO AxioExaminer). Larvae were then freed from the agarose, transferred to fresh embryo media and allowed to recover for one day.

Single Cell Collection

To obtain single gfp positive cells from SAGFF(LF)91B olfactory epithelium, 5 day old fish were anesthetized with tricaine, and mounted in 1% ultralow melting point agarose (Invitrogen, 16520-050). Agarose was cut away in front of the nose so that only the very front (OE) surface was exposed. Trypsin protease solution (0.25% trypsin, 1mM EDTA, in PBS, pH=8) was pre-warmed at 37°C and was then place on the nose. Fish were kept in 37°C incubator for 30 min – 1 hour, until slight digestion was observed. To stop the digestion, fish were taken out of the incubator and stopping solution was placed on nose [pre-chilled (4°C), 10% fetal bovine serum, 1mM $CaCl_2$, in Ringers solution (116mM NaCl, 2.9mM KCl, 1.8mM $CaCl_2$, 5mM HEPES pH 7.4)] to quench digestion.

Glass micropipette tips were used to pick cells off of digested tissue. Glass capillary tubes (3.5' Drummond #3-000-203-G/X) were pulled using the following program: Heat=780, Pull=60, Velocity=50, Time=125, Pressure=500 (Sutter Model P-87 pipette puller). Tips were then manually broken using forceps to get an opening roughly 10μm in diameter. The inside of the pulled tips were then coated in sigmacote (Sigma) to siliconize the inside surface and prevent sticking. Micropipette tips were placed into a droplet of sigmacote and capillary forces allowed the solution to migrate into the micropipette. After 10 minutes positive air pressure, using 20ml Luer-Lok syringe (BD), forced the excess sigmacote out. Siliconized micropipettes were then placed in a customized holder that was fitted for tubing attachment with a 20ml syringe. Flow in and out of the micropipette tip was controlled by air suction, and stopping solution was pre-filled into the tip before collection.

Under a dissecting microscope, cells from the olfactory epithelium of fish larvae were picked off using negative suction pressure from siliconized micropipette tip. Collected OSNs were then placed into a droplet of suspension solution [0.8 mM $CaCl_2$, penicillin 50 U/ml, 10% fetal bovine serum, in Colorless Leibovitz medium L-15 (Gibco), 1:10 RNase Inhibitor (Clonetech) – add 1μl to 10μl suspension solution droplet before collection] using positive pressure to identify gfp positive single cells. Gfp positive cells were then serially diluted using negative and positive

micropipetter tip suction into successive droplets of suspension media until a single gfp positive cell was collected.

Sequencing Library Preparation

The single cell (along with ~1ul of suspension medium) was then manually placed into a pcr tube with 11ul of cell lysis mix from the Fluidigm C1 system. The single cell sample was then immediately placed in lysing program (3min 72°C, 10min 4°C, 1min 25°C). Next, cDNA synthesis and amplification were followed. This incorporates the Clontech SMART-Seqv2 Ultra Low Input RNA reagents (Clontech SMARTer Kit designed for the C1 System) to produce and amplify cDNA. For quality control purposes, any cell with less than 2.0 ng cDNA in total (quantified using a Qubit fluorometer) was excluded. Illumina Nextera tagmentation-based sequencing library synthesis (Nextera XT DNA Sample Preparation Kit) was performed using Nextera v2 index oligos (Nextera XT DNA Sample Preparation Index Kit). Library size was selected using AMPure XP (Beckman Coulter) beads and confirmed using an Agilent Bioanalyzer. Indexed, single-cell libraries were sequenced on Illumina HiSeq 2500 sequencers to produce 50 nt single-end reads.

RNA-Seq Transcript Quantification and Normalization

In our initial analysis, NGS reads were processed with Trimmomatic (version 0.3.2; Bolger et al., 2014), and aligned with Bowtie2 (version 2.2.5; Langmead et al., 2009) to the Zebrafish transcriptome (GRCz10 with RefSeq transcript annotations), which we modified to contain sequences of transgenic transcripts used in our study such as eGFP. Gene expression transcripts per million (TPMs) were derived from the single-cell NGS reads with RSEM (version 1.2.20; Li and Dewey, 2015). We flagged and excluded low quality libraries through a quality assurance pipeline we have recently described elsewhere (Fletcher et al., 2017) that incorporates quality metrics derived in part from FastQC and the Picard suite of alignment metrics. The open-source R package SCONE (https://bioconductor.org/packages/scone; Version 0.0.7) was used to perform quality metric-based cell filtering. The following criteria were used to filter cells: any cell with fewer than 100,000 aligned reads or a percentage of aligned reads below 25% was filtered out.

We assessed several normalization schemes using SCONE , based on a set of data-driven performance metrics as described previously (Fletcher et al., 2017). The first group of performance metrics includes the correlation of expression measures with factors derived from known markers of various zebrafish OE cell types (positive control genes) and the average silhouette width (Rousseeuw, 1987) of the obtained clusters (cluster quality). The second group of metrics include the correlation of expression measures with factors derived from "housekeeping" negative control genes (obtained from RNA-seq experiments on zebrafish OE (Ferreira et al., 2014) and the correlation between expression measures and quality control (QC) measures. According to SCONE, the best performing normalization was full-quantile normalization (Bolstad et al., 2003; Bullard et al., 2010) followed by regression-based adjustment for housekeeping genes. We used one factor which was tied for second place because in our past experience removing more than one factor removed known biological variation.

Following normalization with SCONE, we intersected the genes in the counts matrix with an annotated list of receptor genes, representing all known classes of receptors expressed in the olfactory epithelium, to identify receptor genes expressed by the SAGFF91B transgenic line.

After this initial analysis, we realized that the entire repertoire of ora genes were not represented in our transcript annotation, and we wanted to repeat the analysis with transcript annotations that included all ora genes. We manually annotated and modified the zebrafish genome and Ensembl transcript annotations to include all six ora genes. After processing the reads with Trimmomatic for the single cells that had passed our initial quality metric filtering, we aligned reads to the genome using hisat2 (version 2.0.1, Kim et al. 2015). Transcript assembly and quantification was performed with Stringtie (version 1.3.3b, Pertea et al., 2016), and we examined the TPM output from Stringtie without additional normalization.

RNA-seq data have been deposited in Gene Expression Omnibus. Analysis scripts for this dataset can be found at https://github.com/rufletch/zfOE.

RNA Probe Design

The templates for the following probes were amplified from gBlocks gene fragments (ora4 and ora6, IDT) or by PCR amplification of cDNA (emx3). The ora4 fragment spans the first and second introns in order to limit sequence identity and cross amplification to other sequences. ora6 spans the entire coding region.

Nucleotide sequences of the ora gene fragments:
>ora4 (NCBI reference sequence: XM_005168282.3)
ATGTCTGAGGTCCTGACGGTGGACGCGGTTCTCTTCGGCCTGCTGGTGTTCTCTGGTATCATTGGAAACATCATGGTCATCTATGT
GGTGTTTGACTGTGCTAAATTGTGCGCCTCTCGCCACCTGCCGCCGTCTGACACCATCCTGGTGCACCTGTGTCTGGCTAACCTGCT
GACGTCAGTGTTCCGCACGGTGCCGATCTTCGTGTCGGACCTGGGCCTGCAGGTGTGGCTGACGGCGGGCTGGTGCCGCGTCTTC
ATGCTGCTGTGGGTGTGGTGGCGGGCGGTGGGCTGCTGGGTCACCTTGGCTCTCAGCGCCTTCCACTGCGCCACCCTGCGTCGCCA
GCATGTCTCCATGGGGCCGCTGGGTCACTCGCGGGAGCGTCGCCGCGTCTGGGTCGTCCTGGCGGTGGTGTGGGCTGCAAACCTG
CTGTTCTCGCTGCCGGCGCTGGTCTACACCACACAGGTGCGTGGGAACGCTACGGTGGAGCTGATGGTGAT

>ora6 (NCBI reference sequence: XM_003200787.1)
ATGGTGATGGAGCAGATACAGGTGAATCTCCTCTCTCTGCGCCTCTTCATCTCCATCATTGGTGTTGTGGGAAACACACTGCTCCT
GGTCTCCATCCTGCACACACACACACACCTGAAGTCGTTCGAGCTGTTCCTGCTGGCTCTGTGCTCCGCCAACCTGCAGCAGCTGG
TGATGGTGGATGTGTATGATGTTCTGCTGCTGTGTTCTCCGTCCTGCATCGGTGTGTGTTCCTGCCGCGCGCTGCGCTTCCTGACGG
TGTTCGGGGAGGTCTGCAGCGTGCTCTTCACCGCACTCATCAGCATCTACCGTCACCAGAAGCTCCACGACGTGTTCTCGCATGTG
AACGTGCCCGTGCTGCTGGACAGCCTGCGCTGGGCGGTGTGTATGTGTGTGCTGTGTGTGTGTGTGGCGCTCGCCTTCGGTCTGCC
CACGCTCCTGGTTAACACACACTGGAGTGTCTCCAACTCTTCGCTCGAGCGCTGCCCGGTGGACTTCTTCCAGTGCCCGTCCTCCT
CCCCGTGTCTCACACACATCTACAAGTACGTGTTCCTGCTGGTGTGTGTGGTGCTGCCGCTGCTGGTCGTCACGGTGACGAGTGTG
CTGATGGTGCGGGTCCTGCTGGCGCAGCAGCGCGCCGTGCGGGTTCGAGAGGCGGAGGAGCCCCACCCTCATCACCACCACTCCT
CTCTCCTGCGCAGCACGCTGGCCATCCTGGCGGCCATGTTGCTCTTCCTGCTGGACTGGAGTGTGTATCTGCTCCTGCATTTGGCCT
TTGACCCCTACAGCTTCCCTCTGTGGGCGGAGGTGGAGTTCTTCATCACCACCATTTACACCGCACTCAGCCCGTACGTCTACGGC
ATCGGCAACGACCTCTTCAGCATAAAGCGCTTATACTGCTGA

>emx3 (gene accession number: NM_131279)
cds coordinates: 374..1075

PCR amplification was used with the following primers (each primer set has the T7 promoter site, TAATACGACTCACTATAGG, attached to the 5' end):

ora4- forward, ATGTCTGAGGTCCTGACGGTGGACG
reverse, TAATACGACTCACTATAGGATCACCATCAGCTCCACCGTAGCGT

ora6- forward, ATGGTGATGGAGCAGATACAGGTG
reverse, TAATACGACTCACTATAGGTCAGCAGTATAAGCGCTTTATGCTG
emx3- forward, CATCGGGTTCAGAGTGACCT
reverse, TAATACGACTCACTATAGGGGGCTACTGTCGTCACCTTG

Digoxigenin (DIG) probes were synthesized according to the DIG RNA labeling kit supplier protocol (Roche Molecular Biochemicals).

Whole-mount Fluorescent RNA In-Situ hybridization – Immunohistochemistry Double Labeling

In situ hybridization was essentially performed as previously described (Welten et al., 2006). 5 day old fish were fixed in 4% Paraformaldehyde (PFA) overnight and then dehydrated in 100% MeOH at -20°C for at least 24hrs. Embryos were then rehydrated for 20min in PBS containing 0.1% Tween-20 (PBST) and then digested in Proteinase K (10g/ml, Thermo Scientific) for 30min at room temperature. After brief washes, embryos were refixed in 4% PFA for 20min at room temperature and then washed five times in PBST for 5min. Next embryos were prehybridized for 2-5 hours at 55°C. Hybridization was carried out overnight (ora4) or over 40 hours (ora6) at 55°C in 200µl hybridization buffer (Hyb) containing 50-200ng of digoxigenin-labeled riboprobe.

Samples were then washed in hybridization buffer (without tRNA and heparin) and next washed at 55°C in progressively dilute solutions of Hyb, in 30mM Sodium Citrate solution (SSC). Samples were then placed in stringency washes (50% formamide, 3mM SSC) at 55°C and then room temperature. Samples were then washed in progressively dilute solutions of 3mM SSC in PBST (final solution, 100% PBST) and then blocked in PBST with 0.2% Bovine Serum Albumin, and XX% heat inactivated goat serum for three hours. Pre-adsorbed anti-digoxygenin antibody (1:1000, Roche) and chicken anti-GFP antibody (1:200, Abcam) were diluted in blocking solution and incubated with samples overnight at 4°C.

Primary antibodies were removed with six fifteen-minute washes of PBST and then incubated for 10 minutes with Cy3-tyramide solution in antibody buffer. After two hours of washes, samples were incubated in Alexa Fluor 488 goat anti-chicken antibody (1:200, Invitrogen) in blocking solution overnight at 4°C.

RNA In-Situ Hybridization of Adult Brain Sections

In-situ hybridization was essentially performed as previously described (Ganz et al., 2012). Briefly, after defrosting at room temperature (RT), sections were re-fixed in 4% PFA for 10min and then rehydrated for 15min in phosphate-buffered saline (PBS) and incubated with the probe overnight at 55°C. 100ng of probe was used per slide. The sections were washed at 55°C for 5min in 5xSSC and then 2x 40 min in 0.2xSSC (the last 20min at RT). Sections were incubated for 1-2 hours at RT in blocking solution (0.1M Tris pH 7.4, 0.15M NaCl, 10% HINGS) and incubated with 1:1000 anti-DIG-AP antibody (Goat Anti-Dig-AP, Roche) in blocking solution overnight at 4°C. Subsequently, sections were washed 2x 5min in washing solution 1 (0.1M Tris pH 7.4, 0.15M NaCl) followed by 5min in washing solution 2 (0.1M Tris pH 9.5, 0.15M NaCl, 50mM MgCl2). Sections were stained with the substrate NBT/BCIP. The staining was controlled

using a stereomicroscope. Finally, sections were washed in PBS to stop the reaction, postfixed with 4% PFA for 20min, washed again 2x 10min in PBS, and mounted with 80% glycerol in washing solution 1.

Imaging and Statistical Analysis

Fixed embryos were embedded in 1.5% low-melting-point agarose gel and imaged head-on by confocal microscopy (Zeiss LSM 780 NLO AxioExaminer). Image stacks were analyzed using Imaris, and olfactory epithelial cells were counted using NIH ImageJ and Imaris. Cell counting for statistical analysis was performed blind, with the observer not knowing which population of cells were being counted. Cell quantity was analyzed using a nonparametric Kruskall-Wallis test followed by a pairwise Mann-Whitney Wilcox Rank sum test. All analyses are two-tailed and were done using the R statistical program.

Results

Identification of new olfactory sensory neurons

Previously, gene trap screens of zebrafish were created by using the Tol2 transposon constructs with the Gal4FF transcription activator (Asakawa et al., 2008b). After crossing these lines with UAS:GFP reporter fish, several lines were screened for GFP expression in the olfactory system (Koide et al., 2009). Among these lines was SAGFF91B, which was initially selected because it showed a distinct population of OSNs that expressed GFP in different glomeruli. To examine the trajectories of these OSNs we used whole-mount immunohistochemistry of 5-day-old larvae using the synaptic vesicle protein SV2 antibody, which labels all of the protoglomeruli in the larval OB. The GFP positive axons in SAGFF91b target two glomeruli located in the medial region of the OB, mG2 and mG3 (Fig 2.1A-C). As reported previously, this GFP expression was not limited to OSNs in the olfactory epithelium and bulb. GFP fluorescence is present in other tissues such as the otic vesicle, pineal gland and spinal cord (Koide et al., 2009). Additionally however, we noticed a subgroup of GFP expressing OSNs in the SAGFF91b line that made projections directly to the telencephalon, completely bypassing the olfactory bulb (Fig 2.1C-E, arrows). Extrabulbar projections have been documented in adult zebrafish through anterograde labeling of DiI crystals in the olfactory rosette (Gayoso et al., 2011). However, this is the first observation of extrabulbar projections in larval zebrafish.

Laser ablation reveals a heterogeneous mix of OSNs in the SAGFF91b line

To examine the axonal trajectories of OSNs in the SAGFF91b line, we used laser ablation to selectively target OSNs projecting to distinct OB glomeruli or telencephalon areas. Using a Mai Tai laser (810nm) at 75% power, we were able to selectively ablate each terminal projection region of the 91b OSNs (Fig 2.2A-D). The amount of illumination time required to ablate cell terminals varied. Ablation success was determined by formation of large vacuoles and bubbling which are indicators of cell death and necrosis (Liu and Fetcho, 1999) (Fig 2.2D). Verification of cell death was determined by observing a loss in fluorescence of the cell bodies 24 hours post ablation. For mG2 and mG3 ablations, the terminals in the olfactory bulb were targeted. For the

telencephalon projections, the axons leading up to the telencephalic terminals were targeted (Fig 2.2A, magenta circles). Ablations were highly specific and minimally invasive.

Ablation of axon targets allowed us to observe a heterogeneous population of OSNs expressed by the SAGFF91b line. OSNs varied in shape (bipolar vs. unipolar), location within the OE (anterior-medial vs. posterior), and number (projecting to the olfactory bulb vs. telencephalon) (Fig 2.2A). Within the posterior region of the OE, unipolar and bipolar OSN numbers were significantly reduced after ablation in the two olfactory bulb regions (Fig 2.2E, Table 1). In the anterior region of the OE, unipolar OSNs were significantly reduced only when the telencephalon was ablated Fig 2.2F left, Table 1). On average there were very few bipolar cells in the anterior OE. Bipolar cells were reduced after ablation of both telencephalon and bulb regions (Fig 2.2F right). Taken together, these results show a striking divergence in OSN diversity within the SAGFF91b line. OSNs projecting to the OB (OSNs that are reduced after bulb ablation) are primarily located in the posterior OE and are made of a mix of unipolar and bipolar OSNs. OSNs projecting to the telencephalon are primarily located in the anterior OE and are made up of mostly unipolar OSNs.

Identification of new OSN receptors ora6 and ora4

In an effort to find genes unique to the OSNs of the SAGFF91b line, we selected and isolated OSNs directly from 5dpf OE for analysis by single-cell RNA-seq. By using a low concentration trypsin digestion we were able to dissociate OSNs directly from the fish OE. From these pools of disassociated cells we picked out individual gfp+ cells for single-cell RNA-seq using Illumina sequencing. Cells picked for RNA-seq data were aligned, filtered to eliminate poor quality samples, and normalized to minimize sources of technical variation. Sequencing data from a total of 18 gfp-positive and 4 gfp-negative single cells remained after removing poor quality samples. After examining the normalized data set for the presence of transcripts of known olfactory receptors and other signaling molecules of interest, we noticed increased levels of transcripts encoding members of the ora (v1r-like) receptors in a significant fraction of gfp+ SAGFF91b OSNs. In zebrafish, the ora gene family comprises 6 family members (Saraiva and Korsching, 2007). We then clustered the 18 gfp-positive cells based on expression of all 6 ora genes and found that 28% (5/18) of gfp+ SAGFF91b OSNs expressed elevated levels of ora6 (Fig 2.3). We also found a non-overlapping set of three cells with elevated expression of ora4 and one cell expressing ora2 (Fig 2.3). It is unclear whether the single ora2-positive cell represents a real or spurious signal given the number of cells analyzed. Expression of other ora family members was largely or completely undetectable within this limited sampling of cells. Taken together, these data suggest that at least two mutually exclusive types of cells exist in the SAGFF91b OSN population: those expressing ora6 and ora4.

Verification of ora6 and ora4 expression in OSNs projecting to the OB

To verify the expression of ora6 we performed RNA in-situ hybridization combined with immunohistochemistry staining against GFP. RNA in-situ probe labeling revealed that bipolar OSNs residing primarily in the posterior OE are co-labeled for GFP and ora6. Ablations in the bulb drop ora6 expression nearly to zero while telencephalon ablations do not change ora6 expression at all (Fig 2.4, Table 2). These results show that ora6 expressing OSNs are bipolar and project to the OB.

To more carefully examine which of the two medial OB glomeruli ora6 and ora4 expressing OSNs project to (mG2 or mG3), we performed similar dual RNA in-situ/ immuhistochemistry labeling experiments with ablations to each glomerulus in isolation. Ablations to mG3 but not mG2 caused a significant drop in ora6 expression, showing that ora6 expressing OSNs project to mG3 (Fig 2.5E, Table 3). Ablations to mG2 caused a significant drop in ora4 expression, showing that ora4 expressing OSNs project to mG2 (Fig 2.5F, Table 4). These results verify previous studies that show ora4 expression in OSNs projecting to mG2 (Ahuja et al., 2013; Biechl et al., 2017).

Characterization of telencephalon projecting OSNs

To verify the location of the telencephalon projections to their specific targets in the telencephalon we used in-situ hybridization markers of the amygdala in adult brain tissue. Previous studies have worked out many of the structures in the adult fish brain by using known mouse markers for various pallium (dorsal telencephalon) and sub-pallium (ventral telencephalon) structures, including the amygdala and hippocampus (Perathoner et al., 2016). Accurate markers for brain structures are critical for comparing the forebrain of mammals and fish since the development of each brain follows very different patterns. Rodent brains evaginate after neural tube development while fish in the actinopterygian lineage go through an eversion process, which places certain brain areas in a location opposite from the same area in mammals (Perathoner et al., 2016). The transcription factor *emx3* has been used as a marker for the pallial amygdala, which gives rise to the basolateral and medial amygdala (Ganz et al., 2014; Sah et al., 2003). In these studies, *emx3* shows strong labeling in the pallium, or the medio-dorsal telencephalon (Dm).

Using adult SAGFF91b fish, we used immunohistochemistry labeling against GFP to identify the location of GFP positive OSNs the telencephalon. In the rostral telencephalon, GFP positive cell bodies and axon tracts were scattered throughout the ventricular zone of Dm and V (ventral telencephalon). Some axon tracts were visible on the border of V and the latero-ventral telencephalon (Dlv) (Fig 2.6A, left and middle). In the caudal telencephalon, GFP signal was seen in few scattered cell bodies in Dm and axon tracts both in Dm and V (Fig 2.6B, left and middle). To identify the subdivisions within the telencephalon we used RNA in-situ hybridization of *emx3* to identify where the GFP signal is located in the SAGFF91b telencephalon projecting OSNs (Fig 2.6A and B, right). *emx3* signal was strongest in Dm both in the rostral and caudal telencephalon. The presence of GFP positive cell bodies and axon terminals in the Dm of adult fish shows that the OSNs that project directly from the OE are in fact projecting to the pallial amygdala. These results implicate a sensory circuit that resembles the fast acting Mauthner cells in the startle response circuit in fish (Nissanov et al., 1990). Mauthner cells are connected by very few synapses in order to react quickly to a threatening stimulus. Here, the telencephalon projecting cells may play a similar role in the olfactory system. OSNs that bypass the OB may be used in a fast acting circuit that may play a role in behaviors such as the alarm response.

Discussion

Zebrafish have become an extremely useful model organism due to its amenability to genetic manipulation, optical transparency, and large clutch size (Meyerhof and Korsching, 2009). Understanding the differences between sensory systems of mammals and fish is of vital importance if we are to make accurate comparisons between them.

Here we increase our understanding of the zebrafish olfactory system by uncovering a number of new features in the zebrafish olfactory system. We use forward genetics to uncover and characterize a number of novel OSNs. Previously, in the SAGFF91b line, OSNs were observed that showed projections from the OE to two medial glomeruli in the larval zebrafish OB. They showed no overlap with ciliated or microvillous cells and their expression continued through adulthood (Koide et al., 2009). In this study we quantify these neurons and their projection patterns through immunohistochemistry of GFP and SV2. We have discovered that OSNs labeled by the SAGFF91b line are segregated spatially (medial and posterior) and morphologically (unipolar and bipolar). Neurons projecting to the two medial glomeruli consist of both unipolar and bipolar cells in even proportions and are distributed fairly evenly throughout the OE. Interestingly, we discovered a unique third cell type that has been previously unreported. These OSNs consist of primarily unipolar cells that are confined to the medio-ventral section of the OE. Incredibly, they send projections directly to the ventral telencephalon, completely bypassing the OB altogether. In adults these neurons project to the medio-dorsal telencephalon (Dm), which is the location of the pallial amygdala in zebrafish (Ganz et al., 2014).

After isolating the SAGFF91b gfp+ neurons and examining their RNA expression profile through single cell RNA sequencing, we found an up-regulation of the ora6 receptor in 28% of labeled cells. Through in situ hybridization we have showed that OSNs projecting to the mG3 glomeruli express the ora6 receptor. We also verified the presence of ora4 through our sequencing analysis, and through in-situ hybridization we were able to verify its expression in OSNs projecting to the mG2 glomeruli in the zebrafish larval OB. A summary of the three OSN types in the SAGFF91b gene trap line is illustrated in (Fig 2.7). ora6 OSNs project to mG3 (green), ora4 OSNs project to mG2 (magenta), and the telencephalon projecting cells project to the ventral telencephalon (blue).

This analysis is encouraging because it opens up new ways of thinking about olfactory circuitry. The canonical projection pattern in all olfactory systems discovered to date starts with a sensory epithelium where neurons detect molecules via odorant receptor proteins (Ihara et al., 2013). From here these OSNs send projections to a bulbar location where all OSNs expressing a given receptor project onto two distinct topographically organized clusters known as glomeruli (Buck and Axel, 1991; Mombaerts et al., 1996). Projection neurons from here disperse onto a variety of sensory cortices known collectively as the olfactory cortex. It includes the piriform cortex and the amygdala in mammals and telencephalon, habenula, and hypothalamus in zebrafish (Ghosh et al., 2011; Kermen et al., 2013; Sosulski et al., 2011). Never has there been a characterization of the telencephalon projecting neurons of zebrafish larvae. Extrabulbar primary olfactory neurons have been described in several teleosts and amphibians (Gayoso et al., 2011; Honkanen and Ekström, 1990; Kermen et al., 2013; Riddle and Oakley, 1992). In adult zebrafish, lipophilic tracer dyes have uncovered a small number of bipolar cells projecting to the ventral

telencephalon (Gayoso et al., 2011). While these results uncover the existence of extrabulbar/telencephalon projecting OSNs, we hope to give a more complete picture of the organization and anatomical underpinnings of the projections and their role in zebrafish larvae.

One possible explanation for the telencephalon projecting OSNs is the need for a shortened pathway that requires fast signal processing. One similar system, the escape response in goldfish, shows how primary acoustic afferents from the ear project directly onto Mauthner neurons in the spinal cord, which in turn synapse onto motorneurons that directly innervate trunk muscle (Eaton et al., 2001). Only one action potential is observed throughout the entire system, and no more than four synapses are crossed from sensory input to motor output (Medan and Preuss, 2014; Zottoli, 1977). This system shows how the underlying circuitry for a vital survival behavior in fish can be dependent on few synaptic connections. The telencephalon projections in zebrafish may be an adaptation for a similar escape response. In adult zebrafish, an alarm substance in the skin can cause an olfactory mediated behavioral response in fish (Speedie and Gerlai, 2008). Other chemical mimics of the alarm substance can trigger olfactory mediated alarm behaviors such as diving and freezing (Pfeiffer, 1977; Waldman, 1982). Perhaps the telencephalic or "extrabulbar" projections in zebrafish represent the circuitry involved with processing this olfactory mediated alarm response.

Additionally we have revealed that the ora6 receptor is expressed in OSNs projecting to the mG3 glomeruli in the larval olfactory bulb. Previously, ora4 was shown to be expressed in crypt neurons that project to the mG2 glomeruli (Biechl et al., 2017; Oka et al., 2012). The addition of another member of the ora family showing expression in neurons projecting to the medial olfactory bulb is notable considering there are six members of the ora family and six distinct sub-glomeruli within the larval medial olfactory bulb (Koide et al., 2009; Saraiva and Korsching, 2007). The ora receptors 1-6 are homologous to the mammalian V1R receptors in the mammalian VNO. The V1R receptor family is a fairly new evolutionary family that has undergone rapid expansion in many mammalian species (Pfister and Rodriguez, 2005). V1R receptors detect low molecular weight ligands such as steroids and respond to social cues such as sexual drive in male mice and maternal aggression in female mice (Isogai et al., 2011; Del Punta et al., 2002). More recently ora1 was deorphaned and shown to detect p-hydroxyphenylacetic acid, which elicits olfactory-mediated oviposition behavior in adult zebrafish mating pairs (Ahuja and Korsching, 2014). Taken together, ora4 and ora6 expression in glomeruli within the medial olfactory bulb takes us one step further toward understanding how olfactory social cues may be wired in the fish brain. Since these cells do not overlap with ciliated and microvillous cells, which respond to bile acids, trace amines, and animo acids, we can infer that they too may respond to social cues like ora1. Further investigation into the role of ora4, ora6, and the telencephalon projecting neurons will reveal how social cues and innate behaviors may be processed in the zebrafish olfactory system. It will enable a comparison between the divergent evolutionary pathways of mammalian and fish olfactory systems.

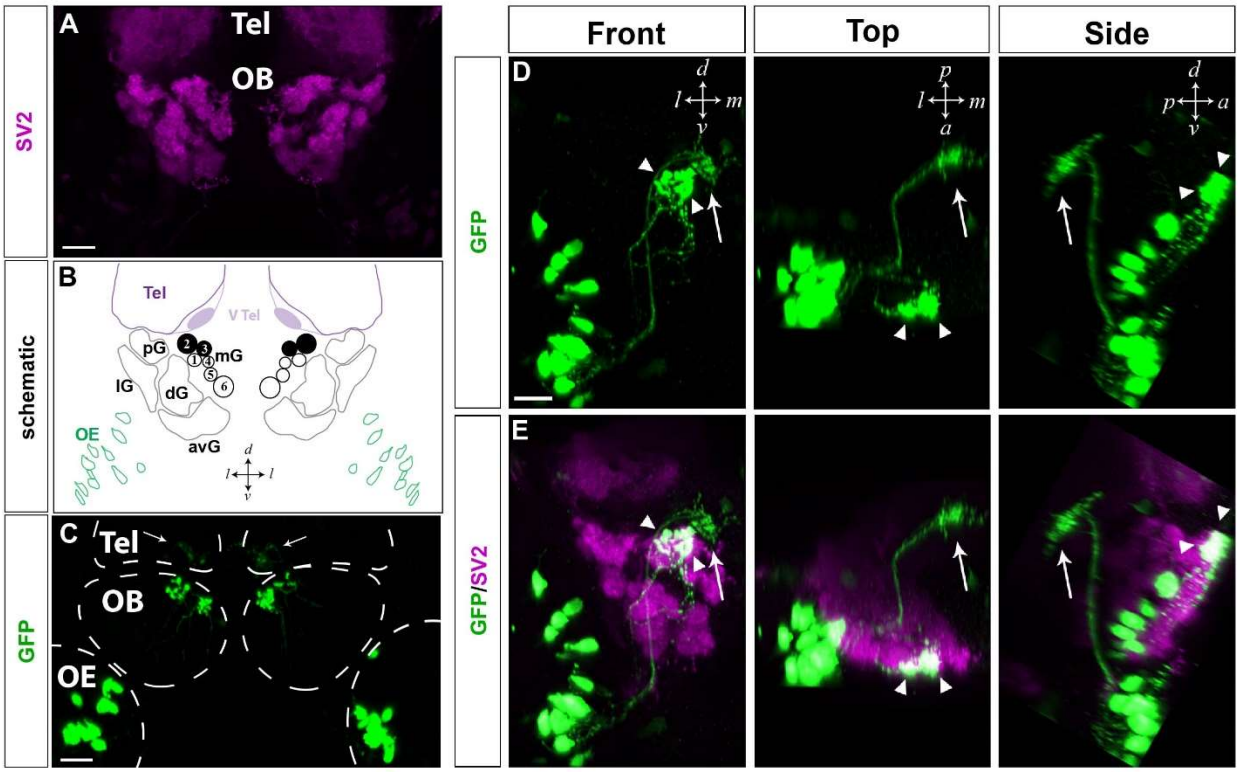

Figure 2.1 SAGFF91b gene trap zebrafish line with Gal4FF expression in OSNs and the forebrain.

GFP expression in 5-day-old larvae of the gene trap Gal4FF-expressing line SAGFF91B crossed with the UAS:GFP reporter strain **(C-E)**. **(A)** Whole-mount immunofluorescence labeling of SV2 (magenta), highlighting the main glomerular clusters present in the larval OB **(B)** Schematic diagram showing the organization of OSNs in the OE (green), OB glomeruli (black) and regions of the telencephalon (purple). OSNs in the SAGFF91b line show strong expression in mG2 and mG3 and weak expression in V Tel **(C)** Frontal view of larvae forebrain showing OSNs in green. Cell bodies originate in the OE and project strongly to the medial glomeruli mG2 and mG3 in the OB and Tel. Immunofluorescence labeling against GFP (green). Arrows highlight the telencephalon end terminals from OSNs originating in the OE. **(D,E)** Front, top, and side views of the OSN projections on the left side of the SAGFF91b larvae forebrain. Arrows point toward the telencephalon projecting OSN terminals. Arrowheads point toward mG2 and mG3 projecting OSN terminals. Whole-mount double-immunofluorescence labeling with antibodies against GFP (D,E; green) and SV2 (E, magenta). Tel, telencephalon; OB, olfactory bulb; V Tel, ventral telencephalon; OE, olfactory epithelium; lG, lateral glomeruli; pG, posterior glomeruli; dG, dorsal glomeruli; avG, anteroventral glomeruli; mG1-6, medial glomeruli 1-6; *d*, dorsal; *v*, ventral; *l*, lateral; *m*, medial; *p*, posterior; *a*, anterior. Scale bars: In A, 20µm; in C, 30µm; in D-E, 10µm.

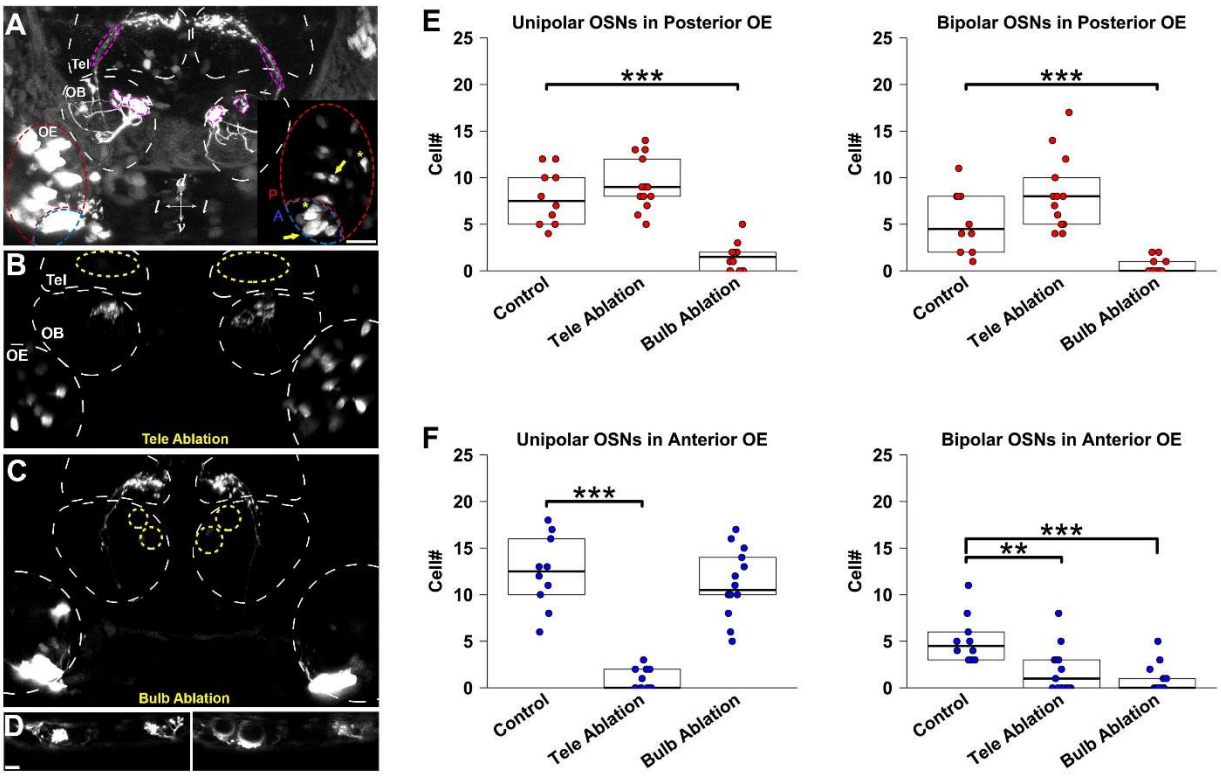

Figure 2.2 Ablation of OSN terminals in the SAGFF91b line reveals organization of heterogeneous population of OSNs

Within the OE of SAGFF91b larvae, OSNs are made up of different morphologies (unipolar and bipolar), are segregated in different areas within the OE (anterior and posterior), and project to different areas (telencephalon and OB). **(A-D)** Whole-mount immunofluorescence labeling with antibodies against GFP. **(A)** Frontal view of a 5-day-old fish larva. OSNs project to the OB and the ventral telencephalon. Magenta dashed circles represent regions of ablation. Either the axon tracks projecting to the telencephalon were ablated (upper 2 magenta circles) or the bulb glomeruli mG2 and mG3 were directly ablated (lower 4 magenta circles). Inset shows a lower gain view of the right OE. The OE is divided into two sections; the anterior (A) region is highlighted in blue, and the posterior region (P) is highlighted in red. Yellow arrows point to unipolar cells. Yellow asterisks (*) are adjacent to bipolar cells. **(B)** Frontal view of a 5-day-old fish after telencephalon ablation. The telencephalon OSN terminals are absent. Yellow dashed circles represent the empty areas normally occupied by the telencephon terminals. **(C)** Frontal view of a 5-day-old fish after medial OB ablations. The OB OSN terminals are absent. Yellow dashed circles represent the empty areas normally occupied by the OB projecting terminals. **(D)** mG2 and mG3 OSN terminals before (left) and after (right) targeted laser ablation. **(E,F)** Box plots show median, upper and lower quartile of OSNs in each condition. Dots represent individual fish. **(E)** The number of unipolar (left) and bipolar (right) OSNs in the posterior region of the OE is significantly diminished when the bulb terminals are ablated (Wilcoxon signed-rank test, ***$p < 0.0003$). **(F)** The number of unipolar (left) OSNs in the anterior region of the OE is significantly diminished only when the telencephalon terminals are ablated. The anterior region has few bipolar cells (right). Telencephalon and OB ablations both lower the number bipolar cells in the anterior OE (Wilcoxon signed-rank test, **$p < 0.01$, ***$p < 0.0003$). Results are

summarized in Table 1. Tel, telencephalon; OB, olfactory bulb; OE, olfactory epithelium; *d*, dorsal; *v*, ventral; *l*, lateral. Scale bars: In A, 20μm; in D, 10μm.

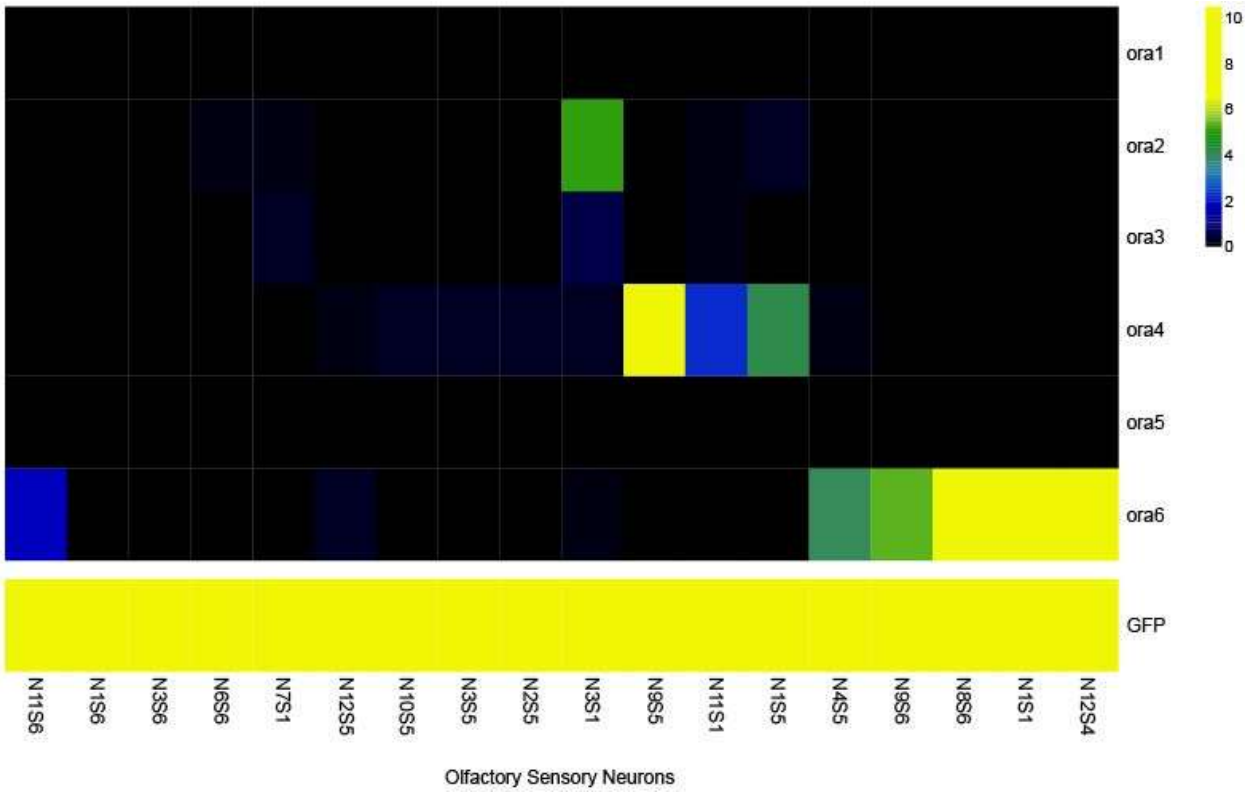

Figure 2.3 Heatmap of ora receptor expression reveals elevated levels of ora6 and ora4 in GFP positive cells

Single cell RNA sequencing analysis of all ora genes reveals an elevated expression of ora6 and ora4 in 28% and 17%, respectively, of GFP positive cells from SAGFF91b fish larvae. Columns represent individual cells. Expression of the ora genes is presented as log2 transformed transcripts per million (TPM). Samples were ordered by hierarchical clustering of ora gene TPMs.

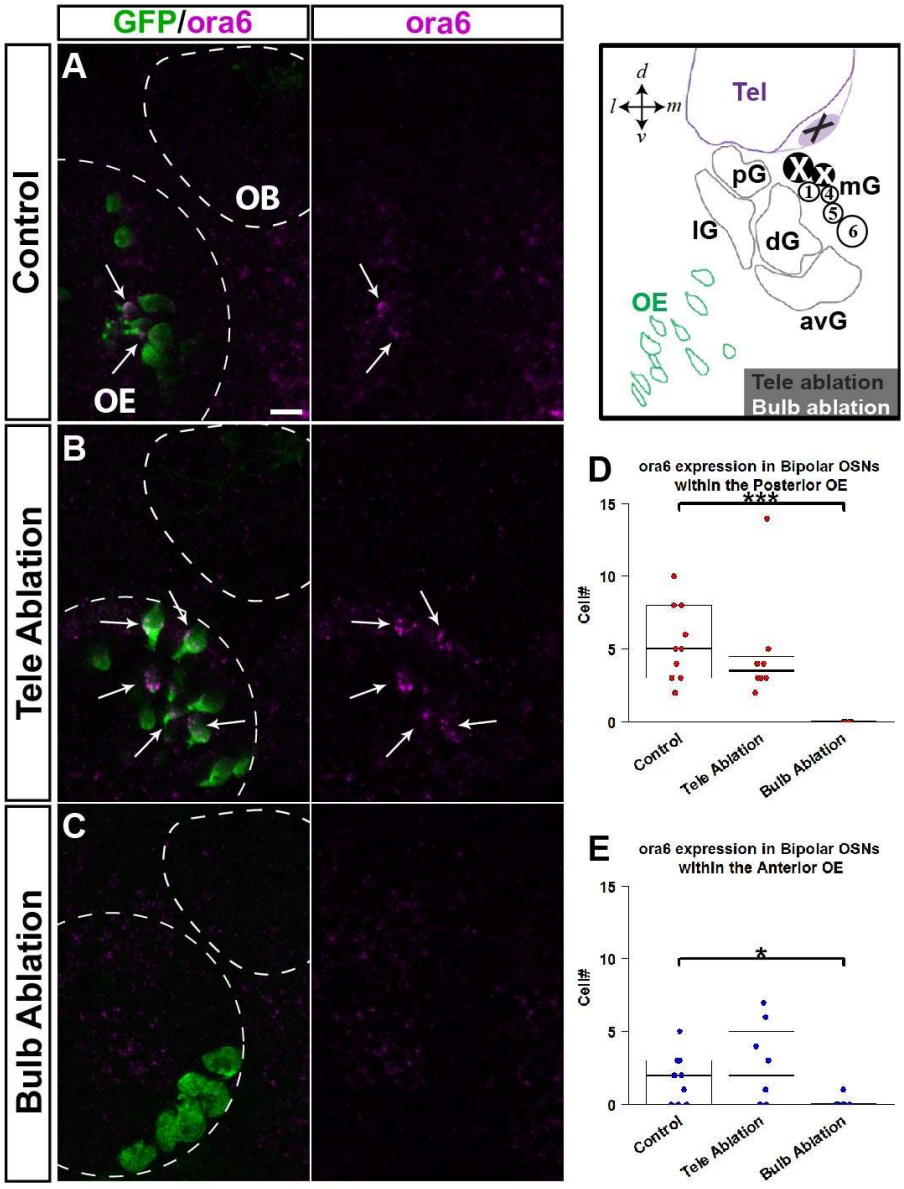

Figure 2.4 ora6 RNA in-situ expression overlaps with OSNs projecting to the OB
ora6 RNA in-situ expression (magenta) and immunofluorescence labeling of GFP (green) in SAGFF91b 5dpf zebrafish larvae. **(A)** ora6 probes overlap with bipolar OSNs in the olfactory epithelium. Arrows highlight co-labeled cells. Schematic: V Tel region (light purple) is ablated (grey X) or bulb glomeruli mG2 and mG3 glomeruli are ablated (white Xs). **(B)** ora6 probes remain even when telencephalon projecting OSNs are ablated. **(C)** ora6 expression drops significantly when bulb projecting OSNs are ablated. **(D**,**E)** The number of ora6 bipolar colabeled OSNs is significantly diminished when the bulb terminals are ablated in the posterior region of the OE (**D**, Wilcoxon signed-rank test, ***$p < 0.0003$) and slightly diminished in the anterior region of the OE **(E**, Wilcoxon signed-rank test, *$p < 0.05$). Results are summarized in Table 2. OB, olfactory bulb; OE, olfactory epithelium; lG, lateral glomeruli; pG, posterior glomeruli; dG, dorsal glomeruli; avG, anteroventral glomeruli; mG1-6, medial glomeruli 1-6; *d*, dorsal; *v*, ventral; *l*, lateral; *m*, medial. Scale bar, 10μm.

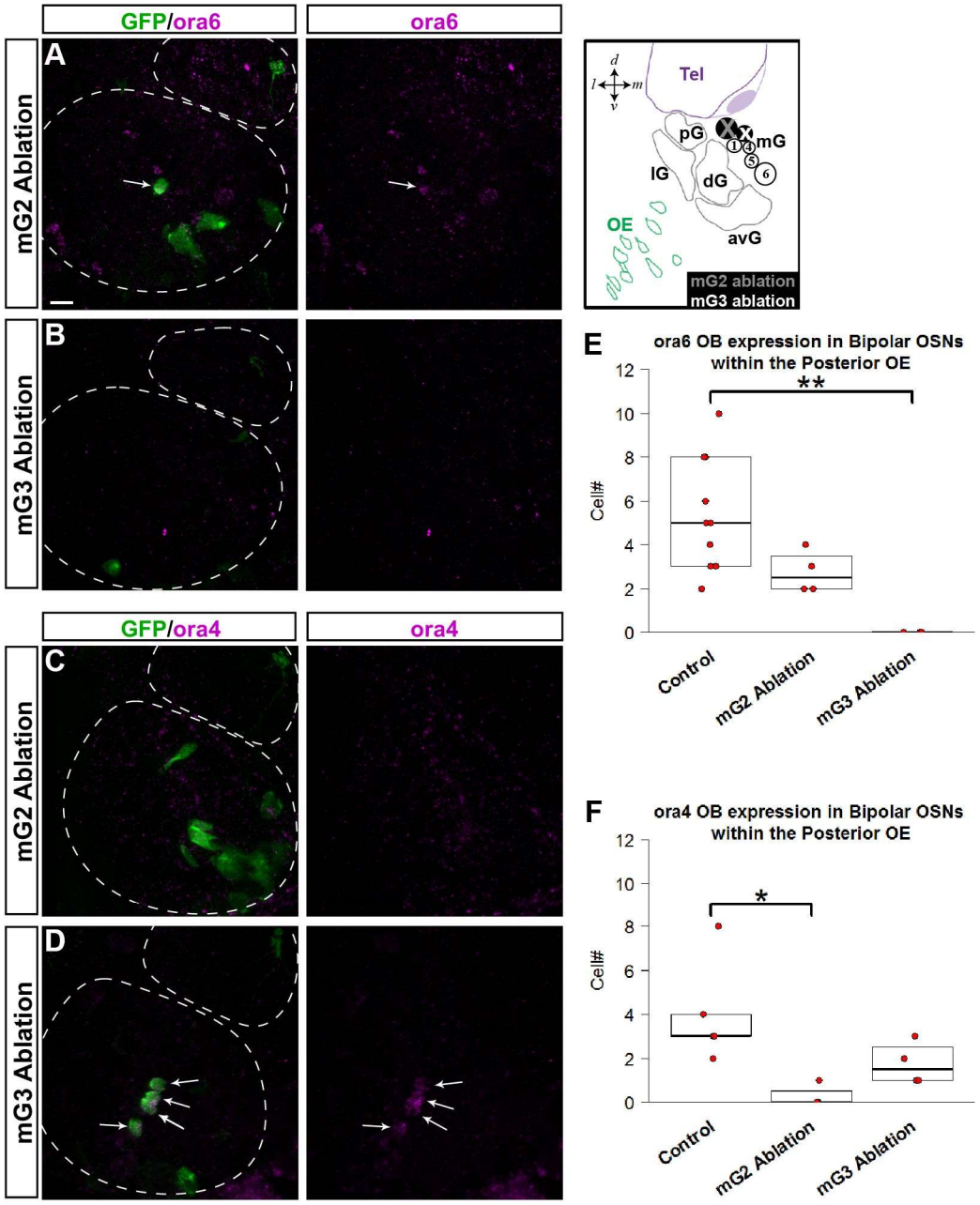

Figure 2.5 ora6 and ora4 RNA in-situ expression overlaps with OSNs projecting to the mG3 and mG2 glomeruli within the OB

ora6 and ora4 RNA in-situ expression (magenta) and immunofluorescence labeling of GFP (green) in SAGFF91b 5dpf zebrafish larvae. **(A)** ora6 probes remain when mG2 projecting OSNs are ablated. Arrows highlight co-labeled cells. Schematic: mG2 is ablated (grey X) or mG3 is ablated (white X). **(B)** ora6 expression drops significantly when mG3 projecting OSNs are ablated. **(C**,**D)** ora4 expression drops when mG2 projecting OSNs are ablated (**C**), but not when mG3 is ablatetd **(D)**. **(E)** The number of ora6 bipolar colabeled OSNs is significantly diminished when the mG3 projecting OSNs are ablated (Wilcoxon signed-rank test, **p < 0.01). **(F)** The number of ora4 bipolar colabeled OSNs is significantly diminished when the mG2 projecting

OSNs are ablated (Wilcoxon signed-rank test, *$p < 0.05$). Results are summarized in Table 3 and 4. OB, olfactory bulb; OE, olfactory epithelium; lG, lateral glomeruli; pG, posterior glomeruli; dG, dorsal glomeruli; avG, anteroventral glomeruli; mG1-6, medial glomeruli 1-6; *d*, dorsal; *v*, ventral; *l*, lateral; *m*, medial. Scale bar, 10μm.

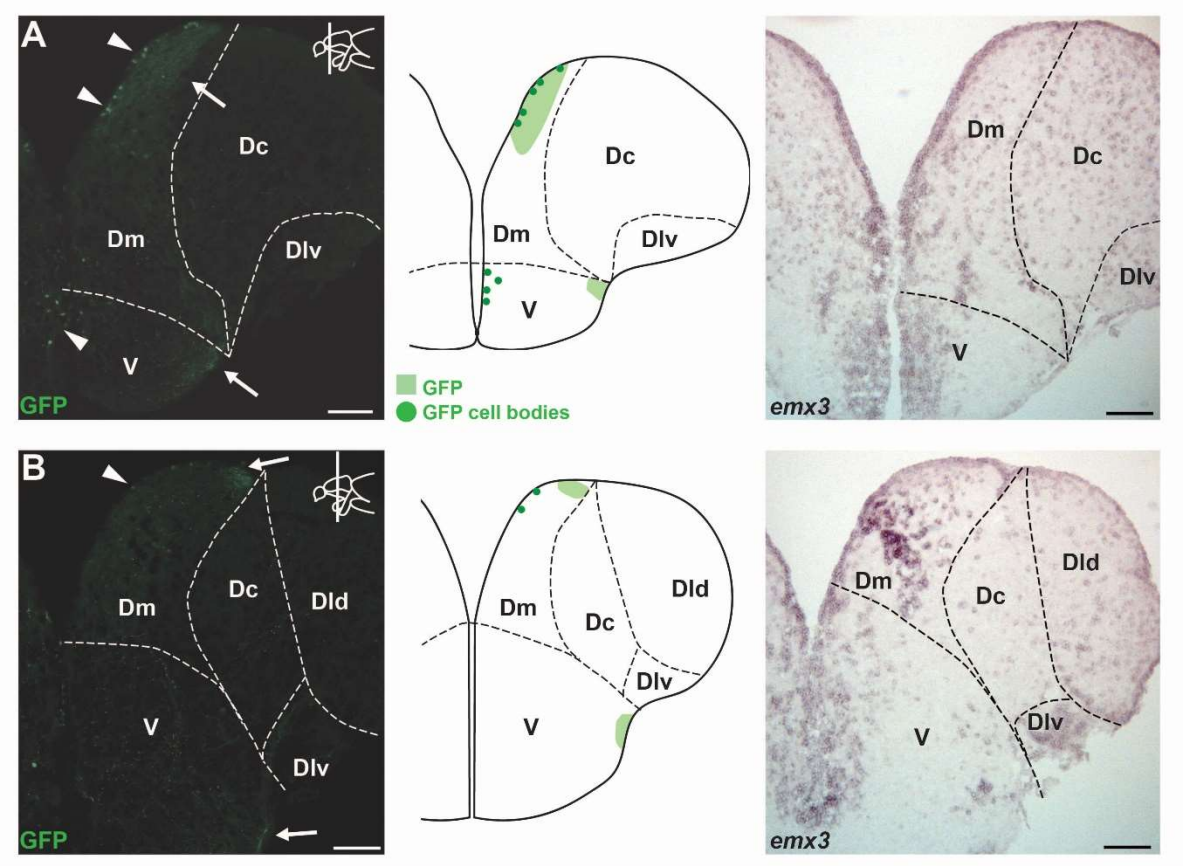

Figure 2.6 Expression of GFP and emx3 in the pallium of adult SAGFF91b fish
Antibodies against GFP and RNA in-situ probes against emx3. (**A**,**B left**) GFP expression in the rostral and caudal sections of the telencephalon. GFP positive cell bodies are seen in the ventral zone of the Dm in both rostral and caudal telencephlon. Cell bodies can also be seen scattered throughout V. (**A**,**B middle**) Summary of the expression pattern of GFP at rostral (**A**) and caudal (**B**) levels of the telencephalon. (**A**, **right**) In the rostral telencephalon, *emx3* expression is present in the ventricular zone of Dm and scattered throughout Dc, Dlv, and V. (**B**, **right**) In the caudal telencephalon, *emx3* expression is strongly present in Dm and Dlv, and scattered throughout Dld and V. Flourescence and brightfield images of cross-sections at the levels indicated through the telencephalon. Dashed lines indicate subdivisions based on previous reports of *emx3* expression. Arrowheads label GFP positive cell bodies. Arrows label GFP positive axon tracts. Dm, medial pallium; Dc, central pallium; Dlv, latero-ventral pallium; Dld, latero-dorsal pallium; V, ventral telencephalon (sub-pallium). Scale bar, 50μm.

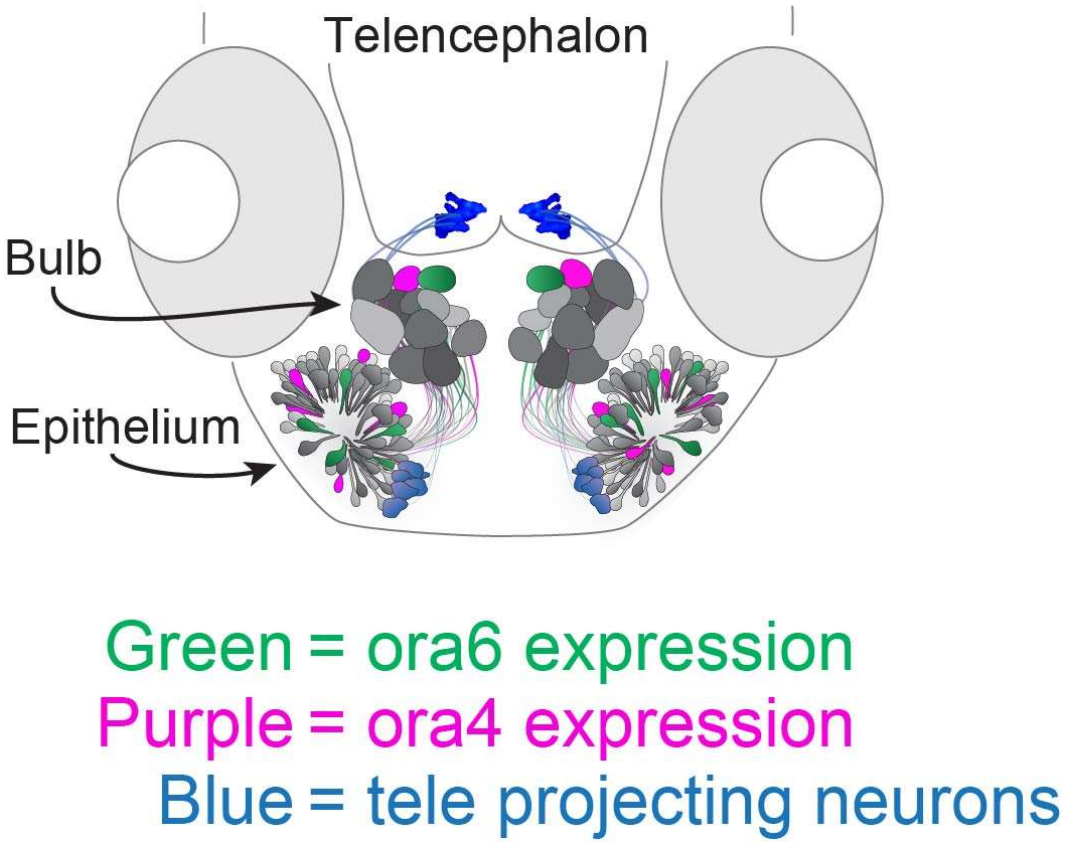

Figure 2.7 Anatomic map of OSNs within the SAGFF91b line
Schematic showing the projection patterns of the three OSN cell types in the 91b line. ora6 and ora4 expression (green and magenta) is observed in bipolar OSNs in the posterior OE projecting to the mG3 and mG2 glomeruli respectively. The telencephalon projecting OSNs (blue) have unipolar cell bodies located in the anterior medial section of the OE.

		Posterior OE					
Number of GFP labeled cells in the SAGFF91b line		Unipolar			Bipolar		
Tele vs Bulb Ablations		no ablation	tele abl	bulb abl	no ablation	tele abl	bulb abl
	mean	7.9	9.3	1.6	5.3	8.3	0.4
	median	7.5	9.0	1.5	4.5	8.0	0.0
	SEM	0.9	0.8	0.4	1.0	1.1	0.2
	n	10	13	14	10	13	14
Kruskal-Wallis test	chi-squared			25.378			25.957
	p-value			3.084E-06			2.310E-06
Mann-Whitney Wilcox Rank Sum test	W		46.5	138		37.5	135
(compared to no ablation)	p-value		0.2612	0.00006912		0.0900	0.0001
		Anterior OE					
	mean	12.4	0.8	11.2	5.2	1.9	0.9
	median	12.5	0.0	10.5	4.5	1.0	0.0
	SEM	1.2	0.3	1.0	0.8	0.7	0.4
	n	10	13	14	10	13	14
Kruskal-Wallis test	chi-squared			25.272			16.016
	p-value			3.253E-06			3.327E-04
Mann-Whitney Wilcox Rank Sum test	W		130	84		111	132.5
(compared to no ablation)	p-value		4.294E-05	0.4262		0.0040	0.0002

Table 1 Cell counts and statistics for GFP positive OSNs in the SAGFF91b line
Statistics for GFP positive cell morphology (unipolar vs bipolar), cell body location (posterior OE vs anterior OE), and axon terminal ablations [telencephalon ablation (tele abl) vs olfactory bulb ablation (bulb abl)]. Highlighted areas correspond to Fig 2.2E and 2.2F.

		Posterior OE					
Number of ora6 GFP double labeled OSNs in the SAGFF(LF)91b line		Unipolar			Bipolar		
Tele vs Bulb Ablations		no ablation	tele abl	bulb abl	no ablation	tele abl	bulb abl
	mean	0.4	0.4	0.0	5.4	4.8	0.0
	median	0.0	0.0	0.0	5.0	3.5	0.0
	SEM	0.2	0.2	0.0	0.8	1.4	0.0
	n	10	8	8	10	8	8
Kruskal-Wallis test	chi-squared			3.3589			17.178
	p-value			1.865E-01			1.861E-04
Mann-Whitney Wilcox Rank Sum test	W		38.5	52		51.5	80
(compared to no ablation)	p-value		0.9145	0.1153		0.3208	0.0002
		Anterior OE					
	mean	0.0	0.0	0.0	1.9	2.6	0.1
	median	0.0	0.0	0.0	2.0	2.0	0.0
	SEM	0.0	0.0	0.0	0.5	1.0	0.1
	n	10	8	8	10	8	8
Kruskal-Wallis test	chi-squared			0.0			6.9031
	p-value			0.0			3.170E-02
Mann-Whitney Wilcox Rank Sum test	W					35.5	66
(compared to no ablation)	p-value					0.7156	0.0125

Table 2 Cell counts and statistics for ora6 GFP double labeled OSNs in the SAGFF91b line, with telencephalon or olfactory bulb ablations

Statistics for GFP positive cell morphology (unipolar vs bipolar), cell body location (posterior OE vs anterior OE), and axon terminal ablations [telencephalon ablation (tele abl) vs olfactory bulb ablation (bulb abl)]. Highlighted areas correspond to Fig 4D and 4E.

		Posterior OE					
Number of ora6 GFP double labeled OSNs in the SAGFF(LF)91b line		Unipolar			Bipolar		
mG2 vs mG3 ablations		no ablation	mG2 abl	mG3 abl	no ablation	mG2 abl	mG3 abl
	mean	0.4	0.5	0.0	5.4	2.8	0.0
	median	0.0	0.5	0.0	5.0	2.5	0.0
	SEM	0.2	0.3	0.0	0.8	0.5	0.0
	n	10	4	4	10	4	4
Kruskal-Wallis test							
	p-value			3.362E-01			3.473E-03
Mann-Whitney Wilcox Rank Sum test							
(compared to no ablation)	p-value		0.6757	0.2781		0.0627	0.0051
		Anterior OE					
	mean	0.0	0.0	0.0	1.9	0.0	0.0
	median	0.0	0.0	0.0	2.0	0.0	0.0
	SEM	0.0	0.0	0.0	0.5	0.0	0.0
	n	10	4	4	10	4	4
Kruskal-Wallis test							
	p-value						1.776E-02
Mann-Whitney Wilcox Rank Sum test							
(compared to no ablation)	p-value					0.0402	0.0402

Table 3 Cell counts and statistics for ora6 GFP double labeled OSNs in the SAGFF91b line, with mG2 or mG3 ablations

Statistics for GFP positive cell morphology (unipolar vs bipolar), cell body location (posterior OE vs anterior OE), and axon terminal ablations [medial glomerulus 2 ablation (mG2 abl) vs medial glomerulus 3 ablation (mG3 abl)]. Highlighted areas correspond to Fig 5E.

		Posterior OE					
Number of ora4 GFP double labeled OSNs in the SAGFF(LF)91b line		Unipolar			Bipolar		
mG2 vs mG3 ablations		no ablation	mG2 abl	mG3 abl	no ablation	mG2 abl	mG3 abl
	mean	1.2	0.0	0.8	4.0	0.3	1.8
	median	1.0	0.0	0.5	3.0	0.0	1.5
	SEM	0.2	0.0	0.5	1.0	0.3	0.5
	n	5	4	4	5	4	4
Kruskal-Wallis test	chi-squared			6.6633			9.1325
	p-value			3.573E-02			1.040E-02
Mann-Whitney Wilcox Rank Sum test	W		20	13		20	17.5
(compared to no ablation)	p-value		0.0108	0.4161		0.0175	0.0786
		Anterior OE					
	mean	0.0	0.0	0.0	0.0	0.0	0.0
	median	0.0	0.0	0.0	0.0	0.0	0.0
	SEM	0.0	0.0	0.0	0.0	0.0	0.0
	n	5	4	4	5	4	4
Kruskal-Wallis test	chi-squared			0.0			0.0
	p-value			0.0			0.0
Mann-Whitney Wilcox Rank Sum test	W		0.0	0.0		0.0	0.0
(compared to no ablation)	p-value		0.0	0.0		0.0	0.0

Table 4 Cell counts and statistics for ora4 GFP double labeled OSNs in the SAGFF91b line, with mG2 or mG3 ablations

Statistics for GFP positive cell morphology (unipolar vs bipolar), cell body location (posterior OE vs anterior OE), and axon terminal ablations [medial glomerulus 2 ablation (mG2 abl) vs medial glomerulus 3 ablation (mG3 abl)]. Highlighted areas correspond to Fig 5F.

References:

Agetsuma, M., Aizawa, H., Aoki, T., Nakayama, R., Takahoko, M., Goto, M., Sassa, T., Amo, R., Shiraki, T., Kawakami, K., et al. (2010). The habenula is crucial for experience-dependent modification of fear responses in zebrafish. Nat. Neurosci. *13*, 1354–1356.

Ahuja, G., and Korsching, S. (2014). Zebrafish olfactory receptor ORA1 recognizes a putative reproductive pheromone. Commun. Integr. Biol. *7*, e970501.

Ahuja, G., Ivandic, I., Saltürk, M., Oka, Y., Nadler, W., and Korsching, S.I. (2013). Zebrafish crypt neurons project to a single, identified mediodorsal glomerulus. Sci. Rep. *3*, 2063.

Ahuja, G., Nia, S.B., Zapilko, V., Shiriagin, V., Kowatschew, D., Oka, Y., and Korsching, S.I. (2014). Kappe neurons, a novel population of olfactory sensory neurons. Sci. Rep. *4*, 4037.

Asakawa, K., Suster, M.L., Mizusawa, K., Nagayoshi, S., Kotani, T., Urasaki, A., Kishimoto, Y., Hibi, M., and Kawakami, K. (2008a). Genetic dissection of neural circuits by Tol2 transposon-mediated Gal4 gene and enhancer trapping in zebrafish. Proc. Natl. Acad. Sci. U. S. A. *105*, 1255–1260.

Asakawa, K., Suster, M., Mizusawa, K., Nagayoshi, S., Kotani, T., Urasaki, A., Kishimoto, Y., Hibi, M., and Kawakami, K. (2008b). Genetic dissection of neural circuits by Tol2 transposon-mediated Gal4 gene and enhancer trapping in zebrafish. Proc. Natl. Acad. Sci. *105*, 1255–1260.

Biechl, D., Tietje, K., Ryu, S., Grothe, B., Gerlach, G., and Wullimann, M.F. (2017). Identification of accessory olfactory system and medial amygdala in the zebrafish. Sci. Rep. *7*, 44295.

Bolstad, B.M., Irizarry, R.A., Astrand, M., and Speed, T.P. (2003). A comparison of normalization methods for high density oligonucleotide array data based on variance and bias. Bioinformatics *19*, 185–193.

Buck, L., and Axel, R. (1991). A novel multigene family may encode odorant receptors: a molecular basis for odor recognition. Cell *65*, 175–187.

Bullard, J.H., Purdom, E., Hansen, K.D., and Dudoit, S. (2010). Evaluation of statistical methods for normalization and differential expression in mRNA-Seq experiments. BMC Bioinformatics *11*, 94.

Chamero, P., Leinders-Zufall, T., and Zufall, F. (2012). From genes to social communication: molecular sensing by the vomeronasal organ. Trends Neurosci. 1–10.

Dulac, C., and Axel, R. (1995). A novel family of genes encoding putative pheromone receptors in mammals. Cell *83*, 195–206.

Eaton, R.C., Lee, R.K.K., and Foreman, M.B. (2001). The Mauthner cell and other identified neurons of the brainstem escape network of fish. Prog. Neurobiol. *63*, 467–485.

Ferreira, T., Wilson, S.R., Choi, Y.G., Risso, D., Dudoit, S., Speed, T.P., and Ngai, J. (2014). Silencing of odorant receptor genes by G protein βγ signaling ensures the expression of one odorant receptor per olfactory sensory neuron. Neuron *81*, 847–859.

Flanagan, K., Webb, W., and Stowers, L. (2011). Analysis of Male Pheromones That Accelerate

Female Reproductive Organ Development. PLoS One *6*, e16660.

Fletcher, R.B., Das, D., Gadye, L., Street, K.N., Baudhuin, A., Wagner, A., Cole, M.B., Flores, Q., Choi, Y.G., Yosef, N., et al. (2017). Deconstructing Olfactory Stem Cell Trajectories at Single-Cell Resolution. Cell Stem Cell *20*, 817–830.e8.

Ganz, J., Kaslin, J., Freudenreich, D., Machate, A., Geffarth, M., and Brand, M. (2012). Subdivisions of the adult zebrafish subpallium by molecular marker analysis. J. Comp. Neurol. *520*, 633–655.

Ganz, J., Kroehne, V., Freudenreich, D., Machate, A., Geffarth, M., Braasch, I., Kaslin, J., and Brand, M. (2014). Subdivisions of the adult zebrafish pallium based on molecular marker analysis. F1000Research *3*, 308.

Gayoso, J.Á., Castro, A., Anadón, R., and Manso, M.J. (2011). Differential bulbar and extrabulbar projections of diverse olfactory receptor neuron populations in the adult zebrafish (Danio rerio). J. Comp. Neurol. *519*, 247–276.

Ghosh, S., Larson, S., Hefzi, H., Marnoy, Z., Cutforth, T., Dokka, K., and Baldwin, K. (2011). Sensory maps in the olfactory cortex defined by long-range viral tracing of single neurons. Nature *472*, 217–220.

Haberly, L.B., and Price, J.L. (1977). The axonal projection patterns of the mitral and tufted cells of the olfactory bulb in the rat. Brain Res. *129*, 152–157.

Hamdani, E.H., and Døving, K.B. (2007). The functional organization of the fish olfactory system. Prog. Neurobiol. *82*, 80–86.

Hansen, A., and Finger, T.E. (2000). Phyletic distribution of crypt-type olfactory receptor neurons in fishes. Brain. Behav. Evol. *55*, 100–110.

Herrada, G., and Dulac, C. (1997). A novel family of putative pheromone receptors in mammals with a topographically organized and sexually dimorphic distribution. Cell *90*, 763–773.

Honkanen, T., and Ekström, P. (1990). An immunocytochemical study of the olfactory projections in the three-spined stickleback, gasterosteus aculeatus, L. J. Comp. Neurol. *292*, 65–72.

Hussain, A., Saraiva, L., and Korsching, S.I. (2009). Positive Darwinian selection and the birth of an olfactory receptor clade in teleosts. Proc. Natl. Acad. Sci. *106*, 4313–4318.

Ihara, S., Yoshikawa, K., and Touhara, K. (2013). Chemosensory signals and their receptors in the olfactory neural system. Neuroscience *254*, 45–60.

Isogai, Y., Si, S., Pont-Lezica, L., Tan, T., Kapoor, V., Murthy, V., and Dulac, C. (2011). Molecular organization of vomeronasal chemoreception. Nature 1–7.

Kawakami, K., Takeda, H., Kawakami, N., Kobayashi, M., Matsuda, N., and Mishina, M. (2004). A transposon-mediated gene trap approach identifies developmentally regulated genes in zebrafish. Dev. Cell *7*, 133–144.

Kawakami, K., Abe, G., Asada, T., Asakawa, K., Fukuda, R., Ito, A., Lal, P., Mouri, N., Muto, A., Suster, M., et al. (2010). zTrap: zebrafish gene trap and enhancer trap database. BMC Dev.

Biol. *10*, 105.

Kermen, F., Franco, L.M., Wyatt, C., and Yaksi, E. (2013). Neural circuits mediating olfactory-driven behavior in fish. Front. Neural Circuits *7*, 62.

Kimmel, C.B., Ballard, W.W., Kimmel, S.R., Ullmann, B., and Schilling, T.F. (1995). Stages of embryonic development of the zebrafish. Dev. Dyn. *203*, 253–310.

Koide, T., Miyasaka, N., Morimoto, K., Asakawa, K., Urasaki, A., Kawakami, K., and Yoshihara, Y. (2009). Olfactory neural circuitry for attraction to amino acids revealed by transposon-mediated gene trap approach in zebrafish. Proc. Natl. Acad. Sci. *106*, 9884–9889.

Langmead, B., Trapnell, C., Pop, M., and Salzberg, S.L. (2009). Ultrafast and memory-efficient alignment of short DNA sequences to the human genome. Genome Biol. *10*, R25.

Liberles, S., and Buck, L. (2006). A second class of chemosensory receptors in the olfactory epithelium. Nature *442*, 645–650.

Liu, K.S., and Fetcho, J.R. (1999). Laser Ablations Reveal Functional Relationships of Segmental Hindbrain Neurons in Zebrafish. Neuron *23*, 325–335.

Matsunami, H., and Buck, L. (1997). A multigene family encoding a diverse array of putative pheromone receptors in mammals. Cell *90*, 775–784.

Medan, V., and Preuss, T. (2014). The Mauthner-cell circuit of fish as a model system for startle plasticity. J. Physiol. Paris *108*, 129–140.

Meyerhof, W., and Korsching, S. (2009). Chemosensory systems in mammals, fishes, and insects. Preface.

Miyamichi, K., Amat, F., Moussavi, F., Wang, C., Wickersham, I., Wall, N., Taniguchi, H., Tasic, B., Huang, Z., He, Z., et al. (2011). Cortical representations of olfactory input by trans-synaptic tracing. Nature *472*, 191–196.

Miyasaka, N., Sato, Y., Yeo, S.-Y., D Hutson, L., Chien, C.-B., Okamoto, H., and Yoshihara, Y. (2005). Robo2 is required for establishment of a precise glomerular map in the zebrafish olfactory system. Development *132*, 1283–1293.

Mombaerts, P. (2004). Genes and ligands for odorant, vomeronasal and taste receptors. Nat. Rev. Neurosci. *5*, 263–278.

Mombaerts, P., Wang, F., Dulac, C., Chao, S., Nemes, A., Mendelsohn, M., Edmondson, J., and Axel, R. (1996). Visualizing an olfactory sensory map. Cell *87*, 675–686.

Mori, K., Kishi, K., and Ojima, H. (1983). Distribution of dendrites of mitral, displaced mitral, tufted, and granule cells in the rabbit olfactory bulb. J. Comp. Neurol. *219*, 339–355.

Nagayama, S. (2010). Differential Axonal Projection of Mitral and Tufted Cells in the Mouse Main Olfactory System. Front. Neural Circuits *4*, 1–8.

Nissanov, J., Eaton, R.C., and DiDomenico, R. (1990). The motor output of the Mauthner cell, a reticulospinal command neuron. Brain Res. *517*, 88–98.

Oka, Y., Saraiva, L., and Korsching, S.I. (2012). Crypt neurons express a single V1R-related ora

gene. Chem. Senses *37*, 219–227.

Oliveira, R.F. (2013). Mind the fish: zebrafish as a model in cognitive social neuroscience. Front. Neural Circuits *7*, 131.

Perathoner, S., Cordero-Maldonado, M.L., and Crawford, A.D. (2016). Potential of zebrafish as a model for exploring the role of the amygdala in emotional memory and motivational behavior. J. Neurosci. Res. *94*, 445–462.

Pfeiffer, W. (1977). The Distribution of Fright Reaction and Alarm Substance Cells in Fishes. Copeia *1977*, 653–665.

Pfister, P., and Rodriguez, I. (2005). Olfactory expression of a single and highly variable V1r pheromone receptor-like gene in fish species. Proc. Natl. Acad. Sci. U. S. A. *102*, 5489–5494.

Del Punta, K., Leinders-Zufall, T., Rodriguez, I., Jukam, D., Wysocki, C.J., Ogawa, S., Zufall, F., and Mombaerts, P. (2002). Deficient pheromone responses in mice lacking a cluster of vomeronasal receptor genes. Nature *419*, 70–74.

Riddle, D.R., and Oakley, B. (1992). Immunocytochemical identification of primary olfactory afferents in rainbow trout. J. Comp. Neurol. *324*, 575–589.

Rousseeuw, P.J. (1987). Silhouettes: A graphical aid to the interpretation and validation of cluster analysis. J. Comput. Appl. Math. *20*, 53–65.

Ryba, N.J., and Tirindelli, R. (1997). A New Multigene Family of Putative Pheromone Receptors. Neuron *19*, 371–379.

Sah, P., Faber, E.S.L., Lopez De Armentia, M., and Power, J. (2003). The amygdaloid complex: anatomy and physiology. Physiol. Rev. *83*, 803–834.

Saraiva, L., and Korsching, S.I. (2007). A novel olfactory receptor gene family in teleost fish. Genome Res. *17*, 1448–1457.

Sato, Y., Miyasaka, N., and Yoshihara, Y. (2005). Mutually exclusive glomerular innervation by two distinct types of olfactory sensory neurons revealed in transgenic zebrafish. J. Neurosci. *25*, 4889–4897.

Sosulski, D., Bloom, M.L., Cutforth, T., Axel, R., and Datta, S. (2011). Distinct representations of olfactory information in different cortical centres. Nature *472*, 213–216.

Speedie, N., and Gerlai, R. (2008). Alarm substance induced behavioral responses in zebrafish (Danio rerio). Behav. Brain Res. *188*, 168–177.

Wakisaka, N., Miyasaka, N., Koide, T., Masuda, M., Hiraki-Kajiyama, T., and Yoshihara, Y. (2017). An Adenosine Receptor for Olfaction in Fish. Curr. Biol. *27*, 1437–1447.e4.

Waldman, B. (1982). Quantitative and Developmental Analyses of the Alarm Reaction in the Zebra Danio, Brachydanio rerio. Copeia *1982*, 1–9.

Welten, M.C.M., de Haan, S.B., van den Boogert, N., Noordermeer, J.N., Lamers, G.E.M., Spaink, H.P., Meijer, A.H., and Verbeek, F.J. (2006). ZebraFISH: Fluorescent In Situ Hybridization Protocol and Three-Dimensional Imaging of Gene Expression Patterns. Zebrafish

3, 465–476.

Zottoli, S.J. (1977). Correlation of the startle reflex and Mauthner cell auditory responses in unrestrained goldfish. J. Exp. Biol. *66*, 243–254.

Chapter 3: A hardwired circuit for olfactory-guided fear in larval zebrafish

In this chapter, the development and analysis of all of the behavioral experiments represents a collaboration with Scott T. Laughlin. S.I. contributed to figures 3.1C and 3.3C,D and is solely responsible for figures 3.5 and Supplementary figure 3.1. S.T.L. created figures 3.1A,B,D-F; 3.2; 3.3A,B; and 3.4.

Background

In nearly every animal model studied to date, chemosensory signals are an important driver of innate behaviors. Knowing the underlying neural circuitry of these behaviors has helped us compare similar behaviors across species. Fruit flies and mice both display innate chemically driven aggressive behaviors that are processed by corresponding olfactory centers in the brain (Ruta et al., 2010; Stowers et al., 2002; Wang and Anderson, 2010). Even within a single animal, we can use the structural differences between learned and innate olfactory behavior circuits to figure out the mechanisms behind a particular behavior. Anxiety and fear can result from a wide variety of sensory inputs and are a common end result of many learned and innate behaviors. Studies examining disorders and mutations of the basolateral amygdala have been shown to cause an altered sense of anxiety in humans and mice (Kim et al., 2014; Truitt et al., 2009). Furthermore, the detection of an alarm pheromone in mice has shown that an innate fear behavior can be driven by a volatile odor (Brechbuhl et al., 2008). Comparing the neural circuitry of innate anxiety in species as diverse as mice, zebrafish and humans can give us a great wealth of knowledge on how fear is organized in the brain and how we can treat anxiety disorders in the future.

Larval zebrafish are a powerful tool for examining the neural circuitry underlying behavior. Their small physical size and transparency enable imaging the entire brain at cellular resolution, even during behavior (Ahrens et al., 2012), and their large clutch size makes them ideal for high-throughput exploration of genetic and pharmacologic modifiers of behavior (Burgess and Granato, 2007; Rihel et al., 2010). Further, zebrafish larvae display a wide array of complex behaviors: they startle (Burgess and Granato, 2007), sleep (Appelbaum et al., 2009; Faraco et al., 2006; Prober et al., 2006; Rihel et al., 2010; Yokogawa et al., 2007), and carefully orient toward prey prior to attack (Gahtan et al., 2005). Zebrafish larvae also have fear-like behaviors, including increased activity upon dark challenge (Emran et al.), dark-avoidance in assays for light/dark preference (Lau et al.), and thigmotaxis (wall-following behavior) (Lockwood et al., 2004; Schnörr et al., 2012). Despite this impressive behavioral repertoire, there are no known olfactory-guided instinctive behaviors in larval zebrafish, limiting the utility of zebrafish for studying olfaction and its downstream neural circuitry.

Here we describe an innate olfactory-guided behavior in larval zebrafish that manifests when larvae are exposed to an extraction of zebrafish skin that contains an alarm pheromone. We show that this behavior is amenable to high-throughput assay and mediated by the olfactory system. This behavior provides a robust platform for examining both olfactory and innate fear/anxiety neural circuitry in the translucent, genetically and pharmacologically tractable zebrafish larva. Furthermore, we can start to identify components of the olfactory system that play a role in alarm behavior

Analysis of innate behaviors in zebrafish larvae have provided detailed insights into the neural circuitry that controls vertebrate behaviors guided by the senses of vision, audition, and somatosensation (Ahrens et al., 2012; Burgess and Granato, 2007; Gahtan et al., 2005; Wyart et al., 2009). Using larval zebrafish to study the neural circuitry underlying olfactory-guided behaviors, however, has been limited by a lack of characterized olfactory-guided behaviors in larval zebrafish. Herein, we describe a combination of olfactory stimulus and behavioral assay that will enable quantitative examination of an olfactory-guided behavior in zebrafish larvae. Based on an innate, olfactory guided fear-like response that occurs in adult zebrafish, the larval fear-like behavior occurs upon olfactory sensation of a zebrafish skin extract containing an alarm pheromone (Jesuthasan and Mathuru, 2008; Mathuru et al., 2012; Parra et al., 2009). We then use this behavior to probe the neural circuitry of the larval zebrafish using our gene trap line, SAGFF91b. By ablating the telencephalon projecting neurons in the SAGFF91b line, we see attenuation of the alarm behavior in larval zebrafish. However, these behavioral results are not significant and remain inconclusive.

Methods

Zebrafish husbandry

Adult fish strains AB (wild type) and fish from the gene trap line SAGFF91b were kept at 28.5 °C on a 14-h light/10-h dark cycle. Embryos were obtained from natural spawnings and were maintained in embryo medium (150 mM NaCl, 0.5 mM KCl, 1.0 mM $CaCl_2$, 0.37 mM KH_2PO_4, 0.05 mM Na_2HPO_4, 2.0 mM $MgSO_4$, 0.71 mM $NaHCO_3$ in deionized (18.0 MΩ·cm) H_2O, pH 7.4) at 25 °C. Embryos and larvae were developmentally staged according to Kimmel and coworkers (Kimmel et al., 1995).

Zebrafish organic skin extraction

Outbred wildtype adult zebrafish were purchased from Aquatica Tropicals Inc. (Plant City, Florida). They were euthanized by tricaine overdose, cooled to 0 °C, rinsed 3x with ice-cold distilled H_20 and frozen at -20 °C. Collections of euthanized zebrafish were exposed to acetone at 1 fish/5 mL for 1 h with gentile agitation and the solution was filtered through cheesecloth, cooled to -20 °C, and filtered again though cheesecloth. The concentration of materials in the skin extract was determined by transferring 250 □l of extract to a tared vial, evaporating the acetone, and weighing the vial. Typical concentrations ranged from 1.25–1.75 mg/ml. The skin extract was used at a final concentration of 4.7 □g/ml.

Individual Open field test

All behavior assays were performed between 10 am and 7 pm at 25 °C. 5 dpf zebrafish in a 10 cm petri dish containing 30 ml embryo media were acclimated to a fluorescent backlight (Gagne Light Box 1012-1) for 1 h prior to behavior assay. At the start of the assay, larvae were transferred to one of 24 transparent wells (22 mm diameter, 2.75 mm height) with equivalent fluorescent backlighting containing 500 l of a test solution while being recorded for four minutes (1920x1080 pixels at 24 frames per second with a Sony NEX-5n camera and 35 mm lens).

Large Group open field test

~50 4dpf zebrafish were raised in one 10cm petri dish at 28.5°C containing 30ml embryo media. Fish were then sequentially and randomly placed into two separate 10cm dishes, each backlit

with fluorescent light (Gagne Light box 1012-1) containing 20ml of embryo media. Fish were given one hour to acclimate to the new conditions before 200µl of skin extract or embryo media (vehicle control) was added to the dish. Skin extract was used at a final concentration of 4.7µg/ml. Dishes were manually swirled immediately after the solutions were added. 2min recordings were taken as each solution was being added (30 seconds before and 1 minutes 30 seconds after solutions were added) and after 1 hour. Positions of all fish were recorded at the end of each before and after video. Only fish physically touching the outer wall of the petri dish were considered to be showing thigmotaxsis.

Behavior quantification

AVCHD format video files were reformatted to MP3 (ArcSoft MediaConverter 7) and the larvae's movement were converted to Cartesian coordinates as a function of time using a custom ImageJ macro. The data were imported to excel and converted to distances traveled in the central region of the assay chamber (defined as a circle in the assay chamber's center with a radius 70% the radius of the assay chamber).

Olfactory nerve lesion

The olfactory system was visualized by lipophilic dye (DiO, DiD) fluorescence. Zebrafish were grown in the presence of phenylthiourea (PTU, 131 µM) from 0–3 dpf. For experiments to control for successful olfactory nerve ablation, 3 dpf zebrafish were immersed in a 1 µM solution of DiO in embryo medium with PTU at 25 °C for 24 h. The fish were washed once by transfer to fresh solution of embryo medium with PTU, anesthetized with tricaine, and mounted in 1% ultralow melting point agarose (Invitrogen, 16520-050) to expose the dorsal surface of the olfactory system. One olfactory nerve was ablated by irradiation at 800 nm (50-75% power at 2 frames/sec, Zeiss LSM 780 NLO AxioExaminer), the larvae were freed from agarose, immersed in a 1 µM solution of DiD in embryo medium plus PTU for 18 h at 25 °C and then imaged by confocal microscopy.

For experiments to determine the role of the whole olfactory system on the larval zebrafish response to alarm pheromone, zebrafish were grown in the presence of 131 µM PTU from 0–3 dpf. At 3 dpf, zebrafish were immersed in a 1 µM solution of DiO in embryo medium (without PTU) at 25 °C for 24 h. The fish were washed once by transfer to fresh solution of embryo medium, anesthetized with tricaine, and mounted in 1% ultralow melting point agarose to expose the dorsal surface of the olfactory system. Both olfactory nerves were destroyed by irradiation at 800 nm (50-74% power at 2 frames/sec) and the larvae were freed from the agarose (larvae spent 50–60 min embedded in agarose during this procedure), transferred to fresh embryo medium (without PTU), and allowed to recover for 18 h prior to behavioral assay. For mock lesion experiments, the above protocol was followed except that the olfactory nerve was not destroyed with laser irradiation. Instead, fish were mounted in ultralow melting point agarose, incubated at ambient temperature for 60 min, freed from agarose, and allowed to recover for 18 h.

For experiments to determine the role of the telencephalon projections and the two olfactory bulb glomeruli, mG2 and mG3, on the larval zebrafish response to alarm pheromone, zebrafish from the gene trap line SAGFF(LF)91b were grown in the presence of 131 µM PTU from 1-3 dpf. At 4dpf, the fish were anesthetized with tricaine, and mounted in 1% ultralow melting point agarose with the dorsal surface of the olfactory system exposed. Olfactory bulb glomeruli, mG2 or mG3,

or the axons of the telencephalon projection neurons were destroyed by creating regions of interest (ROI) around the structures in question and irradiating at 800nm (75% power at 2 frames/sec). Larvae were then freed from the agarose, transferred to fresh embryo media and allowed to recover for two days. Behavior experiments were conducted on 6dpf larvae.

Statistical analysis

Statistical analysis and graphing were performed using Microsoft Excel 2010. Student's *t*-tests were performed to analyse adult zebrafish behaviors in the novel tank diving test, and larval zebrafish thigmotaxis in the open field test. Data are represented as mean +/- the standard error of the mean.

Results

The zebrafish alarm pheromone is produced by specialized club cells in adult zebrafish skin (Pfeiffer, 1977) and is released upon skin rupture into the surrounding water or an experimental solution called "skin extract". When fish are exposed to skin extract, they display a characteristic fear-like response involving darting and diving behaviors. Preparation of the aqueous extraction of zebrafish skin involves making shallow incisions in the fish's skin and soaking them in water. We found this procedure prone to producing batches of skin extract with highly variable behavioral activities. Thus, we simplified the skin extraction procedure by using an organic solvent, acetone, instead of water. Acetone skin extraction serves several purposes: it permeabilized the outer layers of the zebrafish skin, solubilizes the small molecule components, removes most macromolecular components, and improves batch-to-batch extraction reliability. Using the organic skin extraction, we first confirmed that it retained activity in adult zebrafish with the novel tank diving assay that is often used to characterize aqueous skin extract preparations (Egan et al., 2009). In the novel tank diving assay, adult zebrafish were transferred from a home tank to a new tank that contains control (vehicle-treated water), or organic skin-extract treated water, and their movements were recorded (Fig 3.1A). Zebrafish assayed in the novel tank diving assay spend more time near the bottom of the tank when stressed or afraid (Egan et al., 2009). In response to organic skin extract in this assay, fish spent significantly more time near the bottom of the tank than vehicle-treated control fish (Fig 3.1B), indicating that the active molecule or molecules are present in the hydrophobic skin extraction and are likely acetone soluble small molecules.

We next sought to examine the effects of organic skin extract on larval zebrafish behaviors. Our attempt to mimic the novel tank diving assay proved unfruitful, as the larvae's starting vertical positions were highly variable and did not reliably change with the addition of the skin extract solution (Data not shown). Thus, we attempted to apply a well-characterized and robust behavior assay for fear and anxiety that is effective in many organisms to larval zebrafish: the open field test. In the open field test, a subject is placed into an arena and their movement is recorded. In species across the animal kingdom, including humans (Kallai et al., 2007), primates (Ferguson and Bowman, 1990), rodents (Carola et al., 2002), and both adult (Grossman et al., 2010) and larval (Schnörr et al., 2012) zebrafish, the level of anxiety in the subject is proportional to the level of thigmotaxis, *i.e.*, the distance moved near the edges of the test arena. To determine the suitability of the open field test for measuring behavioral responses to organic skin extract, we transferred individual five day post fertilization (dpf) zebrafish larva to circular wells that

contained organic skin extract or control solution. We recorded the movements of the larvae with a video camera for four minutes, and then analyzed the behaviors according to several parameters: the distance of the fish from the edge of the well over time, the distance moved in the central region of the well, and the total distance moved. Examining the representative trace of the control versus organic skin extract-treated fish's movements over the course of the assay suggests that the larvae respond to skin extract by limiting their exploration of the central region of the plate (Fig 3.1C). Quantifying the behaviors reveals that the organic skin extract-treated fish spend more time near the edge of the well over all time points of the assay, but especially during the beginning (Fig 3.1D). Further, by examining the distance moved in the central region of the plate, thereby limiting the effects of any fish with limited movement on the results of the assay, we found that organic skin extract treated fish explored the central region significantly less than vehicle control, indicating heightened thigmotaxis (Fig 3.1E). Importantly, the differences between control and skin extract-treated fish cannot be explained by a simple reduction in the distance moved between the two populations, because there was no significant difference in these values (Fig 3.1F). Further, the behavioral response to skin extract was present in free swimming larvae of different developmental ages, ranging from 4 to 7 days post fertilization (Data not shown). Interestingly, the intensity of the response did not scale directly with increasing concentrations. At very high concentrations of skin extract, the fish explored the test chamber to the same extent as the control population (Data not shown). This result could reflect an alternative behavioral response to non-fear inducing molecules (e.g., feeding cues), or an alternate response to high concentrations of the fear-causing molecules. Regardless, the thigmotaxis response at intermediate concentrations was robust.

In addition to observing thigmotaxsis behavior in isolated fish, we also observed thigmotaxsis behaviors when large groups of fish are placed together. Open field tests using large clutches have been used to detect cAMP-induced anxiety in three day old fish (Lundegaard et al., 2015). We have adapted this assay to observe the effects of skin extract. In these "large group" open field tests, two groups of fish are taken from the same clutch and placed in 10cm petri dishes of either control solution (embryo media alone) or skin extract solution (embryo media plus skin extract). We recorded the positions of the fish before and after adding (one hour) the control or skin extract solution. Fish were determined to be thigmotaxing only if they were directly touching the walls of the petri dish (Fig 3.S1A, yellow dots). We observed a significant increase in the percentage of fish contacting the walls of their dish when exposed to skin extract only (Fig 3.S1B). This result agrees nicely with our previous observation of individual open field test. Both assays together show that larval fish are more likely to position themselves at the edge of their dish when they are exposed to alarm pheromone containing skin extract. This behavior is independent of the size of the dish and the presence of other fish in close proximity.

The observed larval-age innate response to an olfactory stimulus is unprecedented in zebrafish, and in the case of alarm pheromone induced fear behaviors, has not been observed in any species of fish at a larval age. However, the behavioral responses to alarm pheromones have been an area of intense interest in juvenile and adult fish. Several labs have posited that active fear-causing molecules in skin extract are the molecules hypoxanthine N-oxide (Brown et al., 2000; Parra et al., 2009; Pfeiffer and Lemke, 1973), and one report suggests the glycosaminoglycan chondroitin sulfate (Mathuru et al., 2012). Thus, we sought to determine if these proposed alarm pheromones could be the components of the organic skin extract solution that elicit behaviors in larval

zebrafish. We directly analyzed the effects of hypoxanthine N-oxide and chondroitin sulfate on the behavior of larval zebrafish in the open field test. Larval zebrafish were added to wells containing vehicle control or various concentrations of either hypoxanthine *N*-oxide (Fig 3.2A) or chondroitin sulfate from shark fin (Fig 3.2B). In both cases, the molecules did not elicit behavior similar to skin extract-evoked behaviors in larvae. The organic skin extract preparation has activity in both larval and adult zebrafish and both hypoxanthine *N*-oxide and chondroitin sulfate fail to recapitulate the behavior. These results suggest that components of organic skin extract are the true anxiety inducing molecules, or at least, a major component of the active component that acts via a pathway that is conserved throughout development.

We next explored the sensory modality that transmits the behavioral response. In adult fish, crude aqueous skin extract and chondroitin sulfate exert their behavioral effects via the olfactory system. However, there are many explanations for an altered behavioral response upon exposure of larval zebrafish to an extraneous substance. A general onslaught of chemical stimuli is unlikely to be the cause of the observed behavior given the decrease in the response at high concentrations of skin extrac. Nevertheless, we directly assessed this possibility by examining the behavioral responses of larval fish in the open field test to a complex mixture of molecules, an extraction of their food, and we observed no behavioral difference between vehicle control and treated fish (data not shown).

To examine whether olfactory sensation of molecules in the organic skin extract preparation causes thigmotaxis behavior, we lesioned the olfactory nerve, which carries information from the olfactory epithelium to the olfactory bulb. To visualize the olfactory nerve, we labeled the olfactory epithelia at 3 dpf by bathing fish in a solution of the lipophilic fluorescent dye, DiO. This dye labels the membranes of olfactory sensory neurons, revealing their axon tracts into the olfactory bulb. At 4 dpf, the zebrafish larvae we mounted in 1.5% low melting point agarose and their olfactory nerves were lesioned with localized high-intensity illumination with a Ti-Sapphire laser. In a control experiment, the success of the ablation was determined by ablating one olfactory nerve, transferring the fish to a red-shifted variant of DiO, DiD, and then imaging the fish by confocal microscopy 24 h later (Fig 3.3A). To control for alterations in fish behavior unrelated to the lesion, we mock lesioned a population of fish and examined their responses to skin extract in the open field test, finding that these fish displayed behavioral responses to skin extract similar to a strict control population (Fig 3.3B). We then lesioned both olfactory nerves in a population of fish and examined their behavioral responses to organic skin extract in the open field test. As shown in Fig 3.3C, ablation of the olfactory nerve attenuated the response of larval zebrafish to the organic skin extract, suggesting that the behavioral response to skin extract is transmitted by olfaction.

Thigmotaxis in the open field test correlates with anxiety in many species, including human, mice, rats and even larval zebrafish in a similar assay, suggesting that the observed behavior represents a fear response. However, a general aversive response to irritants present in skin extract could be another explanation for the observed larval thigmotaxis behavior. To address this possibility, we examined the responses of larval zebrafish in the open field to a known irritant, mustard oil (Prober et al., 2008). Five dpf fish were assayed in open field test chambers containing skin extract, mustard oil, or vehicle control solutions. Interestingly, the larvae exposed to mustard oil displayed a fundamentally different response than fish exposed to either

skin extract or vehicle. Compared to control, mustard oil-treated larvae moved significantly further during the first 10 s of the assay, and significantly less during the later time points. There was no significant difference in the distance moved at any time point when control and skin extract exposed larvae were compared (Fig 3.4A). These data suggest that the observed behavior cannot be attributed to a general avoidance response in the open field test.

Finally, to determine if the unique neural projections of our previously reported SADFF91b gene trap line play a role in the alarm behavior, we carried out a series of ablations to identify which, if any, neurons affect innate fear. At 4dpf, the zebrafish were mounted in low melting point agarose and either the mG2 and mG3 glomeruli within the olfactory bulb or the axons projecting to the telencephalon were ablated with localized high intensity 800nm laser light (Fig 3.5A-C). After 48 hours of recovery we examined the different fish populations' responses to skin extract. Since we did not see a change in behavior with the bulb ablations we used these ablations as an internal control. As shown in (Fig 3.5D left), ablation of the telencephalon projecting neurons lowered the effectiveness of the alarm behavior significantly, at first. This suggests that these unique cells bind to and are activated by compounds driving innate fear. It also suggests that this behavior is mediated by a circuit that is shorter and faster than any other olfactory circuit known in the zebrafish.

However, repeated experiments have not displayed the same robust results (Fig 3.5D middle, right). These results showed no significant difference between any group, control or skin extract, unablated or ablated. Experiments demonstrating a possible role of the extrabulbar projections have so far been inconclusive. Further comparisons in different conditions may be needed in order to obtain more robust results.

Discussion

Larval zebrafish have become a powerful tool for the analysis of the neural basis of behavior. Our data show that zebrafish adults and larvae display an olfactory-guided thigmotaxis behavior in response to exposure of a zebrafish skin extraction that contains an alarm pheromone. By lesioning the olfactory nerve, we see a loss of the thigmotaxsis behavior showing that the behavior is olfactory driven. The thigmotaxis behavior suggests that the observed behavior represents a larval fear response. Furthermore, the ablation of the telencephalon projecting cells in the SAGFF91b line may cause a slight drop in the thigmotaxis response. This drop however, was fairly inconsistent and didn't conclusively demonstrate a connection between telencephalon projecting cells and thigmotaxsis. These inconsistencies do not nullify our hypothesis that the telencephalon plays a role in fear behavior. Rather they prevent us from making a definite conclusion that the telencephalon does play a role. There is simply not enough significant data to make an interpretation. While we have tried to identify the source of the inconsistencies it is unclear what exactly is causing the problem. Control fish (not ablated and not exposed to skin extract) seem to be thigmotaxing for some reason that we cannot identify. We have tried to pinpoint exactly what may be causing the fearful response (temperature, room placement, batch effects of skin extract, concentration of salts in embryo media, sound) but the cause remains unknown. The behavior does still fit the model, but we simply do not have enough data to make

a definite conclusion. This olfactory-guided instinctive thigmotaxsis behavior in larval zebrafish has allowed us to examine olfactory as well as innate fear neural circuitry.

Comparisons between the structures of alarm circuitry in the brains of different species can reveal interesting evolutionary conservations. The Grüneberg ganglion cells in mice reside in the rostral region of the olfactory cavity. These cells are important for detecting odors that elicit fear responses in conspecifics (Brechbuhl et al., 2008; Grüneberg, 1973). Interestingly, these primary olfactory neurons are unipolar, much like the telencephalon projecting cells in zebrafish. The telencephalon projecting neurons also occupy a distinct region in the medial anterior olfactory epithelium. While this isn't equivalent to the rostral area of the nasal cavity in mice, it does shown the first example of special segregation of primary olfactory neurons in the zebrafish larvae. Perhaps the most important aspect of the telencephalon projecting neurons is that the area these neurons project to in the telencephalon is near the zebrafish amygdala, a primary center for fear processing in animals (Biechl et al., 2017; Ganz et al., 2014; Truitt et al., 2009; Tye et al., 2011).

The amygdala lies at the heart of most fear circuits in mammals, including mice, rats and humans. In fMRI studies, enhanced amygdala-prefrontal functional connectivity has shown a strong correlation with effective treatments of Social Anxiety Disorder (Young et al., 2017). Children with Fragile X syndrome have a mutation in the FMR1 gene, which is an mRNA binding protein essential for the transport and translation of 4-8% of GABAergic synaptic proteins in the amygdala (Bassell and Warren, 2008). This results in reduced fear recognition due to a failure to modulate fear-specific amygdala activation (Kim et al., 2014). In FMR1 knockout mice, inhibitory neurocircuitry in the amygdala is impaired, and in rats with GABAergic lesioning in the basolateral amygdala (BLA), fear/anxiety behaviors are elevated in behavioral assays such as the social interaction test and elevated plus maze (Olmos-Serrano et al., 2010; Truitt et al., 2009). Furthermore, the open field test has been used as a useful test to examine the detailed neurocircuitry between the BLA and the centromedial amygdala (CeM) using optogenetic activation and suppression (Tye et al., 2011). These studies have focused on the role of the amygdala in fear output, or the resulting behavior after many sensory signals have been integrated. Our understanding of fear input is just as important for comparing fear processing systems between species and understanding how our own brain interprets varying fear signals.

The various olfactory systems in the mammalian brain provide an ideal way to compare innate behaviors across and within species. In the mouse, the two main epithelial organs, the main olfactory epithelium (MOE) and the vomeronasal organ (VNO), house over 6 different subsystems of chemosensory neurons that can detect innate social cues (Bear et al., 2016). Main olfactory receptors and TAARs expressed within the MOE can detect social cues that result in aversion and attractive behavior (Bader et al., 2012; Dewan et al., 2013). Interestingly, VR1 and VR2 receptors expressed in the VNO also detect social cues from kairomones, pheromones, and hormones emitted from predators and conspecifics, resulting in a variety of fear, aggressive, and attractive social behaviors (Chamero et al., 2007; Isogai et al., 2011; Papes et al., 2010). How and why do these different olfactory systems encode overlapping social behaviors even though their circuitry is so different? Olfactory sensory neurons in the MOE project onto the main olfactory bulb (MOB) in a highly conserved set of glomeruli while neurons in the VNO sends

projections to the accessory olfactory bulb (AOB) in a distributed pattern varying between organisms (Mombaerts et al., 1996; Wagner et al., 2006). Furthermore, each of these systems sends projections to different subnuclei in the amygdala. Projections form the MOB project onto the cortical amygdala while the AOB sends projections mainly to the medial amygdala (Bergan et al., 2014; Petrovich et al., 2001; Sosulski et al., 2011). Understanding why such distinct structural patterns are used to interpret social cues may reveal key insights into how fear behaviors have evolved and how anxiety disorders arise in humans.

Many explanations have been suggested for why these different subsystems exist. Detecting differences in the characteristics of the signaling molecule itself (small molecule vs large protein) and in the way molecules are encoded (single odorant vs. large mix of odorants) may drive some of the observed differences between how the VNO and the MOE systems are encoded. Others hypothesize that the MOE system detects a narrow range of cues with high selectivity and the VNO system detects a narrow range of cues with high selectivity, regardless of the size and mix of odorants involved (Dulac and Wagner, 2006). Analyzing the structural differences of olfactory social cues in the zebrafish will provide an additional level of understanding in this area. Until now there has never been any behavioral assay used to probe olfactory driven fear in larval zebrafish. Additionally, until now there has never been a set of neurons discovered that project directly from the OE to the telencephalon. Together these two discoveries can be used to probe how the zebrafish brain has evolved to detect olfactory driven social cues. Probing the new class of telencephalon projecting neurons may shed light on how innate fear behaviors evolved and explain the role of the many mammalian olfactory subsystems.

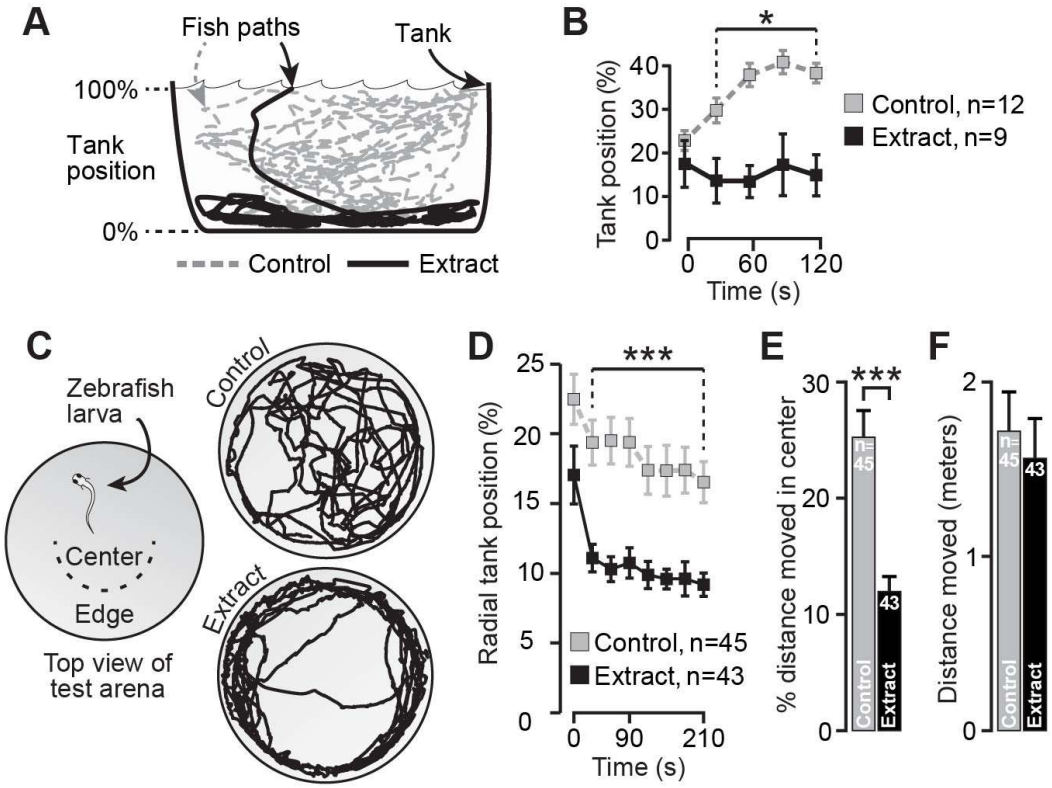

Figure 3.1: 5 dpf larval zebrafish exhibit thigmotaxis when exposed to a skin extract containing an alarm pheromone.

(**A**) The novel tank diving test for examining behavioural responses of adult zebrafish to an organic (acetone) extraction of zebrafish skin. Single adult fish were transferred to novel tank containing an organic skin extract (Extract) or a control solution (Control) and their movements were recorded. (**B**) Adult zebrafish that were exposed to the organic skin extract restricted their movement to the bottom portion of the tank compared to fish exposed to control. (**C**) The open field test for examining behavioural responses of larval zebrafish to an organic extraction of zebrafish skin. 5 dpf larval zebrafish are transferred into a novel circular well that contains skin extract or a control solution and their movements in the x-y plane are recorded from above. (**D**) Average radial position (Center, 100%; edge, 0%) in 5-s bins of fish exposed to skin extract or control solutions in the open field test. (**E**) Plots of the total movement of fish exposed to skin extract or control solutions in the open field test divided by their movement in the central region. (**F**) Plot of the total distance moved of fish exposed to control or skin extract in the open field test. Error bars represent SEM. *, $p \leq 0.05$. ***, $p \leq 0.001$

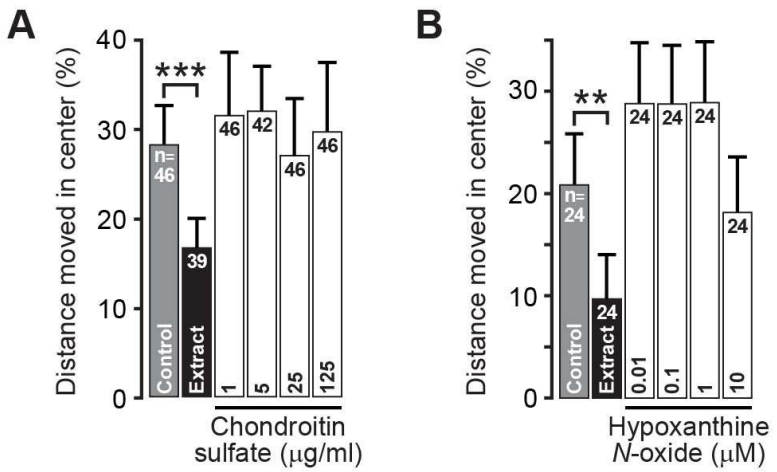

Figure 3.2: Larval zebrafish thigmotaxis behaviors are not caused by putative adult zebrafish alarm pheromones.
(**A**) Open field test responses of 5 dpf zebrafish to vehicle conrol, alarm pheromone-containing skin extract, and varying concentrations of chondroitin sulfate from shark fin. (**B**) Open field test responses of 5 dpf zebrafish to vehicle control, alarm pheromone-containing skin extract, and various concentrations of hypoxanthine *N*-oxide. Error bars represent SEM for samples sizes indicated in the upper portions of each bar. **, $p \leq 0.01$. ***, $p \leq 0.001$.

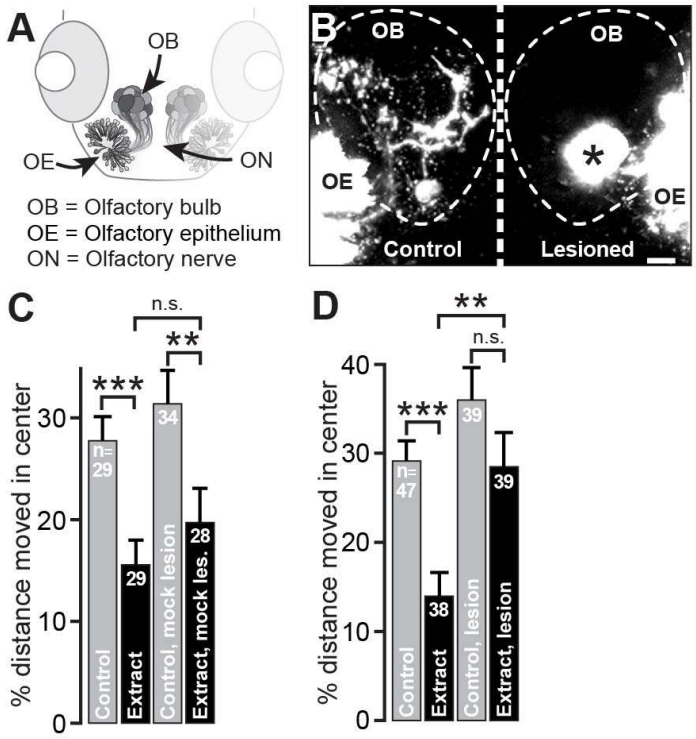

Figure 3.3: Alarm pheromone behaviors are mediated by the olfactory system.
(**A**) Schematic diagram showing the layout of the olfactory system in larval zebrafish looking down on the head. (**B**) Laser ablation of the olfactory nerve persists for 24 h. An olfactory nerve in 4 dpf zebrafish was ablated by 2 photon laser irradiation and then the effect of the lesion on the olfactory system was visualized by immersing the fish in a solution of DiD and imaging the olfactory system at 5dpf. (**C**) A control population, or a mock ablated population were assayed for their responses to alarm pheromone-containing skin extract in the open field test. (**D**) A control population, or a population of 5 dpf fish that had both of their olfactory nerves lesioned at 4 dpf, were assayed for their responses to alarm pheromone containing skin extract in the open field test. OE, olfacroty epithelium. OB, olfactory bulb. *, lesion site. Error bars represent SEM for samples sizes indicated in the upper portions of each bar. N.s., not significant. **, $p \leq 0.01$. ***, $p \leq 0.001$. Scale bar in B, 10μm.

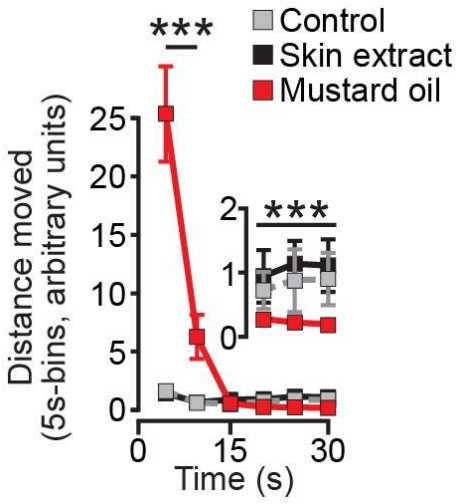

Figure 3.4 Larval zebrafish alarm pheromone response represents fear.
Distances moved in 5-s bins for 5 dpf fish exposed to control, alarm pheromone-containing skin extract, or the irritant mustard oil (n = 24 larvae for each treatment). Inset is a blow-up of time points 20-30 s. Error bars represent SEM, ***, $p \leq 0.001$

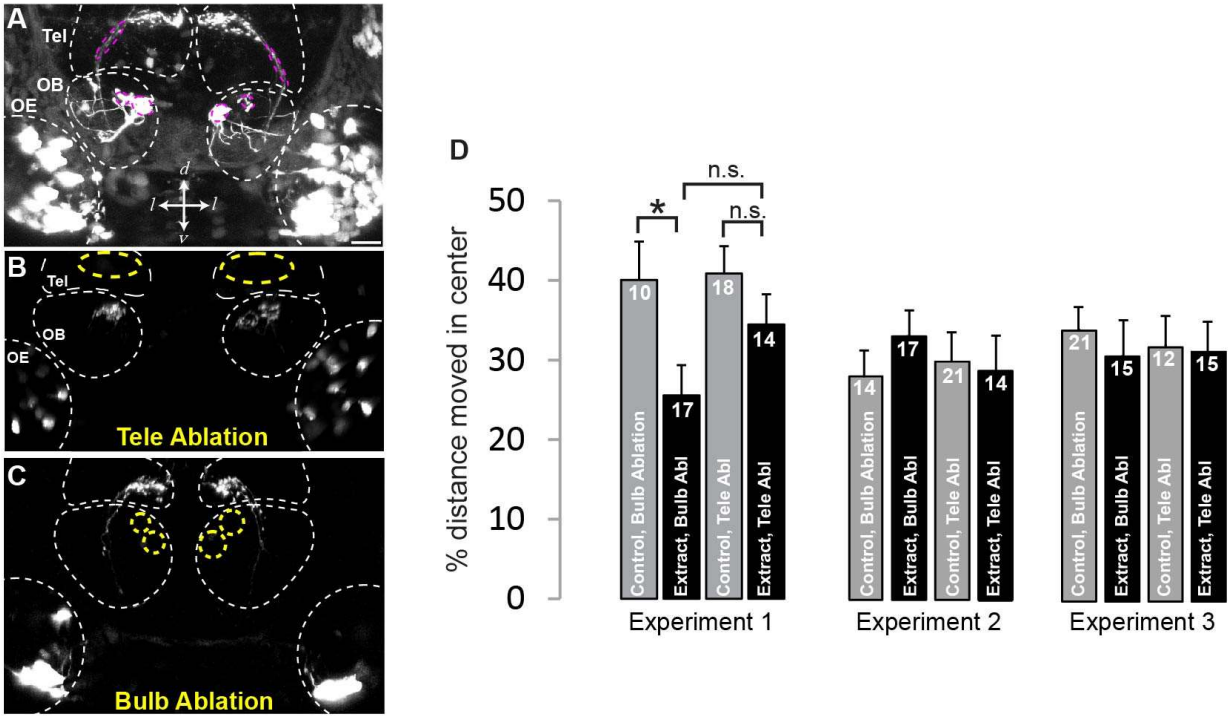

Figure 3.5 Alarm pheromone behaviors are partially mediated by the telencephlon projections.
(**A**) Control fish showing sites of laser ablation of the medial glomeruli, mG2 and mG3, or telencephalon projections. Each ablation was done in 4 dpf zebrafish by 2 photon laser irradiation and then the effect of the lesion on the olfactory system was visualized by the absence of gfp signal at 6dpf. Pink star (*), lesion sites for mG2 and mG3. Pink circles, lesion sites for the telencephalon projections. Yellow circles, sites of telencephalon terminals. (**B**) Results of a telencephalon projection ablation. Yellow circles, estimated sites of where telencephalon terminals should be. (**C**) Results of the bulb ablations of mG2 and mG3. Yellow circles, estimated sites of where mG2 and mG3 terminals should be. (**D**) Three experiments of 6 day old fish, which had either bulb glomeruli (mG2 and mG3) or telencephalon projections ablated at 4 dpf, were assayed for their responses to alarm pheromone containing skin extract in the open field test. Left, telencephalon ablation lowered the effectiveness of the alarm pheromone significantly. Middle and right, further experiments did not replicated significant results. OE, olfactory epithelium. OB, olfactory bulb. Tel, telencephalon. Error bars represent SEM for samples sizes indicated in the upper portions of each bar. n.s., not significant. *, $p \leq 0.05$. Scale bar in A, 20μm.

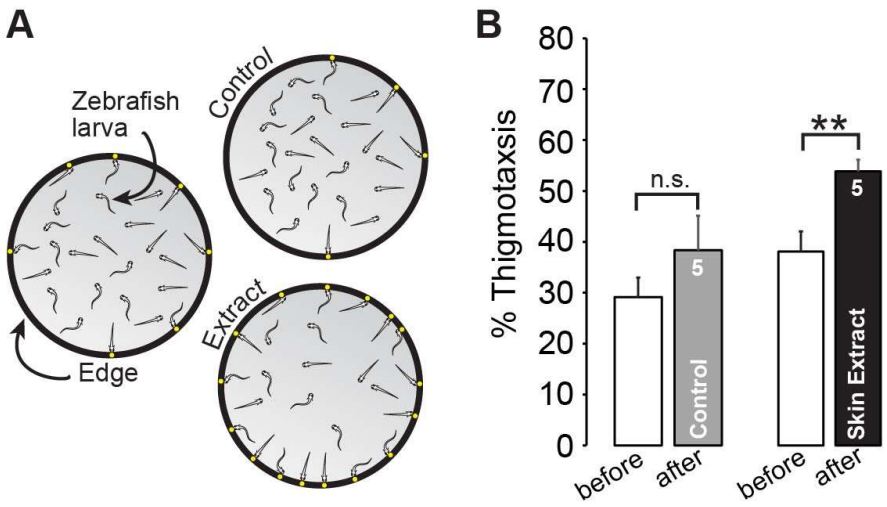

Supplemental Figure 3.1 4 dpf larval zebrafish exhibit thigmotaxis when placed with many other fish larvae and exposed to skin extract.
The open field test for examining behavioural responses of larval zebrafish when grouped with other fish larvae. (**A**) 4 dpf larval zebrafish are transferred from a dish of approx. 50 fish into two novel circular 10cm wide dishes containing either skin extract or a control solution. The percentage of fish touching the edge of the dish after one hour was recorded as % thigmotaxsis (**B**) Plots showing % thigmotaxsis of fish before and after exposure to skin extract or control solutions. Paired student t-test was used to determine significance. Error bars represent SEM. **, $p \leq 0.01$

References:

Ahrens, M., Li, J., Orger, M., Robson, D., Schier, A.F., Engert, F., and Portugues, R. (2012). Brain-wide neuronal dynamics during motor adaptation in zebrafish. Nature.

Appelbaum, L., Wang, G.X., Maro, G.S., Mori, R., Tovin, A., Marin, W., Yokogawa, T., Kawakami, K., Smith, S.J., Gothilf, Y., et al. (2009). Sleep-wake regulation and hypocretin-melatonin interaction in zebrafish. Proc. Natl. Acad. Sci. U.S.A. *106*, 21942–21947.

Bader, A., Klein, B., Breer, H., and Strotmann, J. (2012). Connectivity from OR37 expressing olfactory sensory neurons to distinct cell types in the hypothalamus. Front. Neural Circuits *6*, 84.

Bassell, G.J., and Warren, S.T. (2008). Fragile X Syndrome: Loss of Local mRNA Regulation Alters Synaptic Development and Function. Neuron *60*, 201–214.

Bear, D.M., Lassance, J.-M., Hoekstra, H.E., and Datta, S.R. (2016). The Evolving Neural and Genetic Architecture of Vertebrate Olfaction. Curr. Biol. *26*, R1039–R1049.

Bergan, J.F., Ben-Shaul, Y., and Dulac, C. (2014). Sex-specific processing of social cues in the medial amygdala. Elife *3*, e02743.

Biechl, D., Tietje, K., Ryu, S., Grothe, B., Gerlach, G., and Wullimann, M.F. (2017). Identification of accessory olfactory system and medial amygdala in the zebrafish. Sci. Rep. *7*, 44295.

Brechbuhl, J., Klaey, M., and Broillet, M.-C. (2008). Grueneberg Ganglion Cells Mediate Alarm Pheromone Detection in Mice. Science (80-.). *321*, 1092–1095.

Brown, G.E., Adrian, J.C., Smyth, E., Leet, H., and Brennan, S. (2000). Ostariophysan alarm pheromones: Laboratory and field tests of the functional significance of nitrogen oxides. J. Chem. Ecol. *26*, 139–154.

Burgess, H.A., and Granato, M. (2007). Sensorimotor gating in larval zebrafish. J. Neurosci. Off. J. Soc. Neurosci. *27*, 4984–4994.

Carola, V., D'Olimpio, F., Brunamonti, E., Mangia, F., and Renzi, P. (2002). Evaluation of the elevated plus-maze and open-field tests for the assessment of anxiety-related behaviour in inbred mice. Behav. Brain Res. *134*, 49–57.

Chamero, P., Marton, T., Logan, D.W., Flanagan, K., Cruz, J., Saghatelian, A., Cravatt, B., and Stowers, L. (2007). Identification of protein pheromones that promote aggressive behaviour. Nature *450*, 899–902.

Dewan, A., Pacifico, R., Zhan, R., Rinberg, D., and Bozza, T. (2013). Non-redundant coding of aversive odours in the main olfactory pathway. Nature 1–5.

Dulac, C., and Wagner, S. (2006). Genetic Analysis of Brain Circuits Underlying Pheromone Signaling. Annu. Rev. Genet. *40*, 449–467.

Egan, R.J., Bergner, C.L., Hart, P.C., Cachat, J.M., Canavello, P.R., Elegante, M.F., Elkhayat, S.I., Bartels, B.K., Tien, A.K., Tien, D.H., et al. (2009). Understanding behavioral and physiological phenotypes of stress and anxiety in zebrafish. Behav. Brain Res. *205*, 38–44.

Emran, F., Rihel, J., and Dowling, J.E. Behavioral Assay to Measure Responsiveness of Zebrafish to Changes in Light Increments and Decrements. J. Vis. Exp.

Faraco, J.H., Appelbaum, L., Marin, W., Gaus, S.E., Mourrain, P., and Mignot, E. (2006). Regulation of hypocretin (orexin) expression in embryonic zebrafish. J. Biol. Chem. *281*, 29753–29761.

Ferguson, S.A., and Bowman, R.E. (1990). A nonhuman primate version of the open field test for use in behavioral toxicology and teratology. Neurotoxicol. Teratol. *12*, 477–481.

Gahtan, E., Tanger, P., and Baier, H. (2005). Visual prey capture in larval zebrafish is controlled by identified reticulospinal neurons downstream of the tectum. J. Neurosci. Off. J. Soc. Neurosci. *25*, 9294–9303.

Ganz, J., Kroehne, V., Freudenreich, D., Machate, A., Geffarth, M., Braasch, I., Kaslin, J., and Brand, M. (2014). Subdivisions of the adult zebrafish pallium based on molecular marker analysis. F1000Research *3*, 308.

Grossman, L., Utterback, E., Stewart, A., Gaikwad, S., Chung, K.M., Suciu, C., Wong, K., Elegante, M., Elkhayat, S., Tan, J., et al. (2010). Characterization of behavioral and endocrine effects of LSD on zebrafish. Behav. Brain Res. *214*, 277–284.

Grüneberg, H. (1973). A ganglion probably belonging to the N. terminalis system in the nasal mucosa of the mouse. Z. Anat. Entwicklungsgesch. *140*, 39–52.

Isogai, Y., Si, S., Pont-Lezica, L., Tan, T., Kapoor, V., Murthy, V.N., and Dulac, C. (2011). Molecular organization of vomeronasal chemoreception. Nature *478*, 241–245.

Jesuthasan, S.J., and Mathuru, A.S. (2008). The alarm response in zebrafish: innate fear in a vertebrate genetic model. J. Neurogenet. *22*, 211–228.

Kallai, J., Makany, T., Csatho, A., Karadi, K., Horvath, D., Kovacs-Labadi, B., Jarai, R., Nadel, L., and Jacobs, J.W. (2007). Cognitive and affective aspects of thigmotaxis strategy in humans. Behav. Neurosci. *121*, 21–30.

Kim, S.-Y., Burris, J., Bassal, F., Koldewyn, K., Chattarji, S., Tassone, F., Hessl, D., and Rivera, S.M. (2014). Fear-Specific Amygdala Function in Children and Adolescents on the Fragile X Spectrum: A Dosage Response of the FMR1 Gene. Cereb. Cortex *24*, 600–613.

Kimmel, C.B., Ballard, W.W., Kimmel, S.R., Ullmann, B., and Schilling, T.F. (1995). Stages of embryonic development of the zebrafish. Dev. Dyn. *203*, 253–310.

Lau, B.Y.B., Mathur, P., Gould, G.G., and Guo, S. Identification of a brain center whose activity discriminates a choice behavior in zebrafish. Proc. Natl. Acad. Sci. U.S.A.

Lockwood, B., Bjerke, S., Kobayashi, K., and Guo, S. (2004). Acute effects of alcohol on larval zebrafish: a genetic system for large-scale screening. Pharmacol. Biochem. Behav. *77*, 647–654.

Lundegaard, P.R., Anastasaki, C., Grant, N.J., Sillito, R.R., Zich, J., Zeng, Z., Paranthaman, K., Larsen, A.P., Armstrong, J.D., Porteous, D.J., et al. (2015). MEK Inhibitors Reverse cAMP-Mediated Anxiety in Zebrafish. Chem. Biol. *22*, 1–12.

Mathuru, A.S., Kibat, C., Cheong, W.F., Shui, G., Wenk, M.R., Friedrich, R.W., and Jesuthasan,

S. (2012). Chondroitin Fragments Are Odorants that Trigger Fear Behavior in Fish. Curr. Biol. *22*, 538–544.

Mombaerts, P., Wang, F., Dulac, C., Chao, S., Nemes, A., Mendelsohn, M., Edmondson, J., and Axel, R. (1996). Visualizing an olfactory sensory map. Cell *87*, 675–686.

Olmos-Serrano, J.L., Paluszkiewicz, S.M., Martin, B.S., Kaufmann, W.E., Corbin, J.G., and Huntsman, M.M. (2010). Defective GABAergic neurotransmission and pharmacological rescue of neuronal hyperexcitability in the amygdala in a mouse model of fragile X syndrome. J. Neurosci. *30*, 9929–9938.

Papes, F., Logan, D.W., and Stowers, L. (2010). The Vomeronasal Organ Mediates Interspecies Defensive Behaviors through Detection of Protein Pheromone Homologs. Cell *141*, 692–703.

Parra, K. V., Adrian Jr., J.C., and Gerlai, R. (2009). The synthetic substance hypoxanthine 3-N-oxide elicits alarm reactions in zebrafish (Danio rerio). Behav. Brain Res. *205*, 336–341.

Petrovich, G.D., Canteras, N.S., and Swanson, L.W. (2001). Combinatorial amygdalar inputs to hippocampal domains and hypothalamic behavior systems. Brain Res. Rev. *38*, 247–289.

Pfeiffer, W. (1977). The Distribution of Fright Reaction and Alarm Substance Cells in Fishes. Copeia *1977*, 653–665.

Pfeiffer, W., and Lemke, J. (1973). On the isolation and identification of the alarm substance from the skin of the european minnow Phoxinus phoxinus Cyprinidae, Ostariophysi Pisces. J. Comp. Physiol. *82*, 407–410.

Prober, D.A., Rihel, J., Onah, A.A., Sung, R.J., and Schier, A.F. (2006). Hypocretin/orexin overexpression induces an insomnia-like phenotype in zebrafish. J. Neurosci. *26*, 13400–13410.

Prober, D.A., Zimmerman, S., Myers, B.R., McDermott, B.M., Kim, S.-H., Caron, S., Rihel, J., Solnica-Krezel, L., Julius, D., Hudspeth, A., et al. (2008). Zebrafish TRPA1 Channels Are Required for Chemosensation But Not for Thermosensation or Mechanosensory Hair Cell Function. J. Neurosci. *28*, 10102–10110.

Rihel, J., Prober, D.A., Arvanites, A., Lam, K., Zimmerman, S., Jang, S., Haggarty, S.J., Kokel, D., Rubin, L.L., Peterson, R.T., et al. (2010). Zebrafish behavioral profiling links drugs to biological targets and rest/wake regulation. Science *327*, 348–351.

Ruta, V., Datta, S.R., Vasconcelos, M.L., Freeland, J., Looger, L.L., and Axel, R. (2010). A dimorphic pheromone circuit in Drosophila from sensory input to descending output. Nature *468*, 686–690.

Schnörr, S.J., Steenbergen, P.J., Richardson, M.K., and Champagne, D.L. (2012). Measuring thigmotaxis in larval zebrafish. Behav. Brain Res. *228*, 367–374.

Sosulski, D., Bloom, M.L., Cutforth, T., Axel, R., and Datta, S. (2011). Distinct representations of olfactory information in different cortical centres. Nature *472*, 213–216.

Stowers, L., Holy, T.E., Meister, M., Dulac, C., and Koentges, G. (2002). Loss of Sex Discrimination and Male-Male Aggression in Mice Deficient for TRP2. Science (80-.). *295*.

Truitt, W.A., Johnson, P.L., Dietrich, A.D., Fitz, S.D., and Shekhar, A. (2009). Anxiety-like

behavior is modulated by a discrete subpopulation of interneurons in the basolateral amygdala. Neuroscience *160*, 284–294.

Tye, K., Prakash, R., Kim, S.-Y., Fenno, L., Grosenick, L., Zarabi, H., Thompson, K., Gradinaru, V., Ramakrishnan, C., and Deisseroth, K. (2011). Amygdala circuitry mediating reversible and bidirectional control of anxiety. Nature *471*, 358–362.

Wagner, S., Gresser, A.L., Torello, A.T., and Dulac, C. (2006). A Multireceptor Genetic Approach Uncovers an Ordered Integration of VNO Sensory Inputs in the Accessory Olfactory Bulb. Neuron *50*, 697–709.

Wang, L., and Anderson, D. (2010). Identification of an aggression-promoting pheromone and its receptor neurons in Drosophila. Nature *463*, 227–231.

Wyart, C., Bene, F. Del, Warp, E., Scott, E.K., Trauner, D., Baier, H., and Isacoff, E.Y. (2009). Optogenetic dissection of a behavioral module in the vertebrate spinal cord. Nature *461*, 407–410.

Yokogawa, T., Marin, W., Faraco, J., Pézeron, G., Appelbaum, L., Zhang, J., Rosa, F., Mourrain, P., and Mignot, E. (2007). Characterization of sleep in zebrafish and insomnia in hypocretin receptor mutants. PLoS Biol. *5*, e277.

Young, K.S., Burklund, L.J., Torre, J.B., Saxbe, D., Lieberman, M.D., and Craske, M.G. (2017). Treatment for social anxiety disorder alters functional connectivity in emotion regulation neural circuitry. Psychiatry Res. Neuroimaging *261*, 44–51.